Juvenile Toxicologic Pathology

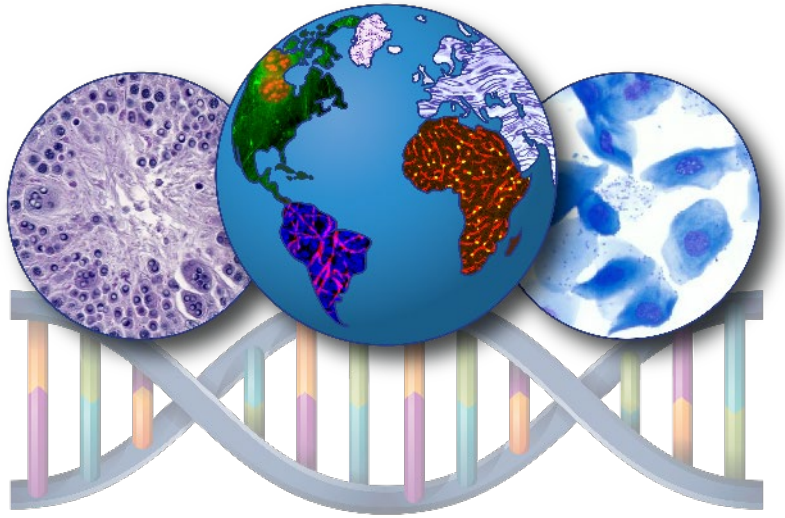

Division of Translational Toxicology Global Toxicologic Pathology Training Program

National Institutes of Health • U.S. Department of Health and Human Services

Abbreviations used in this presentation

ACE – acetylcholinesterase
BRAF – v-raf murine sarcoma viral oncogene homolog B1 (v-raf = rapidly accelerated fibrosarcoma oncogene)
CTA – Comparative thyroid assay
DNT – Developmental neurotoxicity
EDSP – Endocrine disruptor screening program
EOGRTS – Extended one generation reproductive toxicology study
EPA – Environmental Protection Agency
FDA – Food and Drug Administration
GD – Gestation day
H&E – Hematoxylin & eosin
IHC – Immunohistochemistry
ICH – International Council for Harmonisation
JAS – Juvenile animal study
JNS – Juvenile neurotoxicity study
OECD – Organisation for Economic and Cooperative Development
PAS/H – Periodic acid Schiff/hematoxylin
PND – postnatal day
PPND – Pre and postnatal development
PTFA – Pubertal and thyroid function assay
VEGF-R – Vascular endothelial growth factor receptor

Juvenile Toxicologic Pathology Outline

- Introduction
- Safety assessment studies involving juvenile animals
- Nervous system (brain, spinal cord)
- Eye
- Respiratory system (lung)
- Cardiovascular system (heart)
- Urinary system (kidney)
- Gastrointestinal system
- Liver, pancreas and salivary gland
- Reproductive system (female and male)
- Endocrine system
- Musculoskeletal system
- Skin and mammary gland
- Immune System
- Specific factors to consider in studies involving juvenile animals
- References
- Acknowledgements

Introduction

- Juvenile tissues are commonly examined in certain pre-clinical safety studies.
- This presentation covers 1) unique and selective features of normal postnatal development of major tissues in the rat to assist the pathologist when evaluating histopathology of young animals; and 2) examples of toxicity unique to juvenile laboratory animal species.
- In classical publications, the juvenile stage for the rat (and human) constitutes only one (1) of five (5) postnatal developmental stages. In this presentation "juvenile" will be used in the more general sense as the stage between birth and adulthood, unless otherwise specified.

Five Stages of Postnatal Development		
Stage	**Rat (age)**	**Human (age)**
Neonatal	0-7 days	0-28 days
Infantile	8-20 days	1-23 months
Juvenile	21-32 days	2-13 years
Peripubertal	33-55 days	13-16 years
Adult	> 55 days	> 16 years

Safety Assessment Studies Involving Juvenile Animals

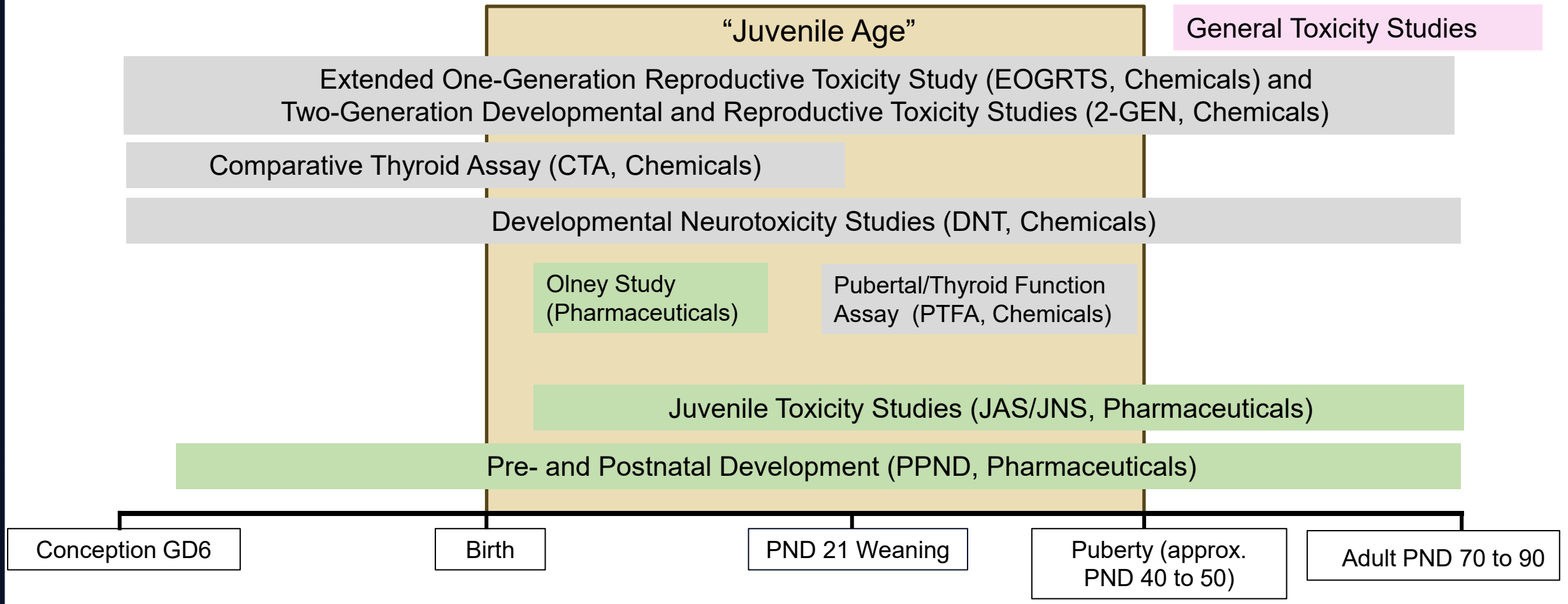

There are at least 8 safety assessment studies that involve dosing or evaluation of juvenile animals. The grey and green bars indicate the period of exposure to test article (chemical or pharmaceutical agent, respectively). Pale yellow box indicates the juvenile age. Note that General Toxicity Studies (pink bar) do not involve dosing or evaluation of juvenile animals.

Safety assessment studies that involve dosing or evaluation of tissues from juvenile animals

Study	Industry	Guideline or Regulations
Extended One Generation (EOGRT)	Chemical	OECD (2018). Test No. 443: Extended One-Generation Reproductive Toxicity Study.
2-Generation (2-GEN)	Chemical	OECD (2001). Test No. 416: Two-Generation Reproduction Toxicity Study.
Developmental Neurotoxicity Study (DNT)	Chemical	EPA (1998). Health Effects Test Guidelines OPPTS 870.6300 Developmental Neurotoxicity Study. OECD (2007). Test No. 426: Developmental Neurotoxicity Study.
Comparative Thyroid Assay (CTA)	Chemical	EPA (2005). Guidance for Thyroid Assays in Pregnant Animals, Fetuses and Postnatal Animals, and Adult Animals.
Pubertal and Thyroid Function Assay (PTFA)	Chemical	EPA (2009). EDSP Test Guidelines OPPTS 890.1450 Pubertal Development and Thyroid Function in Intact Juvenile/peripubertal Female Rats. EPA (2009). EDSP Test Guidelines OPPTS 890:1500 Pubertal Development and Thyroid Function in Intact Juvenile/peripubertal Male Rats.
Juvenile Animal Study (JAS) or Juvenile Neurotoxicity Study (JNS)	Pharmaceutical	FDA (2021). Guidance for Industry: S11 Nonclinical Safety Testing in Support of Development of Pediatric Pharmaceuticals.
Olney Lesion Study	Pharmaceutical	None.
Pre- and Postnatal developmental toxicity study (PPND)	Pharmaceutical	ICH (2020). S5(R3). Guideline on Detection of Reproductive and Developmental Toxicity for Human Pharmaceuticals.

Nervous System, Rat

Brain

- Prenatal development of the brain involves neuronal proliferation and migration in most areas of the brain. This proliferation and migration of neurons is complete by birth, except for three areas of the brain: the olfactory bulbs, hippocampus and cerebellum.
- Postnatal development of the brain involves some neuronal proliferation and migration (limited mostly to olfactory bulbs, hippocampus, and cerebellum). Neurons proliferate from the undifferentiated germinal cells lining the ventricles and surface of the cerebellum. They migrate into position along radial glial cells, which provide the scaffold. These radial glial cells eventually differentiate into astrocytes.
- Neuronal differentiation, neuronal apoptosis, gliogenesis (development of astrocytes, oligodendrocytes), myelination, and synaptogenesis are postnatal events that occur during brain development. The brain is histologically “mature” at PND 21, though there is continued gliogenesis, myelination and synaptogenesis until brain reaches adult size by PND 90.
- Gliogenesis is considered a postnatal process with peak activity around PND 7 to PND 21.
- Apoptosis of neurons occurs in 60-70% of cortical neurons during early postnatal life (PND 1 to PND 14). Peak apoptosis occurs around PND 7.
- Myelination in the brain is a postnatal event (PND 0 to PND 37).
- The blood brain barrier (BBB) is considered adult-like at PND 21.
- There is a brain growth spurt (PND 8 to PND 12).

Spinal Cord

- Most spinal cord development is prenatal. Postnatal change in the spinal cord is limited to myelination, which is generally complete by PND 14. There is some apoptosis of neurons and glial cells at around PND 1 to PND 8.

Developmental Sequence in Proliferation and Migration of Neurons

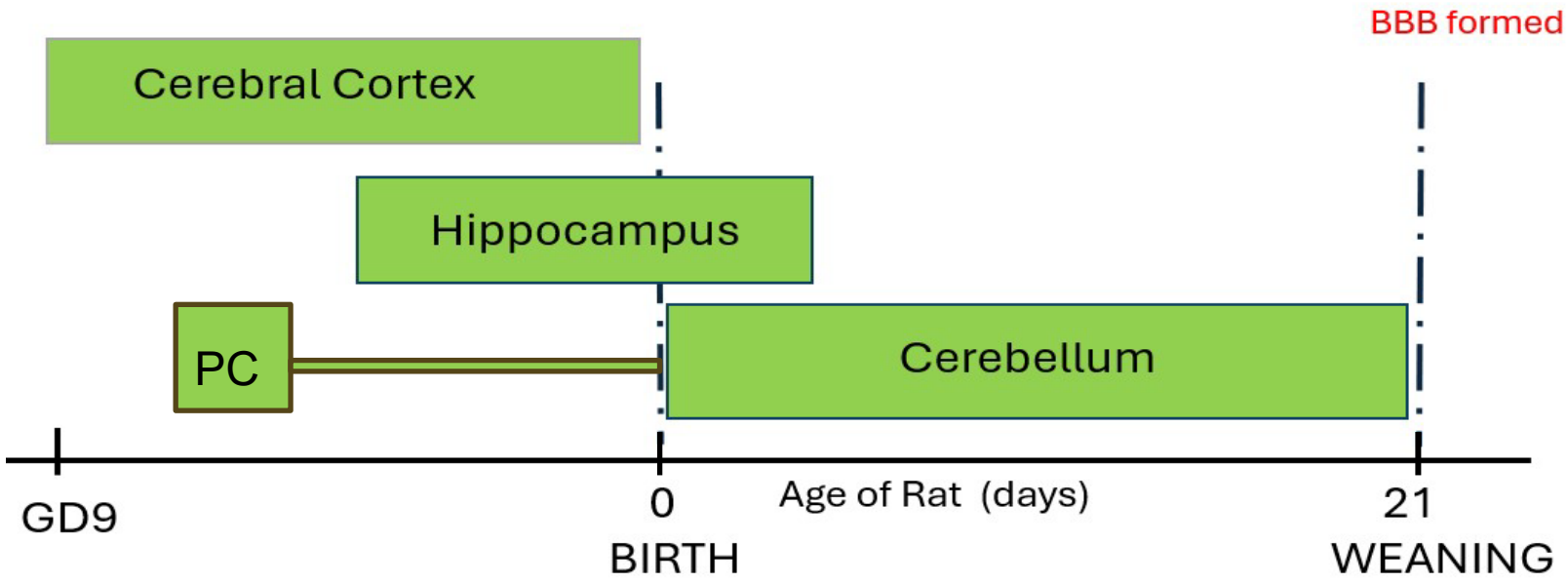

The three areas of brain (cerebral cortex, hippocampus, and cerebellum) are highlighted here because these three areas are the focus of morphometry for developmental neurotoxicity studies. Neuronal proliferation (from germinal matrix cells) and neuronal migration into position are mostly prenatal events in the cerebral cortex, in the Purkinje cells of the cerebellum, and in the hippocampus (predominantly Ammon's horn). Postnatal neuronal migration and proliferation occurs in the hippocampus (predominantly the dentate gyrus) and for all neurons (other than Purkinje cells) in the cerebellum. PC = Purkinje cells; BBB = blood brain barrier

Brain, rat, PND 1

- Postnatal neuronal proliferation and migration occurs in the hippocampus, cerebellum, and olfactory bulbs.
- The primary germinal matrix lines the lateral and third ventricles and provides the precursors of the neurons, which migrate into appropriate positions along radial glial cells. The dark blue of the primary germinal matrix still contains undifferentiated cells ready to proliferate and migrate into position in the hippocampus and olfactory bulbs. The extension of the primary germinal matrix into the olfactory bulbs is called the “rostral migratory stream”.
- There is a secondary germinal matrix lining the surface of the cerebellum which will lead to proliferation of neurons of the cerebellum.

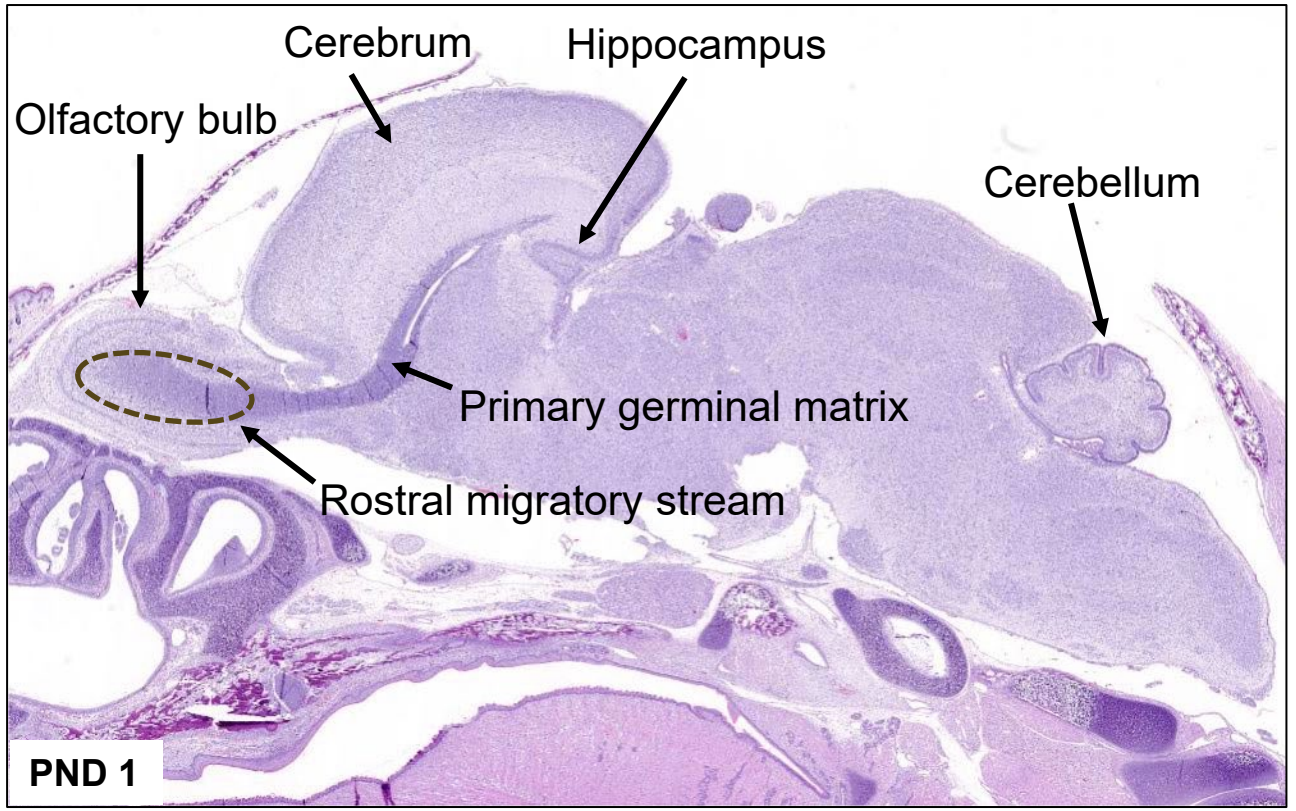

Cerebral cortex, rat, PND 1 and 21

- These images show the dramatic change in the cerebral cortex between PND 1 and PND 21. H&E stain.
- All neurons are formed and positioned in place in the cerebral cortex at birth, resulting in a very dense population of closely approximated neurons.
- Physiological apoptosis results in loss of 60-70%of neurons during the PND 1 to PND 14. Apoptosis can be detected with Caspase 3 or Caspase 9 but is difficult to detect on H&E-stained sections.
- Apoptosis (and loss) of neurons, along with neuronal differentiation (expansion of dendritic branching, elongation of axons) results in the less cellular and histologically adult-like cerebral cortex by PND 21. Note the increased size of the nuclei of the neurons at PND 21 compared to the undifferentiated neurons at PND 1. Also note the relative density of neurons (boxes) at PND1 versus PND 21.

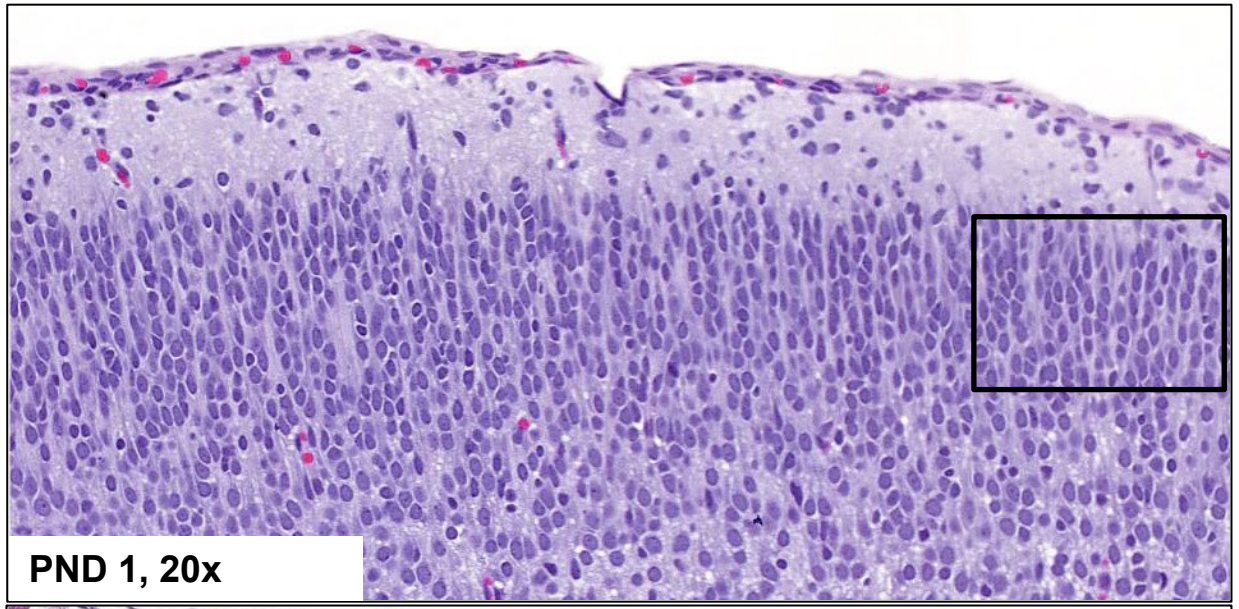

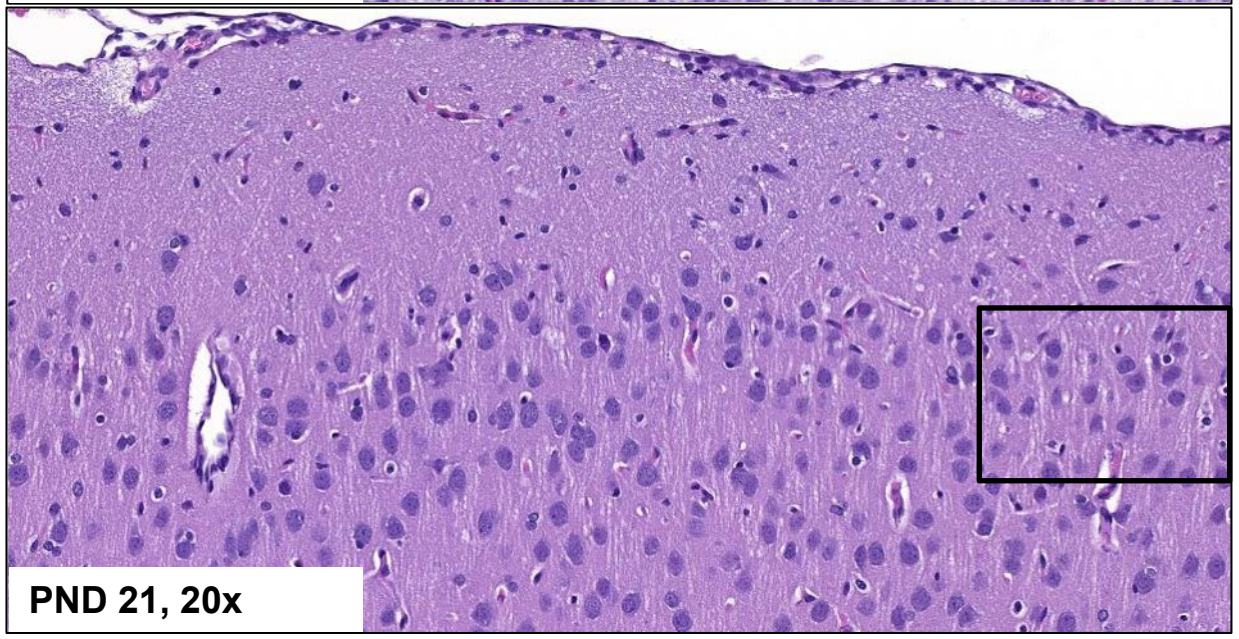

Cerebellum, rat, PND 1, 7, 14 and 21

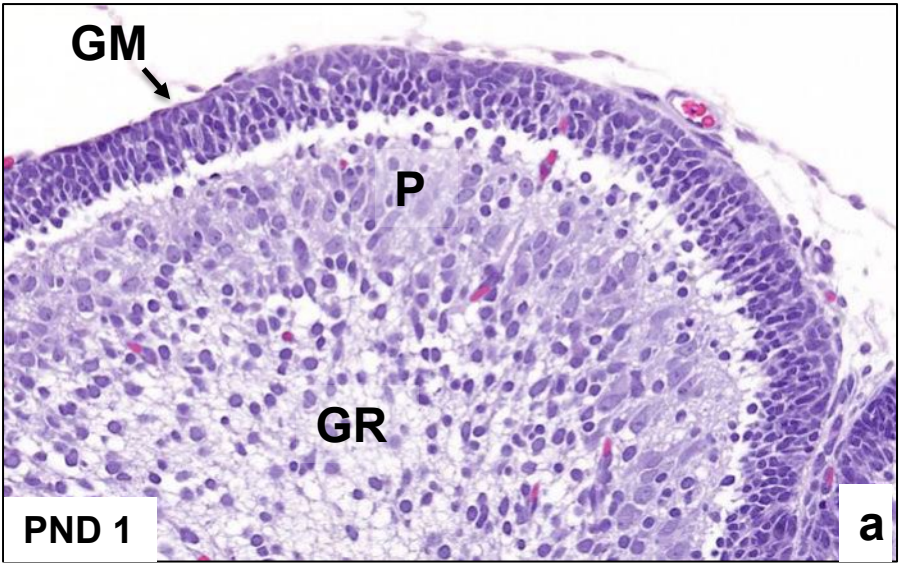

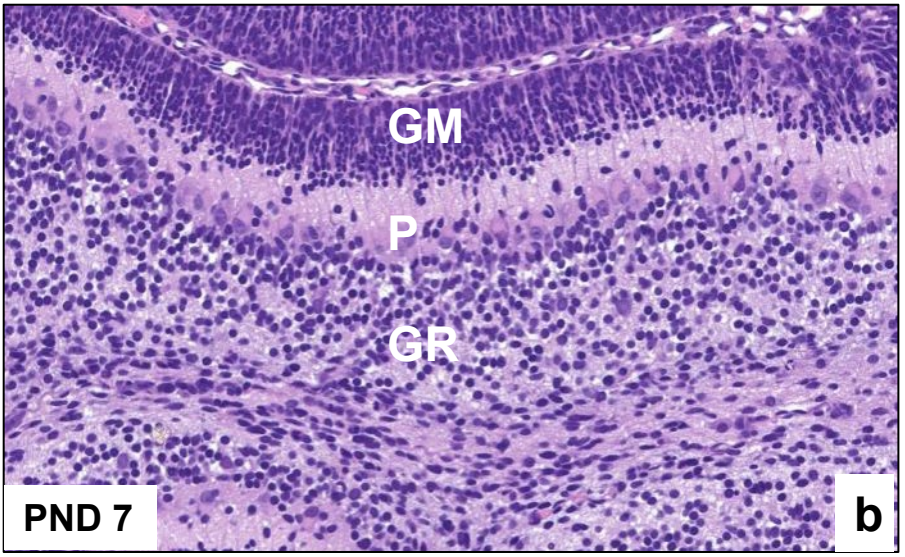

These images (a – d) show the postnatal morphologic development of the cerebellum.
a) At PND 1, a cluster of Purkinje cells (P) are present and form no particular pattern. The germinal matrix (GM) on the surface is robust. The granule cell layer (GR) is nearly devoid of neurons.
b) At PND 7, the germinal matrix is giving rise to new neurons that migrate into position to populate the granule cell layer (GR). Purkinje cells (P) spread out in a linear distribution as cerebellum expands.
c) At PND 14, germinal matrix is still present, and the granule cell layer (GR) has increased neuron density (when compared to PND 7). Some dark staining cells in the molecular layer (M) represent active migration of granule cell neurons from the germinal matrix to the granule cell layer. The Purkinje cells (P) are enlarged and more differentiated compared to those at PND 7.
d) By PND 21, the cerebellum is histologically mature, with loss of the germinal matrix.

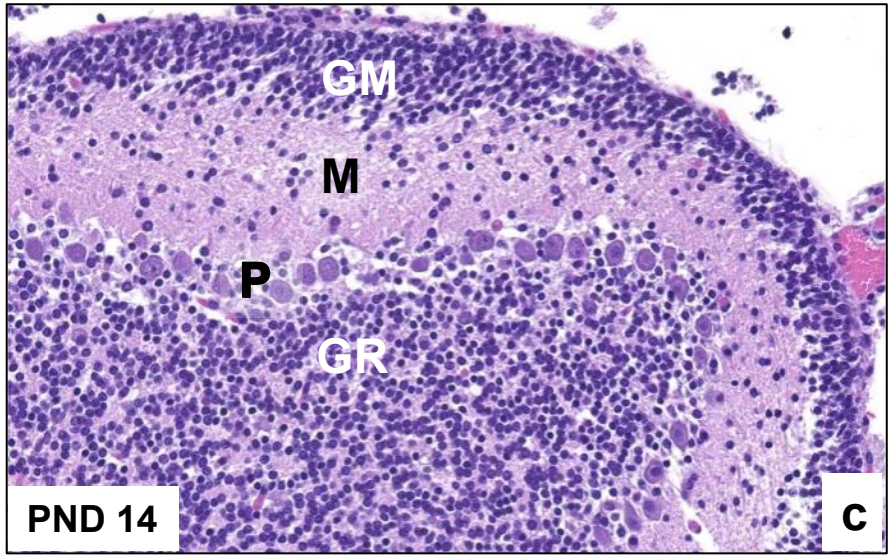

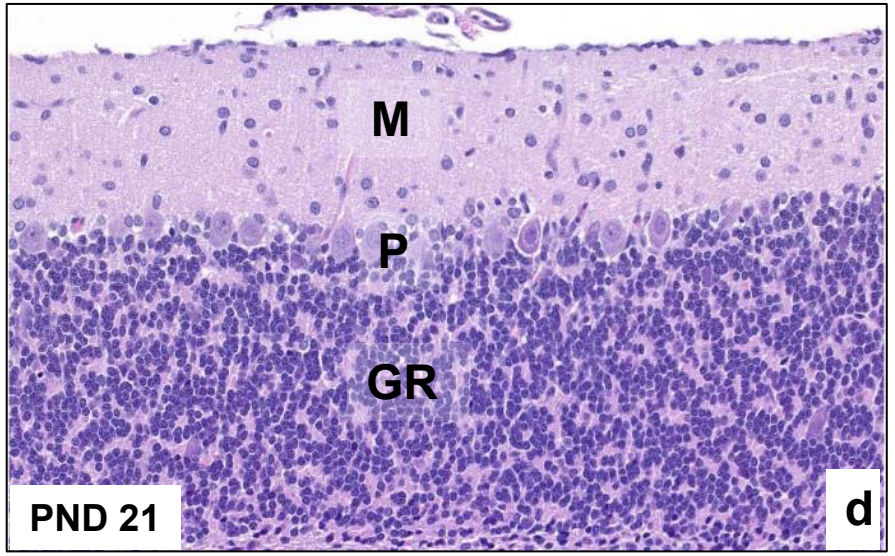

Cerebellum, rat, PND 22 and PND 78, Luxol fast blue/cresyl violet stain

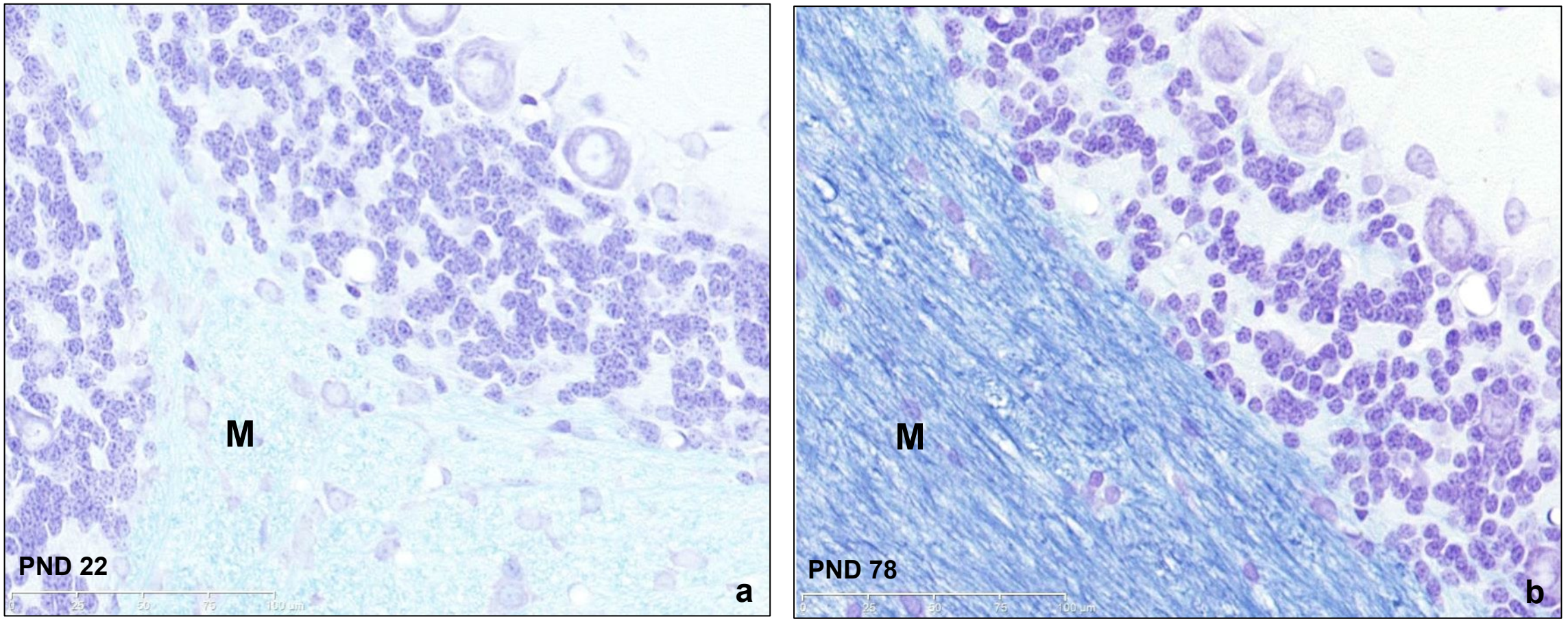

Myelination occurs postnatally in the rat and is complete by about PND 37. a) Myelin (M) at PND 22 barely stains blue with luxol fast blue/cresyl violet stain in the white matter of the cerebellum, as compared to b) the dense blue staining of myelin (M) in cerebellar white matter of the adult brain (PND 78). The pale blue staining at PND 22 indicates incomplete myelination.

Brain, rat, PND 21 and PND 8, selected microscopic findings

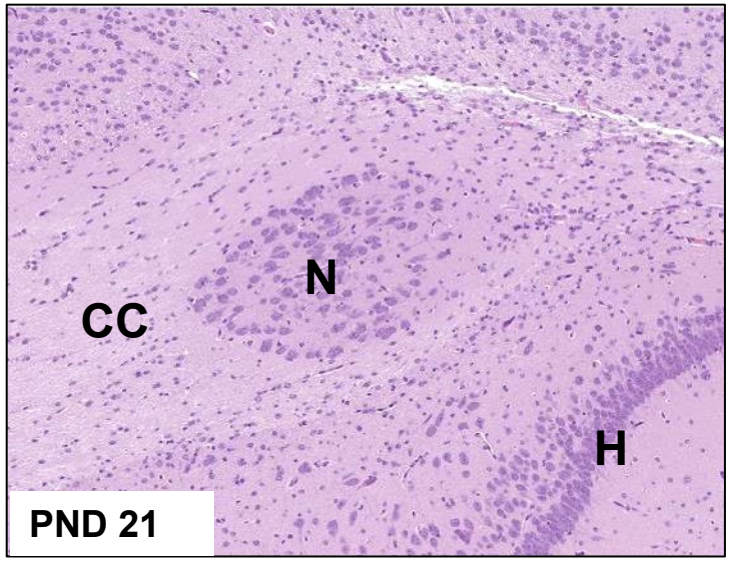

Heterotopia. Note the abnormal cluster of neurons (N) in the corpus callosum (CC). Hippocampus (H). H&E stain.

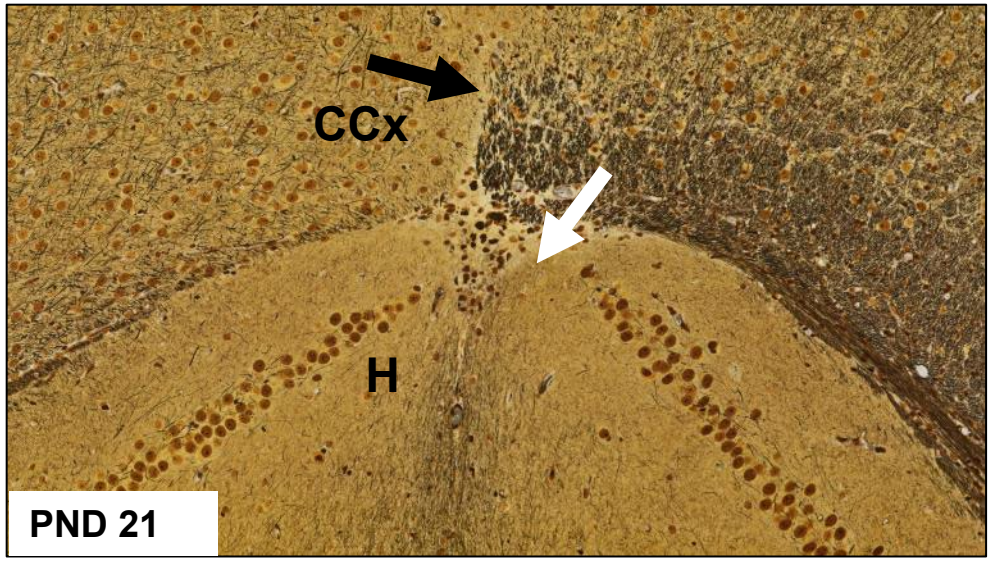

Dysplasia of hippocampus (H) and cerebral cortex (CCx). Note loss of continuity (or disruption) of neurons of hippocampus (white arrow) and the linear disruption of the cortex (black arrow). Bielschowsky stain.

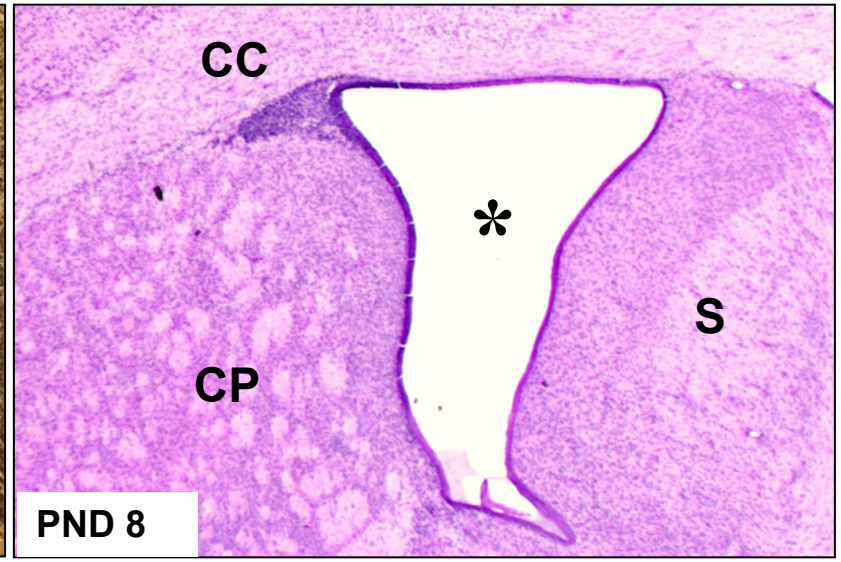

Ventricular dilatation (*). Caudate putamen (CP), corpus callosum (CC), septal nuclei (S). H&E stain.

Xenobiotic-related microscopic alterations in developing rat brains may include heterotopia, dysplasia, and/or ventricular dilatation (DTT nomenclature is dilation). The illustrated heterotopia was due to gestational and lactational exposure to a thyrotoxicant, and the hippocampal dysplasia was due to gestational and lactational exposure to tetrahydrocannabinol. Ventricular dilatation (*) is a common background finding in developing rat brains. In this PND 8 brain from an Olney lesion study, the finding was considered to represent a background finding.

Brain, rat, PND 22, hypoplasia of corpus callosum from a DNT study

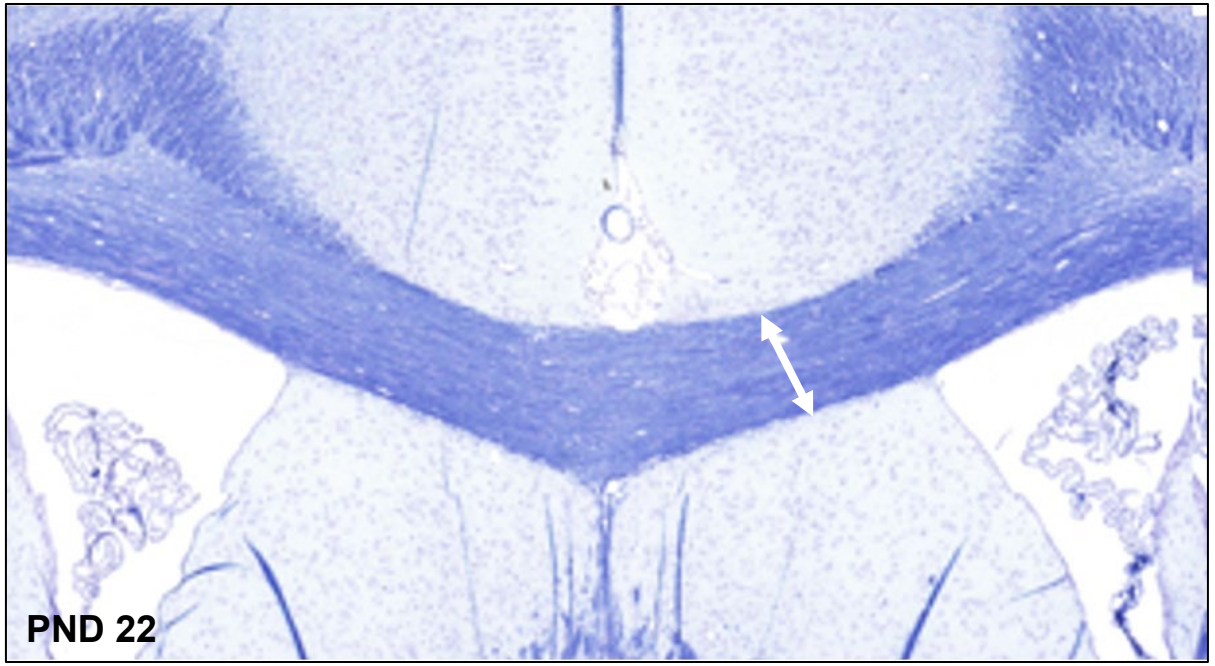

Normal rat corpus callosum. Note the thickness of the corpus callosum (double-headed arrow). LFB/CV stain, 20x.

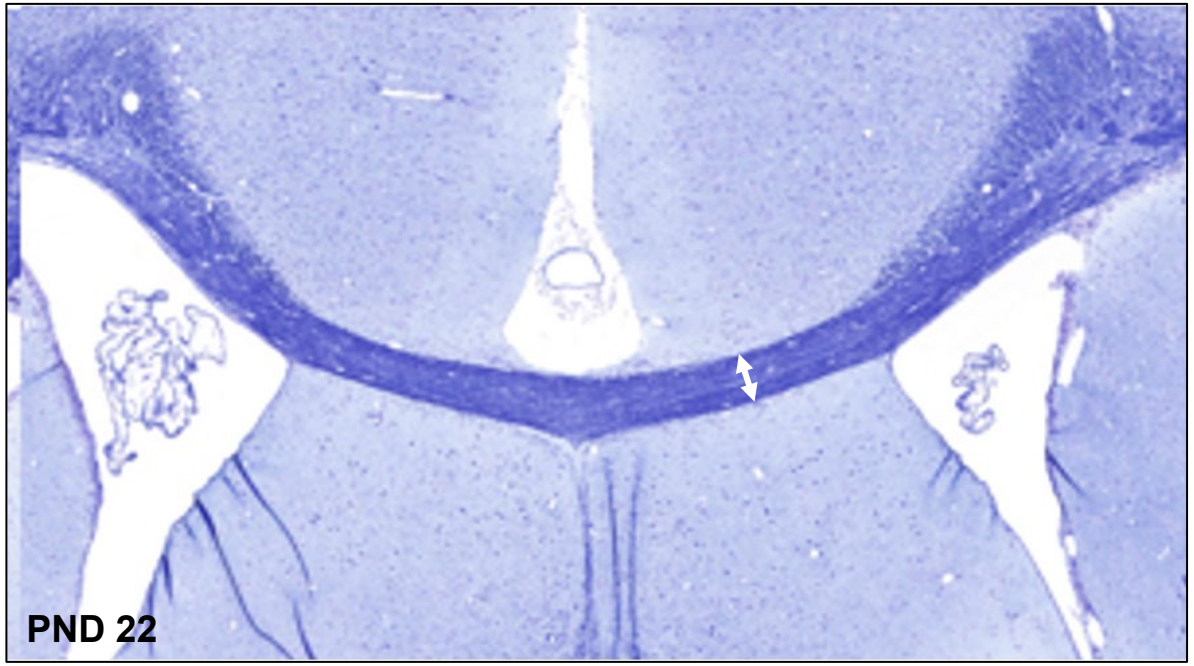

Rat corpus callosum hypoplasia, following exposure to tetrahydrocannabinol. Note the decreased thickness of the corpus callosum (double-headed arrow) compared to normal image (left). LFB/CV stain, 20x.

Thinning or hypoplasia of the corpus collosum is another developmental finding from developmental neurotoxicity studies that may be detected by light microscopy. The rat on the right was exposed to tetrahydrocannabinol during gestation and prior to weaning. Morphometry measurements are usually used to objectively identify test article-related differences in size of sub-anatomic brain sites but, in this instance, light microscopy was sufficient to identify the marked effect on the corpus callosum.

Brain, rat, PND 8, neuronal necrosis from Olney study

- Neonatal rat brain is often evaluated to detect test article-related neuronal necrosis. Neuronal necrosis is also known as the Olney lesion when caused by NMDA-receptor antagonists or GABA-agonists.
- a) The aminocupric silver stain is used to identify necrotic neurons. These necrotic neurons (black) are commonly seen in the septal nuclei (oval outline) in the forebrain. 40 µm frozen, gelatin-embedded section, aminocupric silver stain, 4x.
- b) Necrotic neurons can also be identified on H&E-stained paraffin sections. The bottom image (b) shows necrotic neurons (arrows) and necrotic debris in the thalamus of a MK-801 positive control PND 8 rat on an Olney lesion study. Necrotic neurons have swollen eosinophilic cytoplasm, and a pyknotic nucleus. H&E stain, 25x.
- Note that in brain tissue at PND 8, it is difficult to differentiate neuronal necrosis (caused by test article) from the normal physiologic apoptosis occurring at this time. Physiological apoptotic neurons tend to be widely scattered, while xenobiotic-mediated necrotic neurons tend to be clustered in specific areas of the brain. In the cerebral cortex of neonatal rats (PND 8) with relatively immature brain tissue, the neuropil stains pale blue with H&E stain.

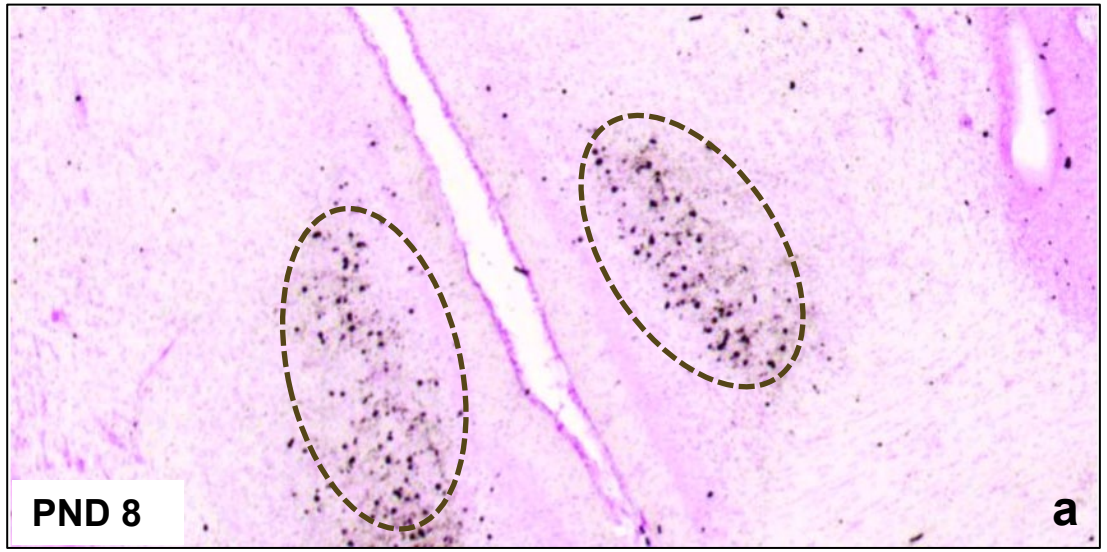

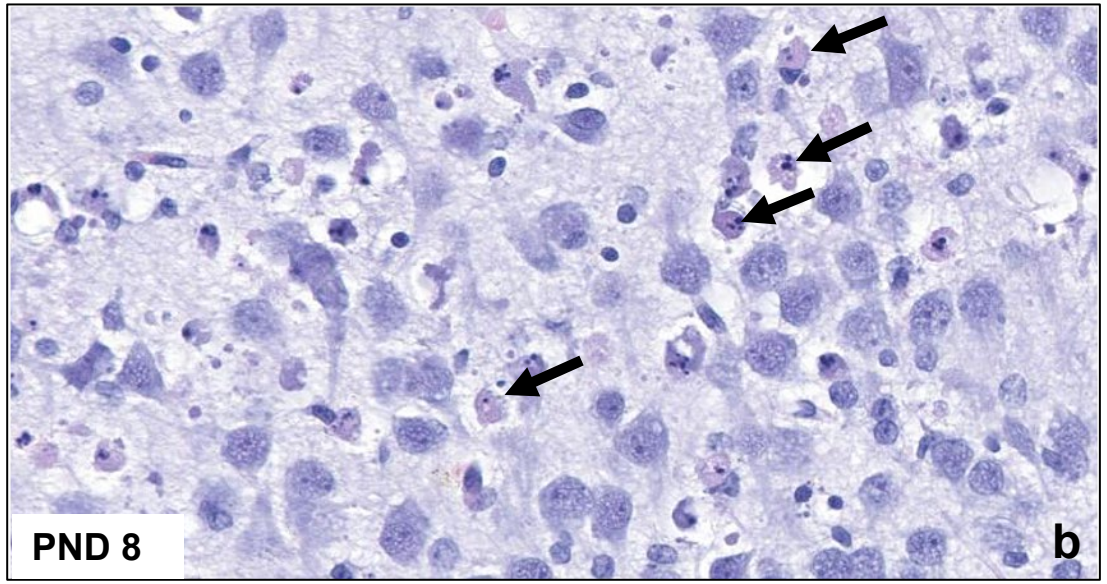

Eye

- The eye of the rat at birth is equivalent to the eye of humans at gestation week 26. The uvea, lens, eyelid and optic nerve are morphologically mature by PND 14 to 16, and the retina and cornea at PND 21.

- **Cornea** – At birth, the corneal epithelium is 1 to 2 cell layers and increases to 4 to 5 cell layers thick when the eyelid opens (at PND 14). The eyelid covers the cornea and is fused from PND 1 to PND 14. The epithelium reaches the thickness of an adult eye by PND 21 to PND 28. During this time frame, the corneal stroma and Descemet's membrane also increase in thickness. The maturation of the cornea progresses from the center of the cornea to the periphery (limbus).

- **Lens** – The lens is relatively flat at birth, but rapidly becomes more spherical, occupying 2/3 of the intraocular cavity at PND 16. At birth, the lens is vascular with blood supplied from the hyaloid vessel. The lens grows by division of a subcapsular layer of anterior epithelium into specialized fiber cells at the equator. These cells elongate and form an onion skin of fibers, and the nuclei spread out to form the characteristic nuclear bow.

- **Retina** – All retinal cells develop from neuroblastic multipotent cells. During prenatal life, these neuroblastic cells differentiate and/or commit to a certain cell type (i.e., cone, rods, bipolar, Muller, amacrine, horizontal cells, etc.). The neuroblastic cells and these committed cells form a thick solid monolayer visible by light microscopy at birth. After birth, committed cells start migrating into position. At PND 7, all layers are discernable. At PND 14, all cells are postmitotic and neuroblasts no longer exist. At PND 21, the retina has the histology of the adult retina. The most peripheral aspect of the retina may lag somewhat behind this development schedule.

Eye, rat, PND 1 and PND 14

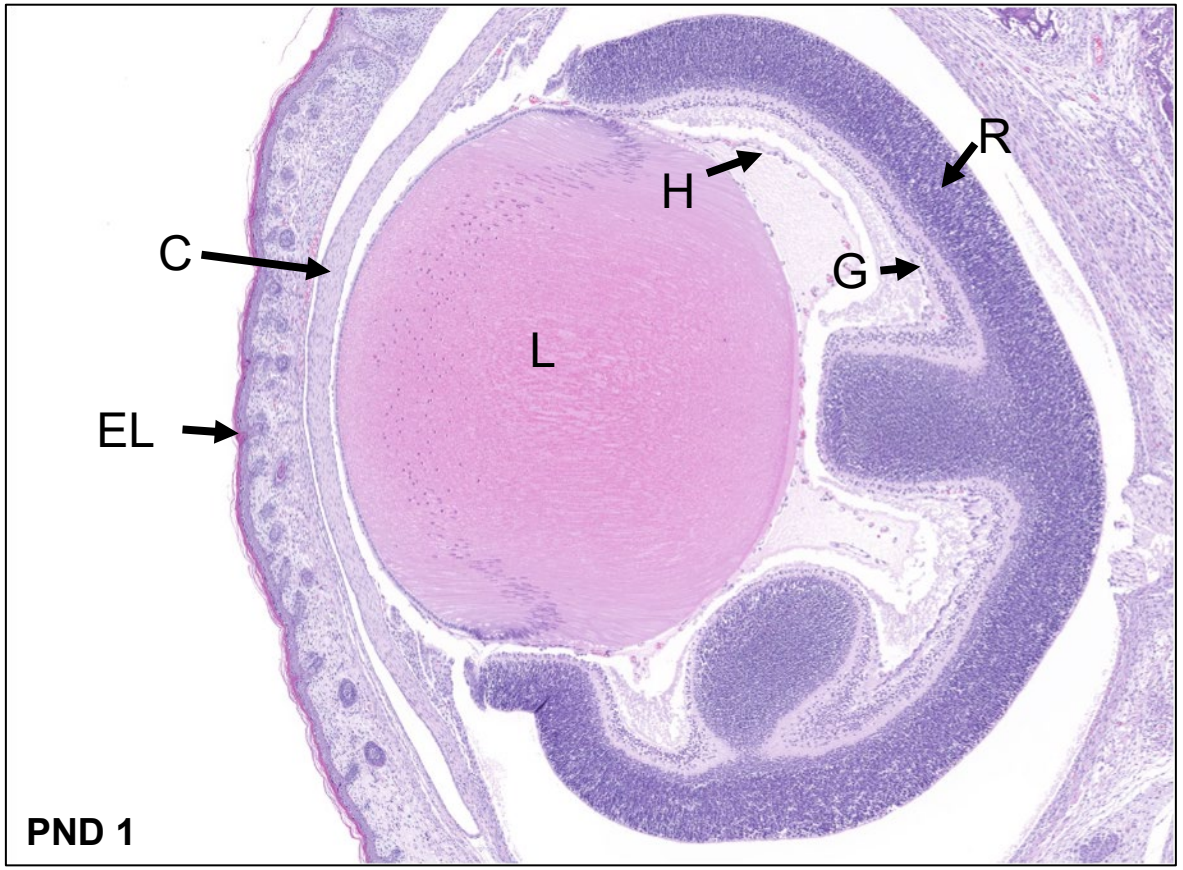

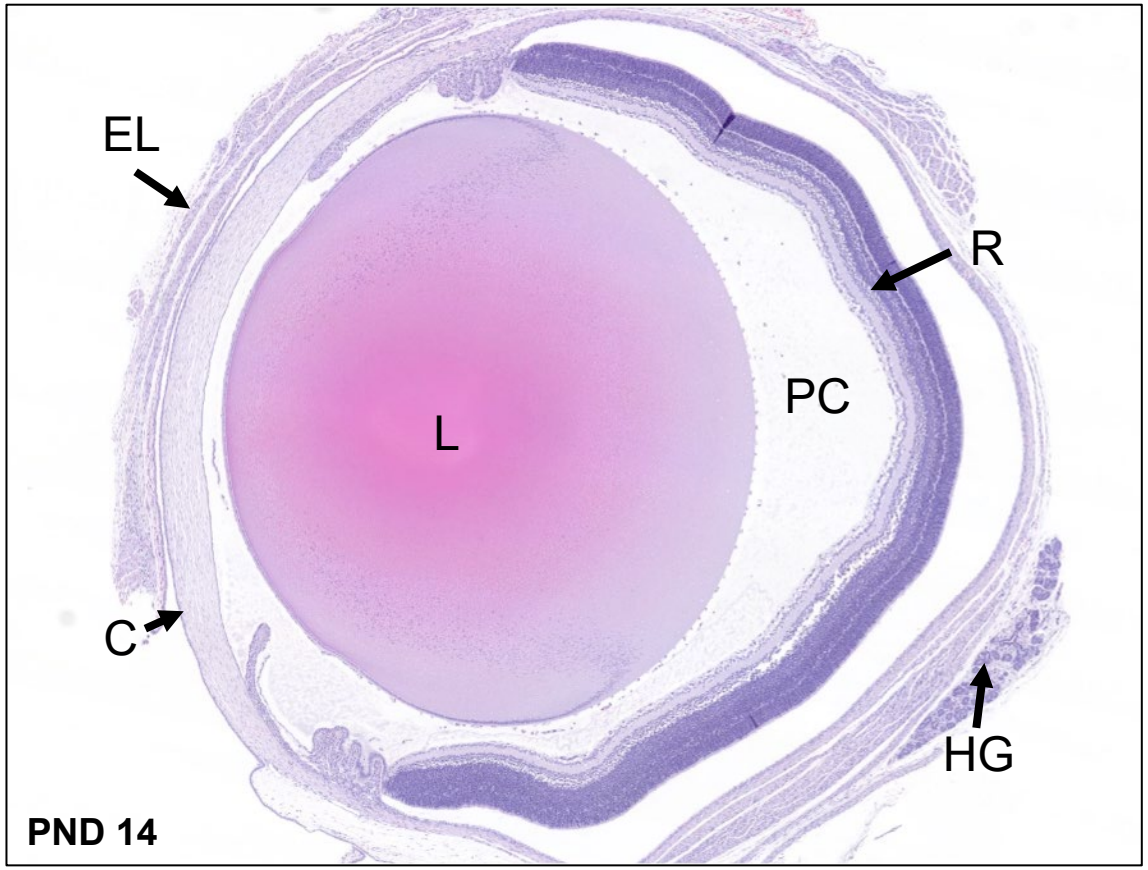

At PND 1, the retina (R) consists of a monolayer with only the ganglion cell layer distinguishable. Note the thick layer of skin (fused eyelid; EL) covering the relatively thin cornea (C). The early postnatal period is a critical time in eye development and represents an important window for toxic injury. By PND 7, the retina has the distinctive layers but remains morphologically immature. C = cornea; EL = eyelid; G = ganglion layer; H = hyaloid vessels; HG = harderian gland; L = lens; PC = posterior chamber. H&E stain.

Eye, rat, PND 7 and PND 21

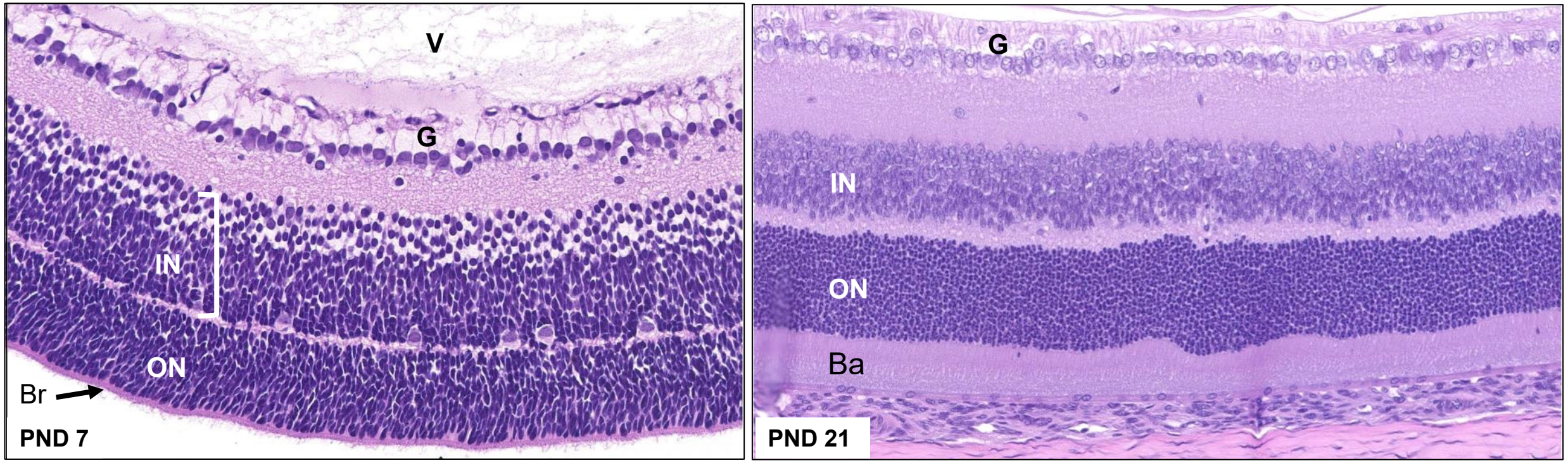

Rat retina, PND 7 (40x) and PND 21 (30x). At PND 7, note that all retinal layers are discernible, even though the layers do not have adult proportions as seen at PND 21. At PND 7, the inner nuclear layer (IN) is thicker than the outer nuclear layer (ON) and subdivides into segments of amacrine, bipolar and Muller cells. Bruch's membrane (Br) is histologically mature, and no apparent bacillary zone of the receptors of the rods and cones is present. At PND 21, when morphologically mature, the inner nuclear layer is thinner than the outer nuclear layer (of rods and cones), and the bacillary zone (eosinophilic receptor layer of rods and cones [Ba]) is noticeable. IN = inner nuclear; ON = outer nuclear; V = vitreous ; G = ganglion cell. H&E stain.

Eye, rat – lesions associated with exposure to ally isothiocyanate during juvenile age

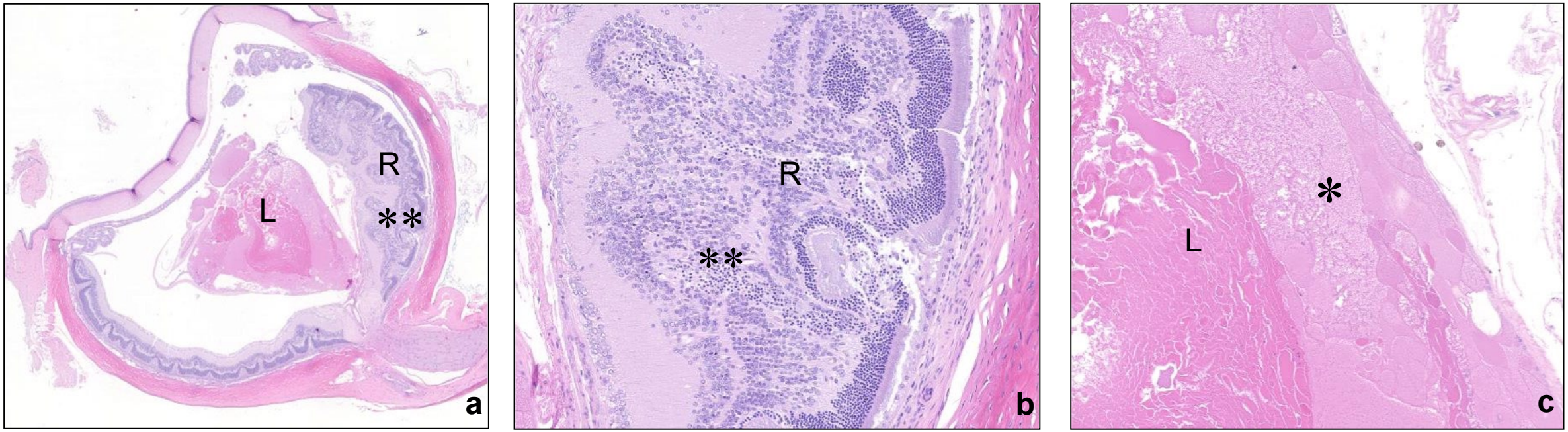

Rats exposed to allyl isothiocyanate (AITC) through fetal life and suckling and then administered the test article directly by oral gavage through PND 70 developed grossly visible microphthalmia, cataracts, and retinal dysplasia. Prior studies with AITC did not include direct exposure of juvenile rats from fetal life through PND 56, and those prior studies had no eye lesions. The test article-related effects appear to be both developmental (micropthalamia and retinal dysplasia) as well as degenerative (cataracts). Note the hyalinized pale and swollen fibers in the lens indicative of cataracts (*) and the disruption of the normal architecture to the retina (**). This case study underscores the need to conduct juvenile studies where exposure occurs at time points not otherwise included in routine toxicity studies. L = lens. R = retina. H&E stain.

Respiratory System (Lung)

- The lung develops through morphologically distinct stages of maturation, including embryonic (prenatal), pseudoglandular (prenatal), canalicular (prenatal), saccular (pre- and postnatal), and alveolar (postnatal).
- From GD 21 to PND 4, the lung of the rat is in the saccular stage. From PND 4 to PND 21, the lung undergoes a process of bulk alveolarization and then continued alveolarization, involving formation of primary and secondary septae, with remodeling of collagen and smooth muscle. The “bulk” stage represents a surge of this morphologic change, while the change is less dramatic but still ongoing during the “continued” stage of alveolarization. Microvascular maturation by vascular remodeling occurs during alveolarization to help form alveoli with higher air-blood surface area and increased oxygen exchange. The lung is morphologically mature at PND 21.

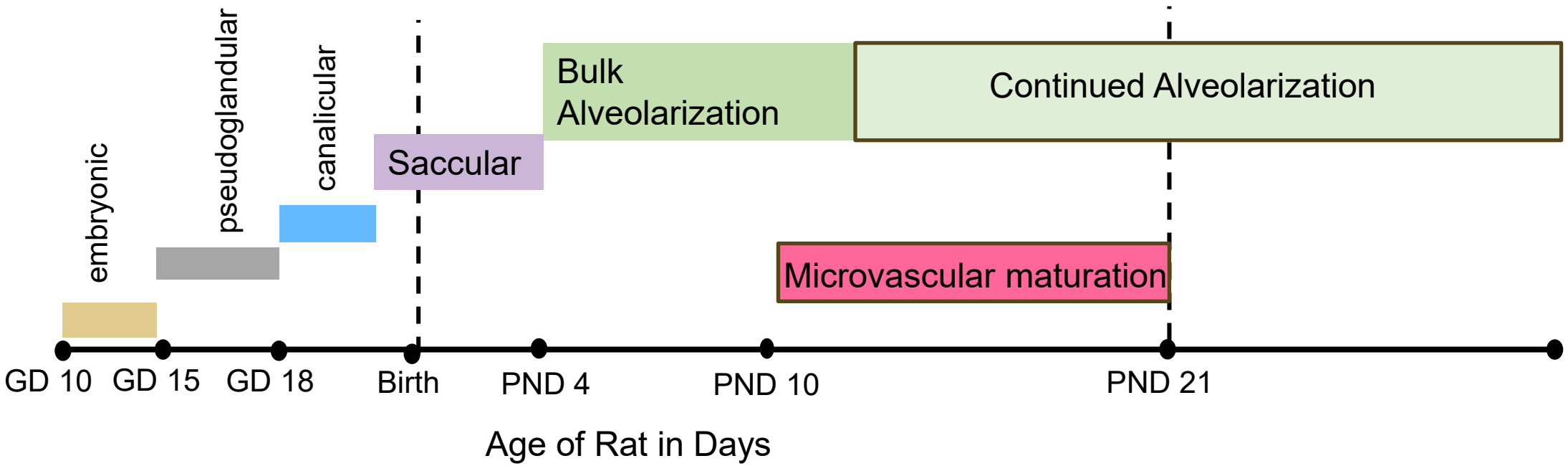

GD = gestation day; PND = postnatal day

Lung, rat, PND 1

- At the saccular stage, the lung has thick septae with a capillary on each side of the septum (arrows). There are no secondary septae. The saccular stage is densely cellular and should not be confused with interstitial pneumonia or atelectasis. H&E stain, 26x.
- Hyperoxia can cause “delayed maturation” of lung (an animal model for premature births), and, under those conditions, this saccular appearance may persist beyond PND 4.

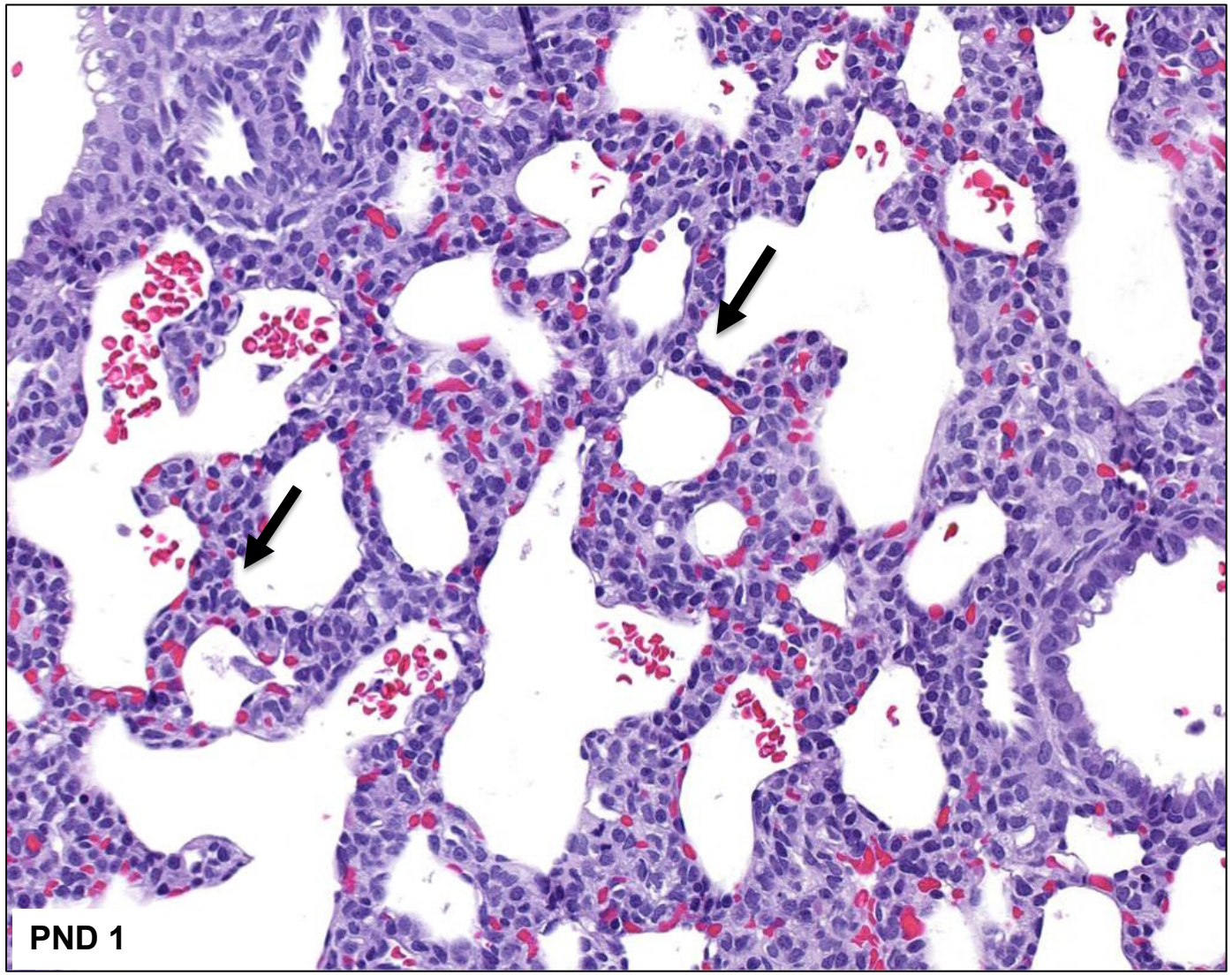

Lung, rat, PND 14

- Alveolarization is a piece-meal process, therefore, at PND 14, not all septae have reached the mature alveolar stage.
- During alveolarization, the airspaces divide to increase air:tissue surface area for more effective oxygen exchange.
- Note some septae have a capillary on each side of the septum (arrows) while the mature septae have a single capillary following vascular remodeling (arrowhead). H&E stain, 33x.

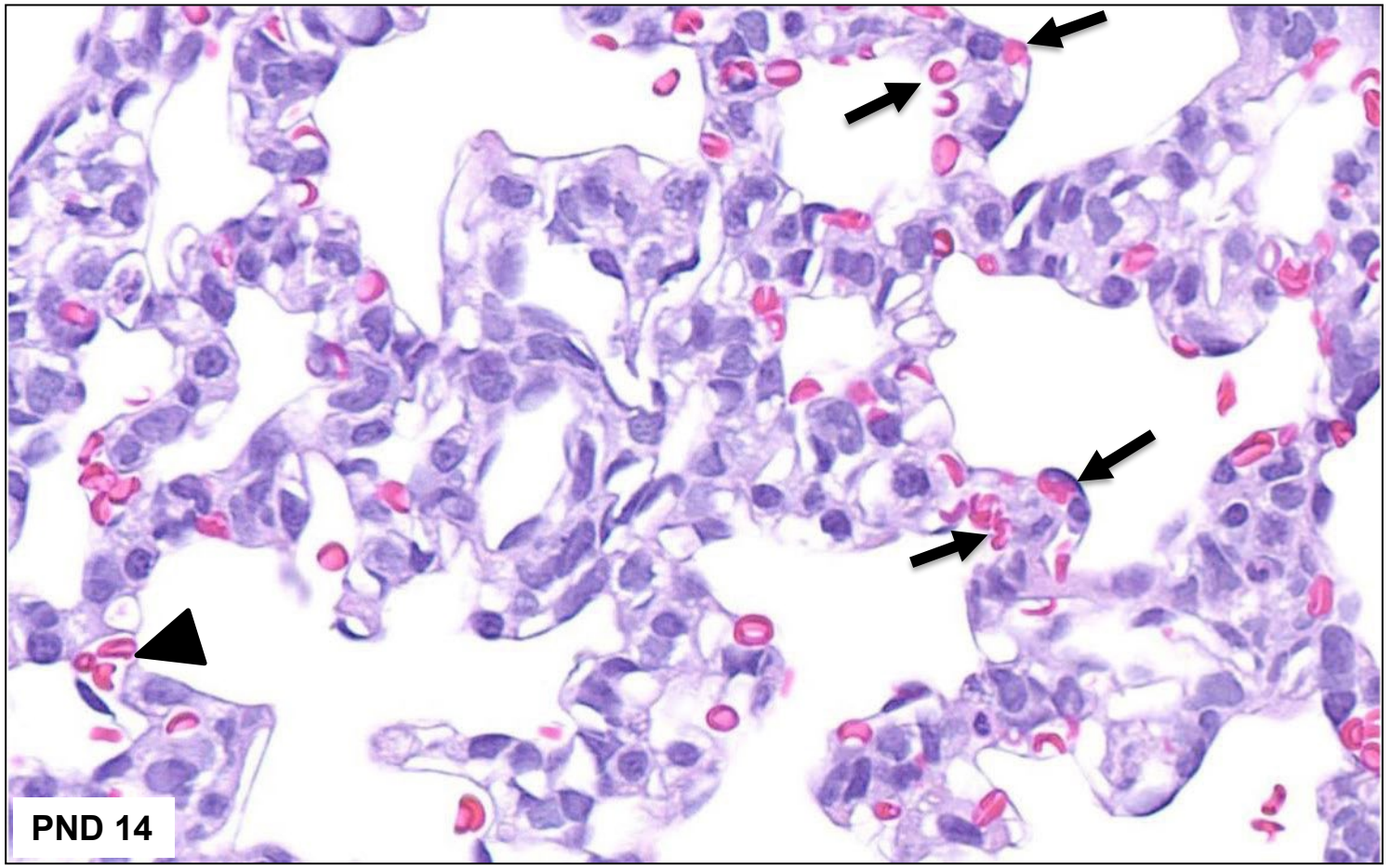

Lung, rat, PND 21

- By PND 21, the lung is histologically mature with thin capillary septae. A few alveolar macrophages (thick arrowhead) may be present in the lung.
- Thin secondary septae (arrows) are characteristic features of alveolar stage lung tissue. These secondary septae are more blunted during bulk alveolarization. H&E stain, 20x.

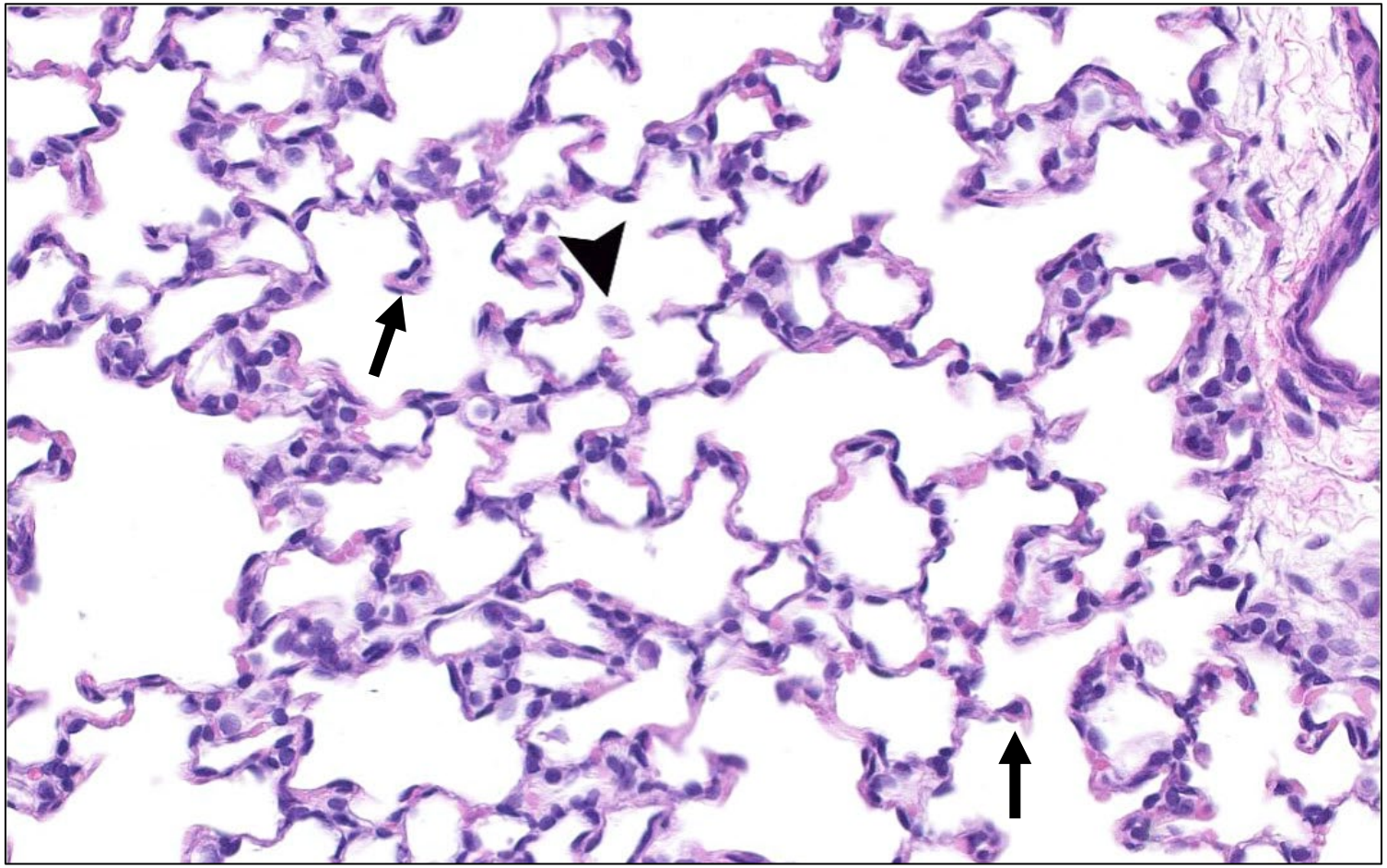

Cardiovascular system (Heart)

- The myocardium undergoes rapid growth as the fetus transitions from fetal to postnatal circulation after birth. This growth is especially prominent in the left ventricle.

- The atria and ventricles are dilated at birth, and right and left ventricular walls are of equal thickness. Within the first postnatal week, the left ventricular free wall becomes three times as thick as that of the right ventricular wall.

- The cardiomyocyte has three microscopic stages of postnatal growth:
  - Stage 1 – PND 1 to 6: proliferative phase. Cardiomyocyte nuclear division without cell division, resulting in multinucleated cardiomyocytes and the presence of mitotic figures.
  - Stage 2 – PND 7 to 14: transitional phase. There is both proliferation and hypertrophic change in the cardiomyocytes.
  - Stage 3 – PND 15 to about PND 30: hypertrophic phase. The individual cardiomyocytes continue to grow in size, but there is little to no proliferative activity.

Heart, rat, PND 1 and PND 7

- The rat heart at PND 1 has dilated left and right ventricles and the left (arrow) and right ventricular free walls and the septum have roughly equivalent dimensions.
- By PND 7, the left ventricular free wall (arrow) is thicker and can be up to three times the thickness of the right ventricular free wall.
- Subgross images of heart. H&E stain.

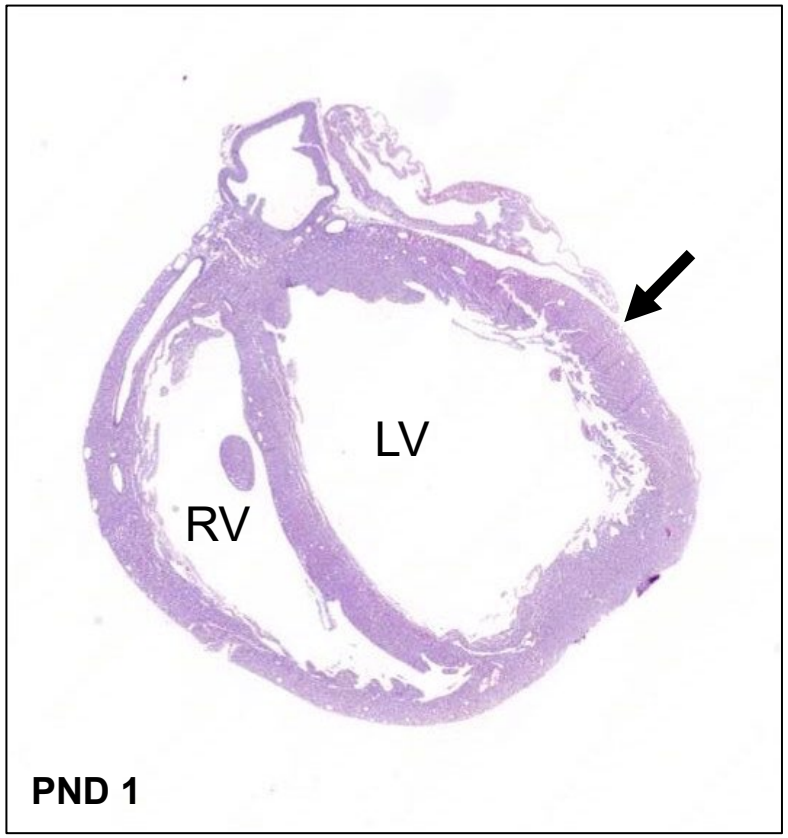

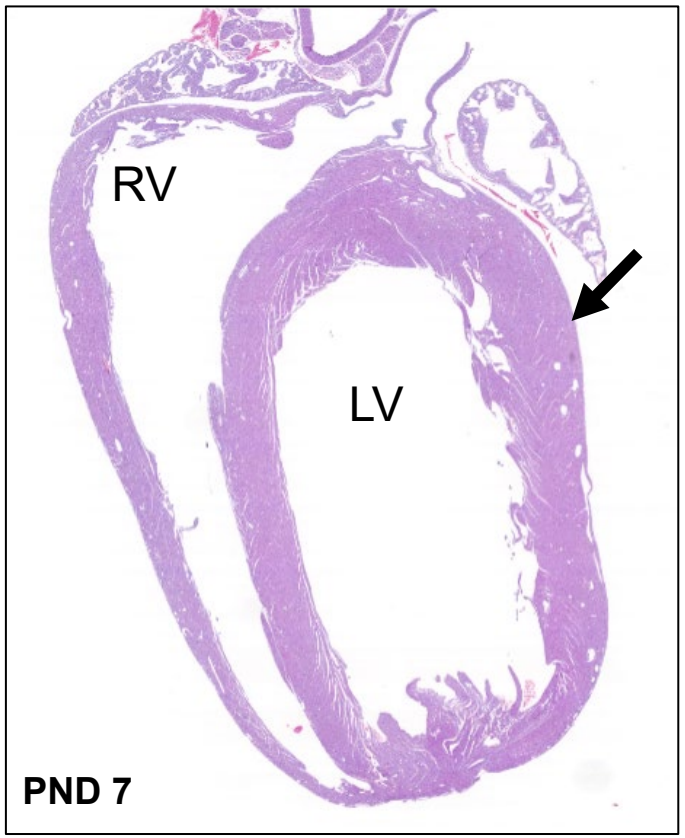

Heart, rat, PND 1 and PND 21

- At PND 1, the myocardium is in the proliferative phase of development. There is a dense population of myocyte nuclei with relatively sparse sarcoplasm, and the nuclei are densely packed. Note the mitotic figures (arrows). H&E stain, 40x.
- At PND 21, the myocardium is morphologically adult-like. Note the lower density of nuclei due to the increased amount of sarcoplasm associated with the hypertrophic stage of development. H&E stain, 40x.

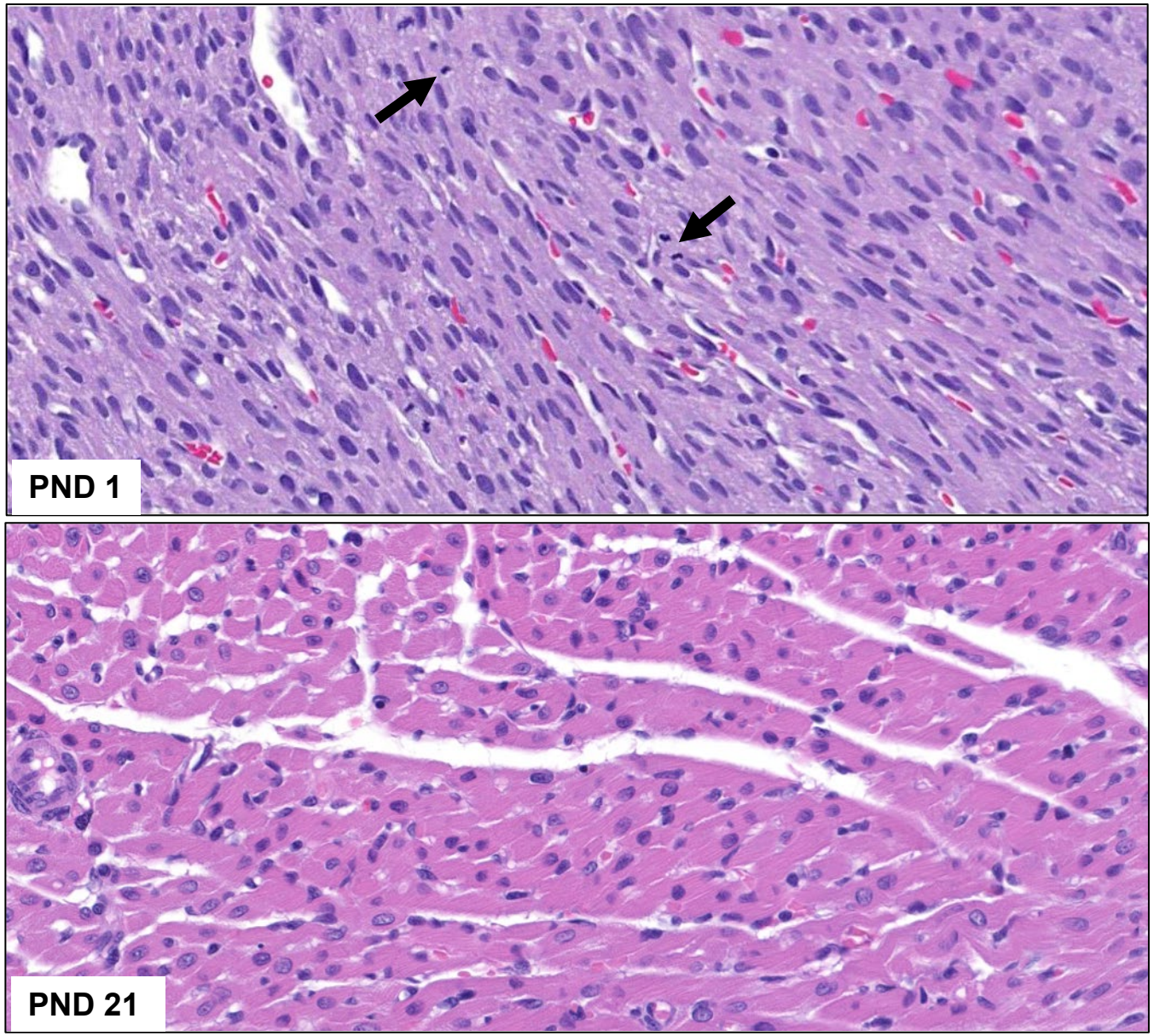

Urinary System (Kidney)

- At birth, the rat kidney is histologically similar to a fetal human kidney.
- Nephrons arise *de novo* (i.e., anew) from undifferentiated nephroblasts in the nephrogenic zone, and new nephrons are induced up through PND 4. Thereafter, the nephrons (and glomerular tufts) mature through four (4) stages of development, and the kidney is histologically mature by PND 28.
- Induction of new nephrons (i.e., nephrogenesis) is entirely a prenatal event in mice, nonhuman primates, and humans.
- Adult nephron morphology is achieved by PND 28 (rats), PND 14 (dogs), and PND 21 (pigs).
- Acid-base equilibrium increases dramatically between birth and PND 17, and anion and cationic transporters are mature by PND 28.
- In general, functional maturity lags behind morphologic maturity of the nephron, as the glomerular filtration rate (GFR) is stable at PND 42.

Kidney, rat, PND 1

- In this kidney at PND 1, the basophilic “nephrogenic zone” (*) containing newly formed glomeruli is prominent and located in the superficial aspect of the renal cortex. This zone gives rise to new nephrons through PND 4. These nephrons will continue to mature to stage IV nephrons by PND 14. H&E stain.

- During pre- and postnatal formation of new nephrons, the pattern of growth is centrifugal. This means that new nephrons are induced in tissue more superficial to the older nephrons, and the cortex expands outward. The more developed nephrons are located deeper in the cortex, and the most immature nephrons reside in the most superficial (subcapsular) location.

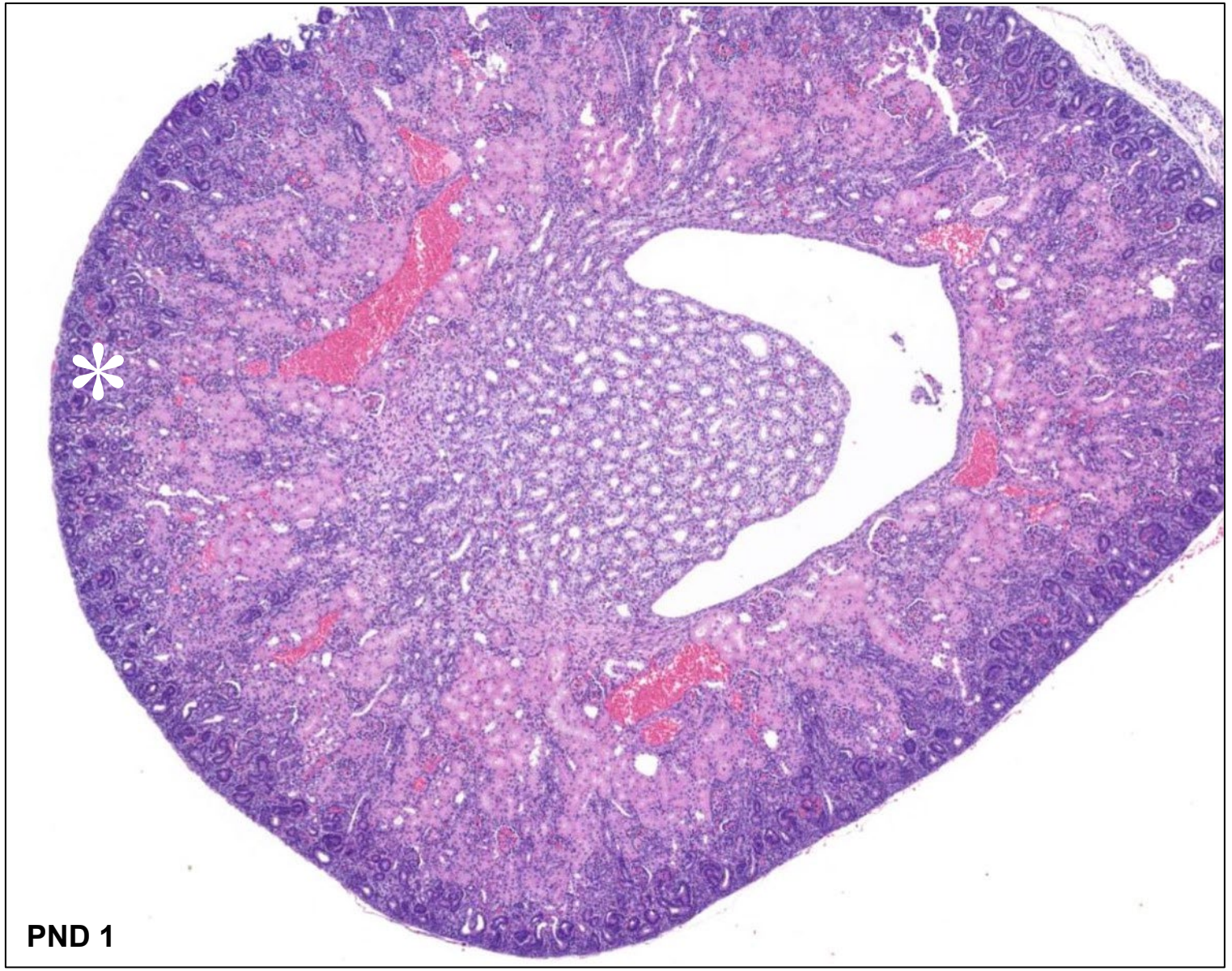

PND 1

Kidney, rat, PND 1

There are 4 stages of nephron development that can be distinguished based on the appearance of the glomerular tuft. These 4 stages are present in a rat kidney at birth:

- Stage 1 – Ellipsoid shape (in subcapsular nephrogenic zone). The developing glomerulus forms an oval or ellipsoid shape.
- Stage 2 – Comma- or S-shaped (subcapsular nephrogenic zone). The developing glomerulus folds in on itself forming convoluted or bent contours.
- Stage 3 – The developing glomerulus is recognizable now as a glomerulus, and these stage 3 structures reside just deep to the nephrogenic zone. The tufts commonly have a layer of plump cuboidal podocytes on surface of tuft.
- Stage 4 – Stage 4 is a mature glomerulus and resides deep in the cortex beneath the nephrogenic zone. Stage 4 glomerular tufts have open capillary loops and no longer have the continuous layer of plump podocytes on their surface.
- Note how the more immature nephrons are close to capsular surface, and the more mature nephrons are deeper in cortex. H&E stain.

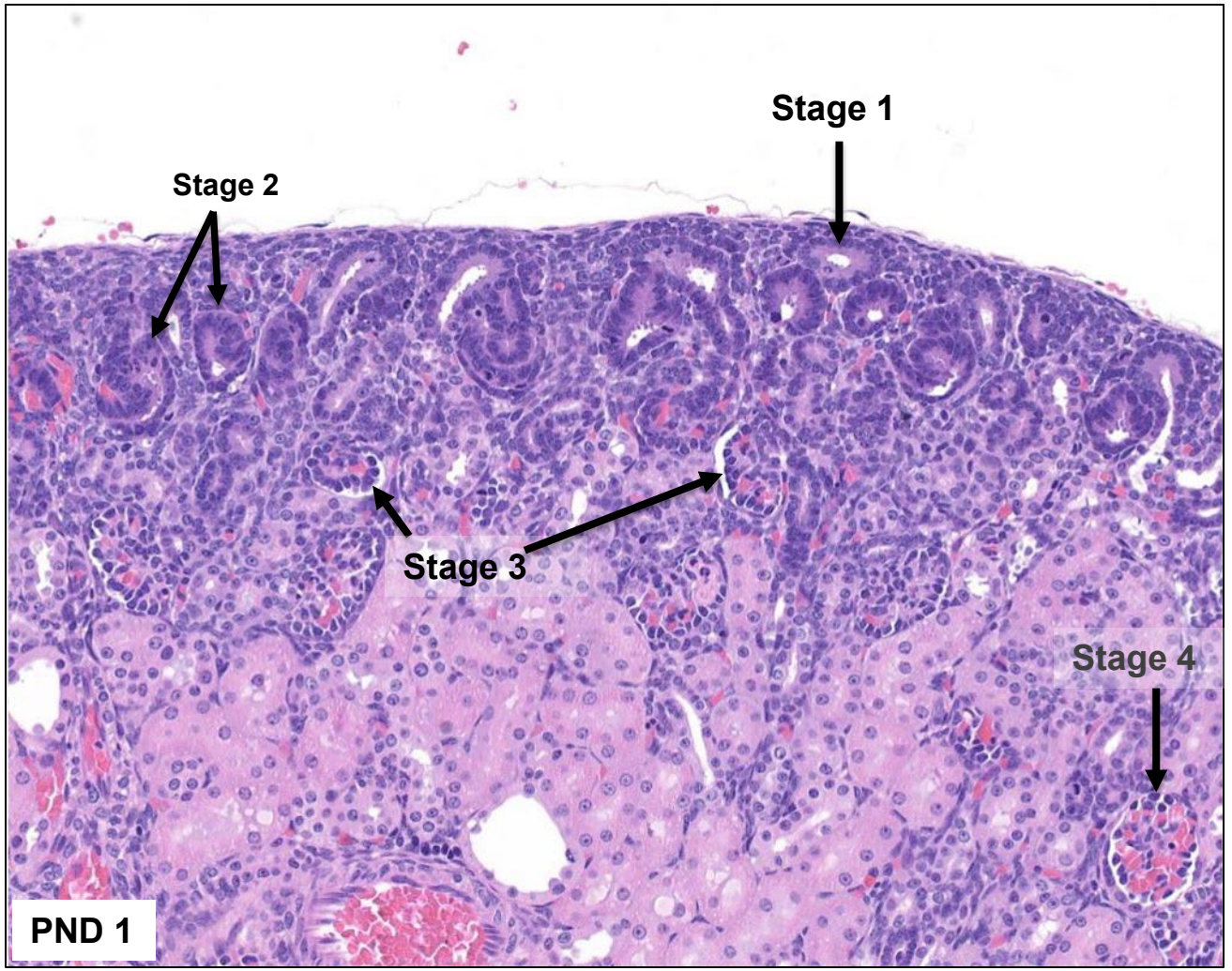

Juvenile kidney toxicology

- The juvenile kidney may have increased or decreased susceptibility to nephrotoxicants when compared to the adult kidney. Whether there is increased or decreased toxicity depends on the test article and how that test article or metabolic byproduct is handled by the kidney.

- Cytochrome P-450 (CYP) enzymes mature at different ages and the kidney tissue can be exposed to different amounts of either the original test article, or its metabolic breakdown products, than the adult kidney.

- The juvenile kidney has less concentrating ability and reduced perfusion, when compared to the adult kidney, and, thus, the juvenile kidney may be exposed to less test article (e.g., Gentamicin and Cisplatin) than the adult kidney when given the same exposure.

- The maturation of the organic anion transporters and the cationic organic transporters occurs between PND 8 to 15. These transporters affect excretion of test articles and/or their metabolic byproducts. The immature development of these transporters in juvenile rat kidneys may either increase or decrease the susceptibility of the kidney to various test article toxicity, when compared to that of the adult kidney.

- Certain test articles affect the kidney during certain windows of opportunity, and determining this window may require multiple studies with different exposure time frames. Some examples of these windows of opportunity include:
  - Acetylcholinesterase (ACE) inhibitors causing tubule dysgenesis and acute tubular necrosis when given to rats between PND 1 to PND 14.
  - Dabrenafib (a BRAF kinase inhibitor) causing crystal deposits and obstructive nephropathy (cortical cysts and tubular dilation when given to rats between PND 7 to 13). (BRAF = v-raf murine sarcoma viral oncogene homolog B1; v-raf = rapidly accelerated fibrosarcoma oncogene)
  - Pazopanib 9a (vascular endothelial growth factor receptor [VEGF-R] inhibitor) causing glomerulopathy when given to rats between PND 9 to 21.

Kidney, rat, PND 60, toxic mineralization

- Until PND 17, the juvenile rat kidney has deficient acid-base homeostasis. Acid-base homeostasis is important in calcium:phosphate (Ca:PO4) regulation. Juvenile kidneys are prone to developing crystals or mineralization (DTT nomenclature is mineral) within tubules.
- When rats are exposed to test articles that disrupt acid-base and/or Ca:PO4 homeostasis during the second postnatal week or are fed a diet with a low Ca:PO4 ratio, the kidneys readily develop mineralized deposits at the corticomedullary junction.
- In the images on the right, the rat was exposed indirectly through a soy-deficient diet having a low Ca:PO4 ratio, albeit high Ca and PO4 levels. Exposure was indirectly through the placenta and milk of the dam and then directly to the juvenile following weaning. The top image (stained with alizarin red for calcium) and the bottom image (higher magnification, stained with H&E) show abnormal mineralization of tubules (arrows) at the corticomedullary junction. This mineralization was caused by exposing the suckling and post-weaned juvenile rats to a soy-deficient diet.
- Dabrenafib (BRAF kinase inhibitor) is a test article that also causes mineralized or crystalline deposits in the tubules leading to obstructive nephropathy when given directly to rats between PND 9 to13. The pathogenesis was an obstructive nephropathy, but the underlying cause was an acid-base imbalance that led to crystal formation and tubule obstruction.

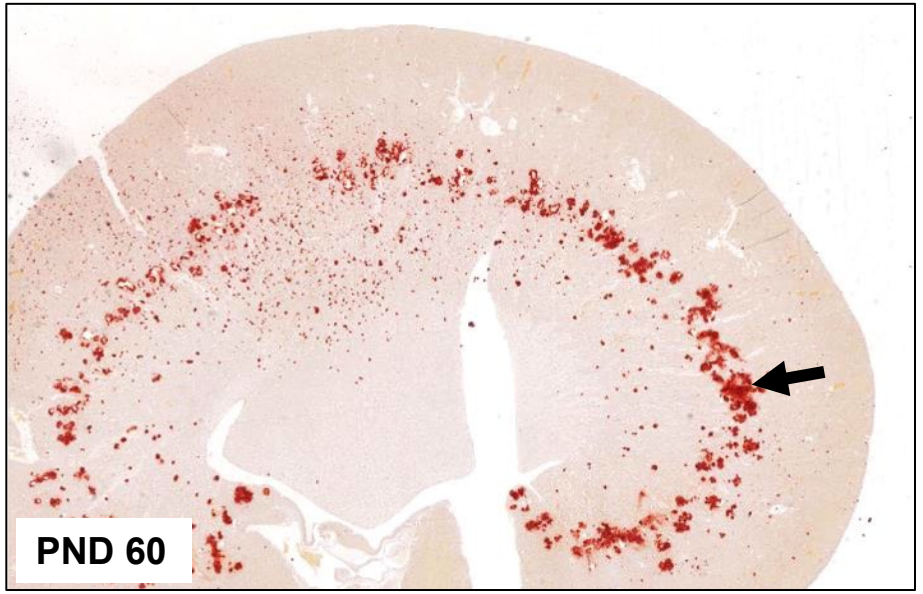

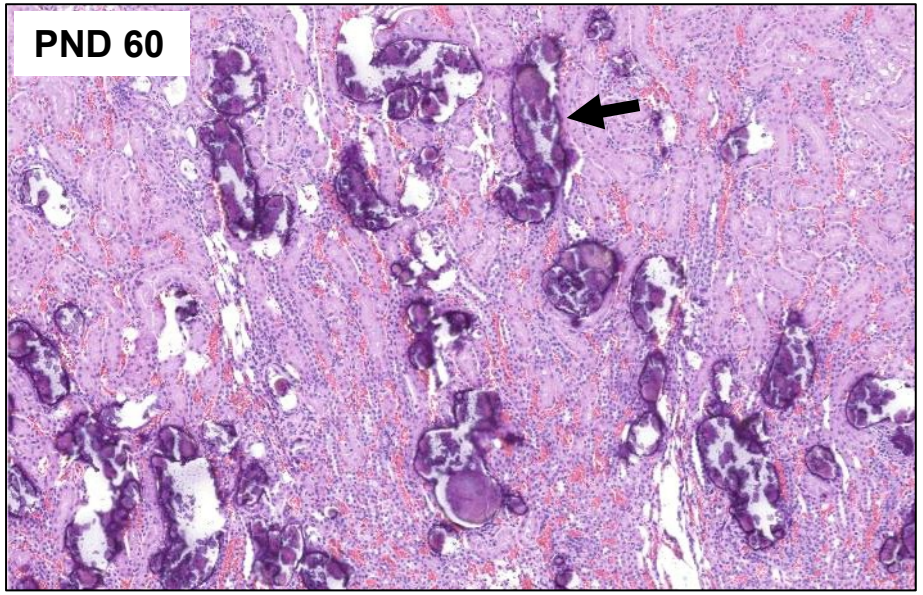

Kidney, rat, PND 28, basophilic tubules and PND 18, tubular dilatation

- a) There is an increase in basophilic tubules (*) in a PND 28 rat, which was a test article-related effect in this juvenile animal study. Basophilic tubules can also be a background finding. Compare to normal tubules (**). H&E stain.
- Other background findings in the kidneys of juvenile rats include pelvic dilatation, tubular cysts, and tubule dilatation.
- b) There is a cluster of dilatated tubules/cysts (arrow) in the cortex of a control female rat at PND 18. H&E stain.

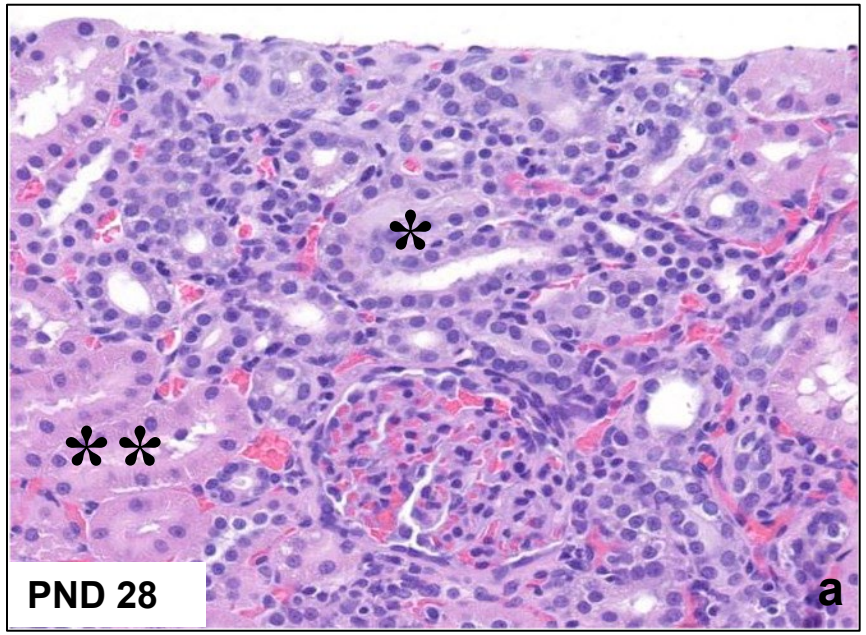

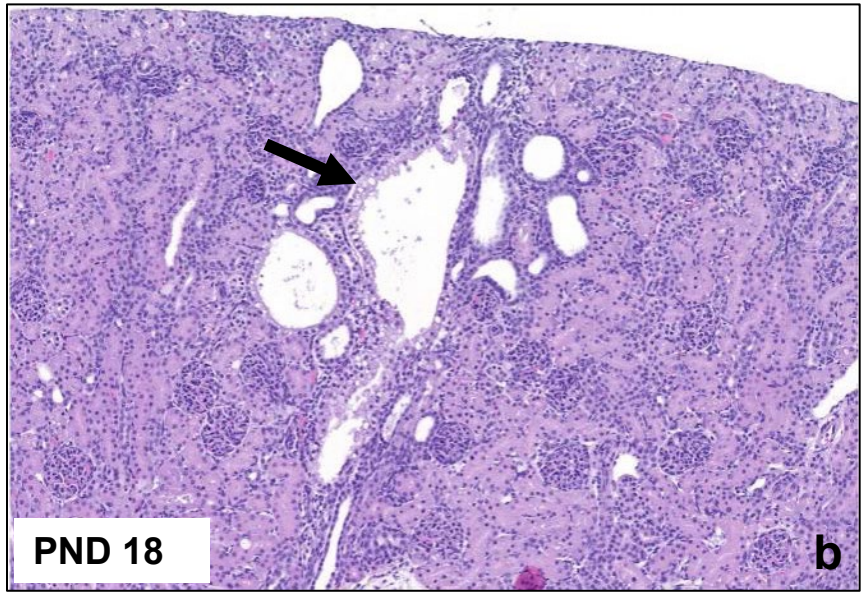

Kidney, rat, PND 28, hydronephrosis and pyelonephritis

- Gamma aminobutyric acid (GABA) is a neurotransmitter mediating sensory fibers from the ureters. A test article that modulates GABA has been associated with hydroureter and hydronephrosis (DTT nomenclature is pelvis dilation) in perinatal studies in rats (Petrere, 1994).
- This images on the right are of a rat kidney at PND 28 treated by oral gavage from PND 4 through PND 28 with a test article that modulates GABA. At PND 28 necropsy, there was test article-related bilateral renal pelvic dilatation (*) and inflammation (arrows). Markedly dilated renal pelvis, termed hydronephrosis, is shown in panel (a). Secondary inflammation of the kidney, termed pyelonephritis (DTT nomenclature is inflammation), is shown in panel (b). H&E stain.
- Renal pelvic dilatation at minimal to mild severities can be seen as a background finding in control rats during the juvenile age.

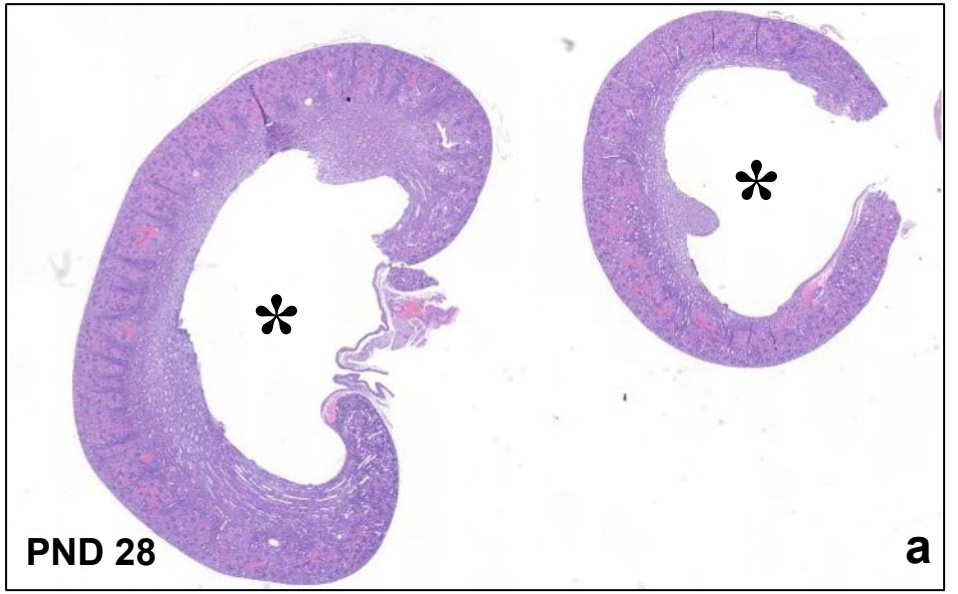

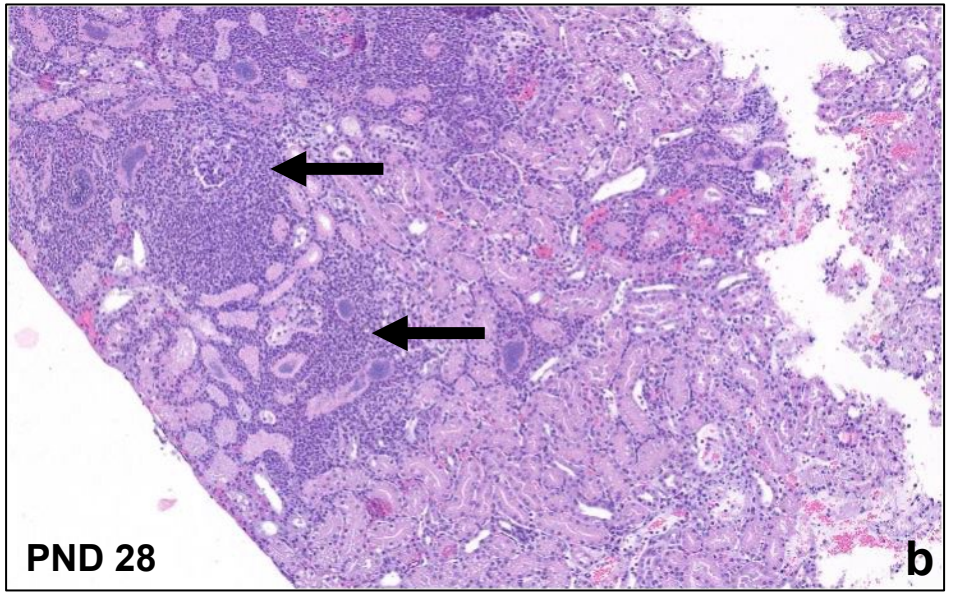

Gastrointestinal (GI) system

- The GI system includes all tissues from the tongue to the anorectal junction.
- The anterior sections of the GI tract (tongue, esophagus, and non-glandular stomach) mature by PND 21, which is earlier than the more posterior sections of the GI tract (glandular stomach through the rectum), which mature microscopically at PND 28.
- The high functional capability of the anterior segments is advantageous since the rat must be able to suckle milk as soon as it is born. Lipase, the earliest digestive enzyme, is produced by the tongue's serous glands at birth to help enable the breakdown of milk.
  - In contrast to the anterior segments, the posterior segments have little to no digestive enzyme capability.
- There are some structures that exist in the digestive tract of young animals during the first 2 weeks of age: transient villi in the glandular stomach and colon to increase absorptive surface area, highly vacuolated small intestinal cells due to lipid and protein absorption, and a hyperplastic deeply basophilic appearance to the mucosa that occurs during the dynamic event of weaning.
- The major GI maturation factors glucocorticoid (GC) and/or thyroxine (TH) surge in second to third postnatal weeks. These hormones result in:
  - Upregulation of gastrin receptors on gastric parietal cells causes increased hydrochloric acid production
  - Conversion of small intestine brush border enzymes from lactase to sucrase/maltase. This conversion is necessary since rat pups start to eat carbohydrate-rich solid food at approximately PND 16
  - An increase in the proliferative activity of the crypt to form a deeply basophilic, mitotically active mucosa that can appear "hyperplastic" by PND 21
- Maturation is genetically programmed and does not depend on diet or weaning. Stress and thyroid hormone levels can influence this maturation process. Excess glucocorticoid that may result from stress if the pup is orphaned or not nurtured will result in precocious maturation of the gastrointestinal tract. This precocious maturation is a natural survival mechanism.

Stomach and colon, rat, PND 1

- There are 3 stages of stomach development:
  - 1. Bland phase – PND 0 to 14, pH = 6.0. Proteins are absorbed rather than denatured by acid.
  - 2. Transitional phase – PND 14 to 20. Glucocorticoid surge at week 2 causes ↑ gastrin production and gastrin receptors, leading to ↑ acid production. pH goes down to 4.0.
  - 3. Acidic phase – PND 21+. Pepsinogen production increases. Final adult pH of 2.0 not achieved until PND 42.
- Gastric pH may influence xenobiotic ionization and absorption, with possible effects on PK data.
- The left image represents a rat nonglandular and glandular stomach at PND 1. Note pseudovilli (arrow, left and right images) in glandular regions of the stomach and colon. In neonatal rats, the glandular stomach and colon have transient pseudovilli that increase absorptive area.

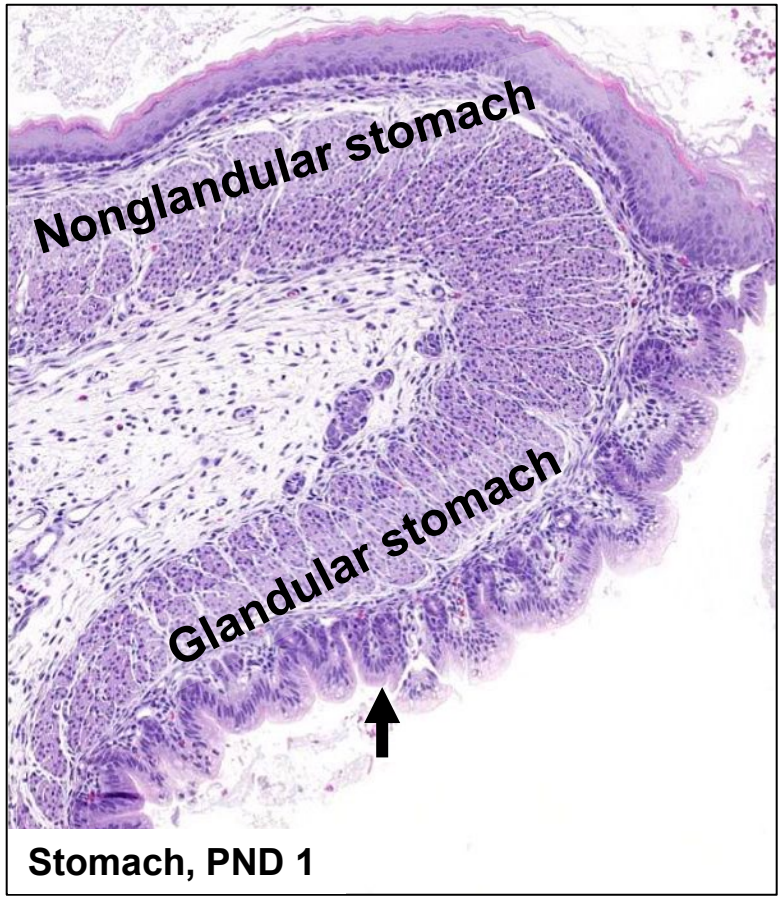

Stomach, PND 1

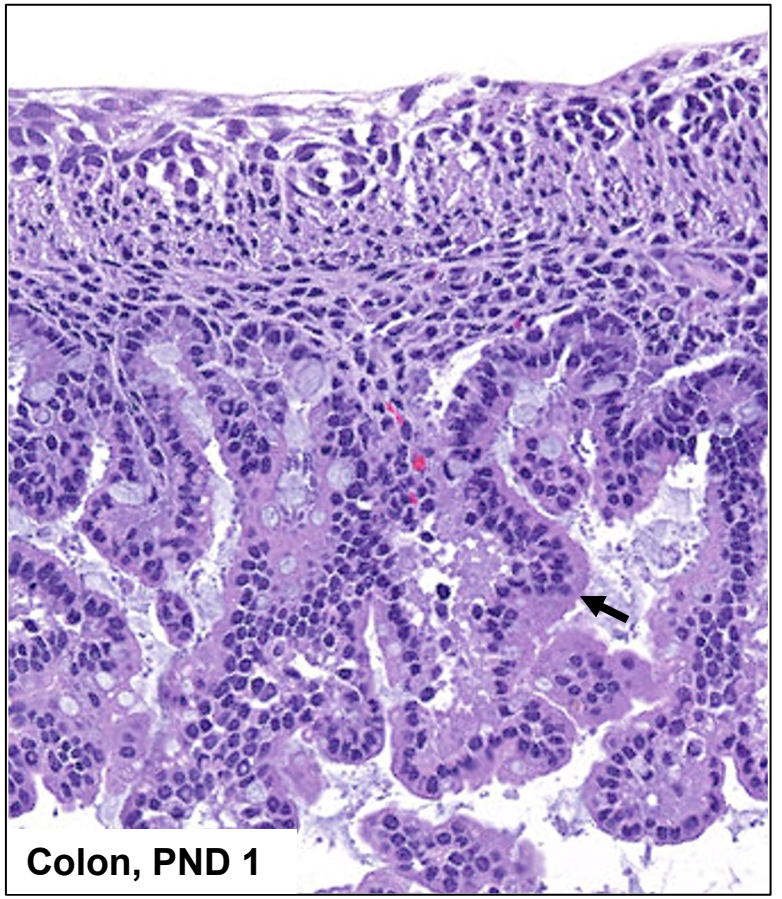
Colon, PND 1

Small intestine, rat, PND 7 (Swiss roll)

The Swiss roll technique is an excellent method for microscopic evaluation of the entire small intestine of rodents. In this Swiss roll preparation, the ileum is in the center of the roll and the duodenum is at the periphery. H&E stain.

For further reading, see Moolenbeek, C. and E. J. Ruitenberg (1981). "The "Swiss roll": A simple technique for histological studies of the rodent intestine." *Laboratory Animals*, *15*(1), 57–59. https://doi.org/10.1258/002367781780958577

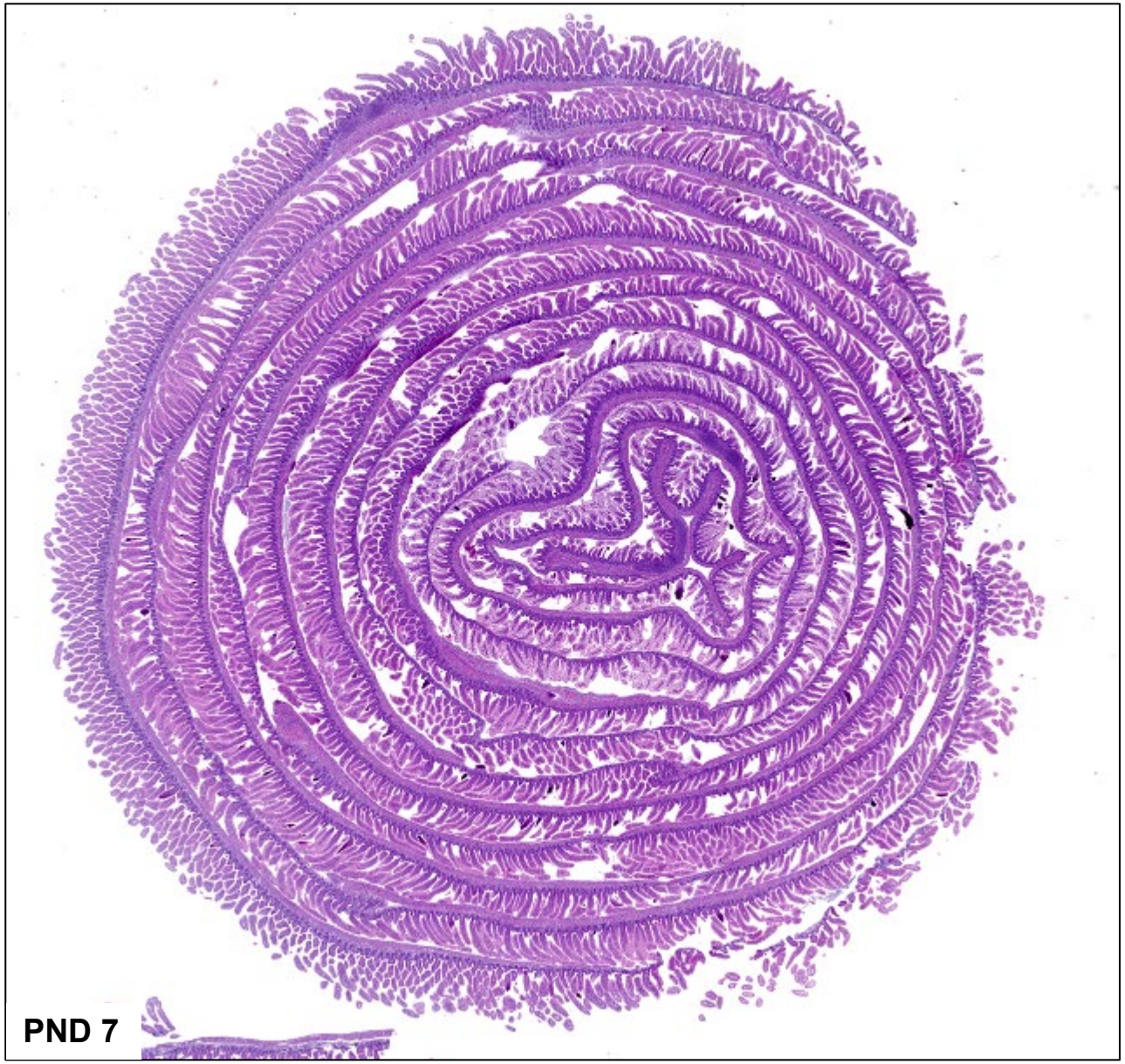

Small intestine, rat, PND 7

Right: In this Swiss roll preparation of entire small intestine of a PND 7 rat, contrast the non-vacuolated jejunum with the highly vacuolated ileum (right side of dashed line) associated with protein and lipid absorption. Due to the low level of gastrointestinal enzymes, lipid and protein at this early age are digested intracellularly after absorption. H&E stain.

Below: In this higher magnification image of the ileum at PND 7, the discrete intracytoplasmic eosinophilic droplets within vacuoles within villus epithelial cells are pronounced. H&E stain, 47x.

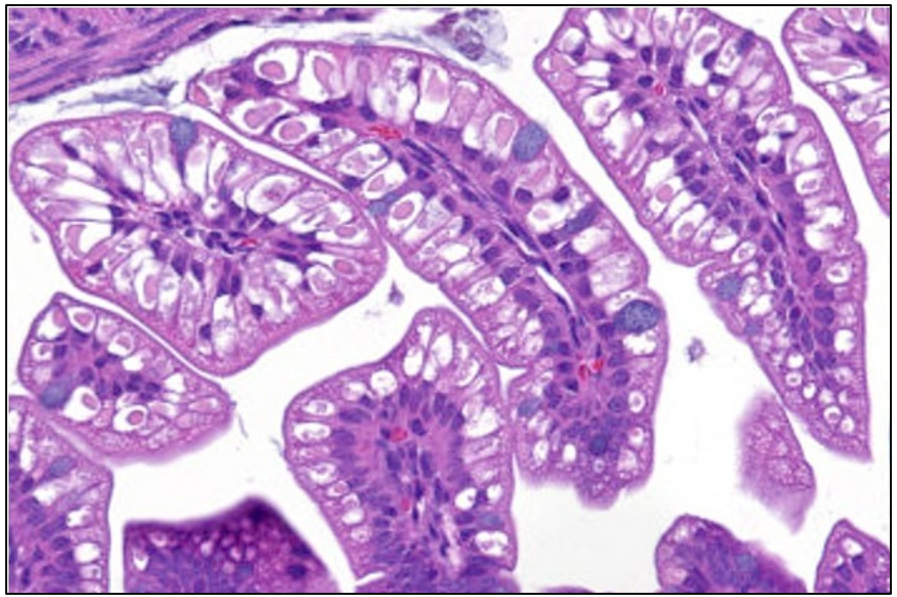

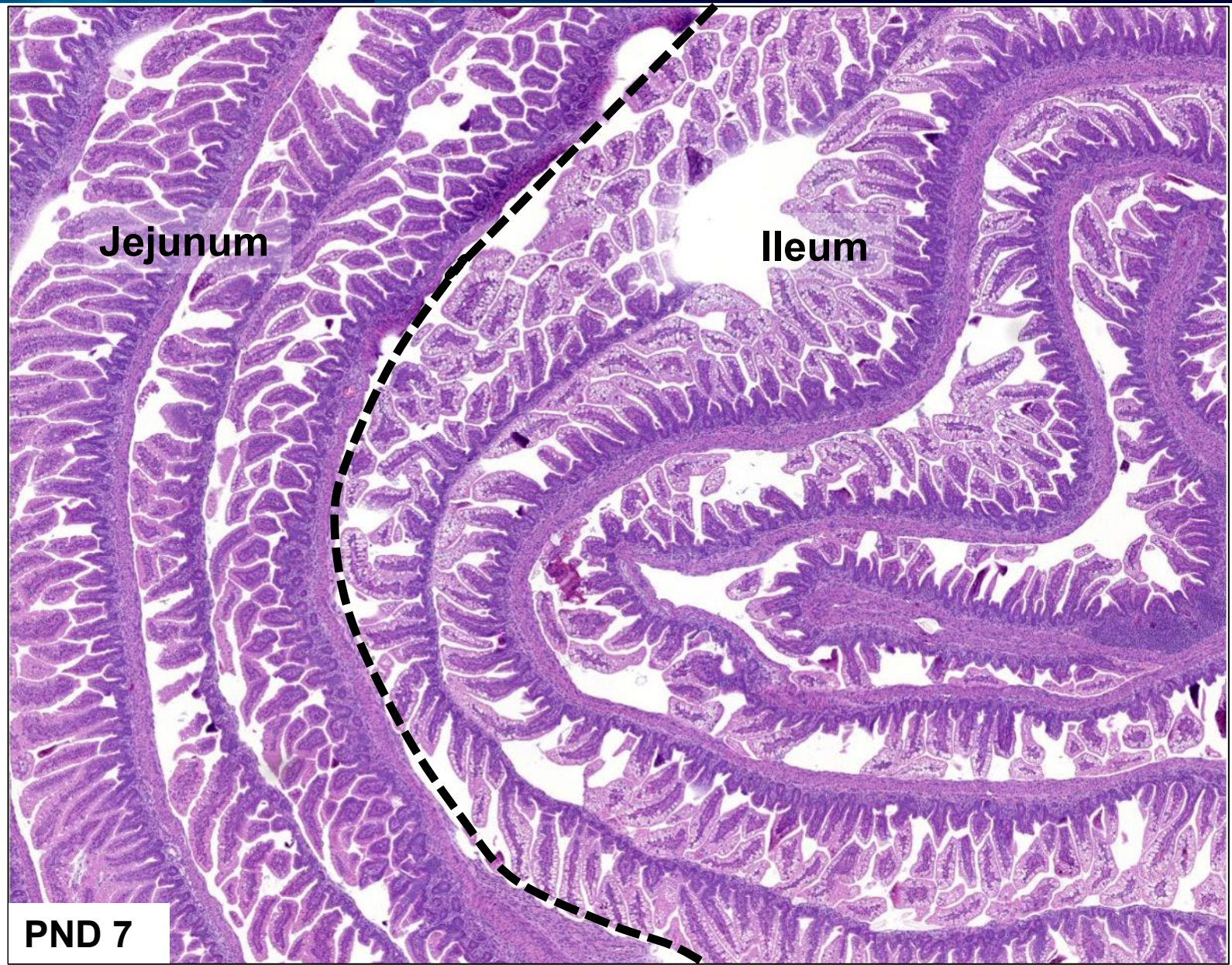

Small intestine, rat, PND 14 and PND 21

- Thyroxine and glucocorticoid influence the proliferation of the crypt epithelial cells.
- The images on the right show a rat ileum at PND 14 (a) and PND 21 (b).
- a) At PND 14, there is a relatively quiescent-appearing mucosa that has sparse mitotic figures (arrow) in basophilic crypt epithelial cells (C). Note the highly vacuolated epithelial cells in the villi (V) as they absorb protein and lipid (without initial enzymatic digestion) (arrowhead). H&E stain.
- b) At PND 21, the ileum is much more proliferative appearing and the crypt epithelium (C) has increased basophilic cytoplasm and a high mitotic rate (arrows). The increase in mitotic activity occurs throughout the gastrointestinal system in association with a surge in glucocorticoids and thyroxine that starts during the second postnatal week in rats. H&E stain.

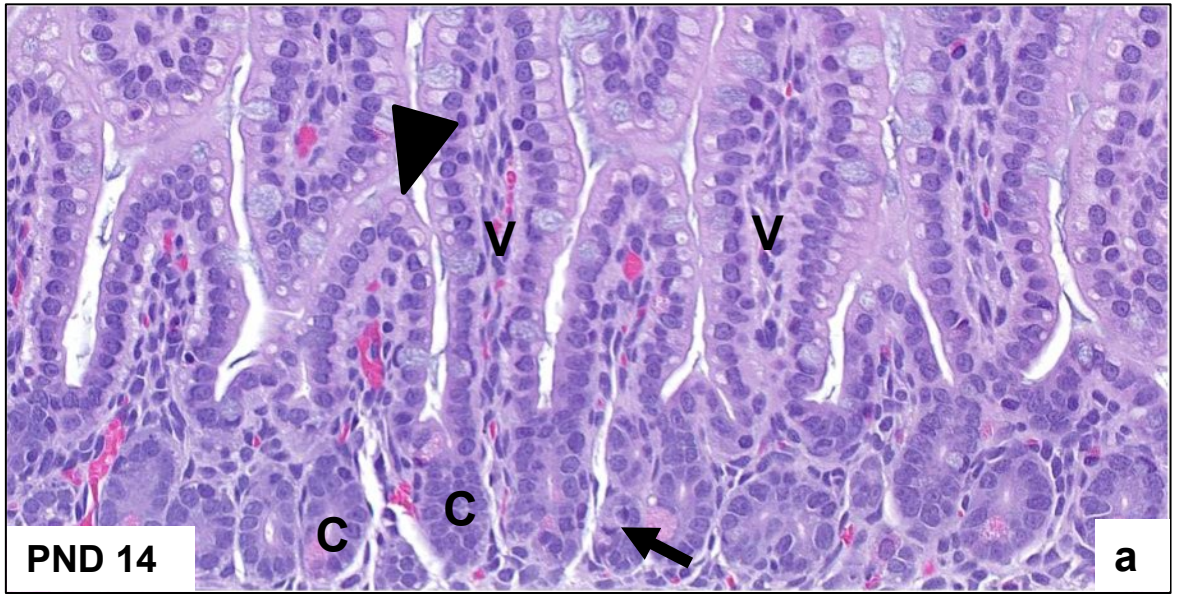

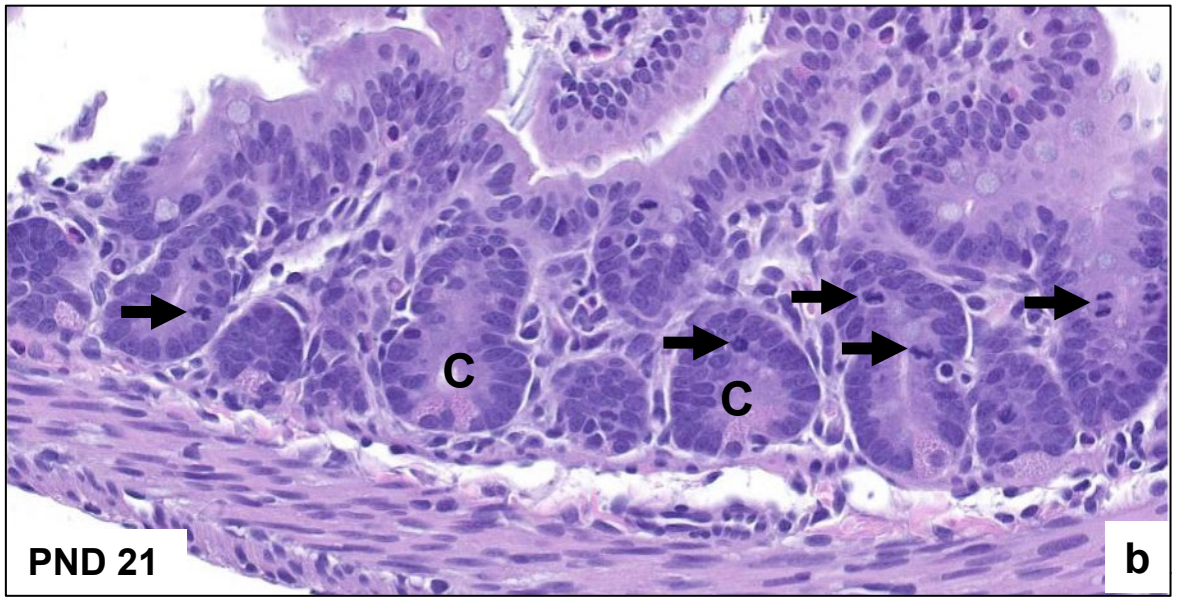

Pancreas, rat, PND 0 and PND 3

The sequence of postnatal development of the pancreas is as follows:

- At PND 0 (figure a), acinar cells (*) are engorged with zymogen granules, as seen by their densely eosinophilic cytoplasm. Note the well-developed pancreatic islets (arrows) with basophilic cytoplasm at PND 0 (a, inset) and PND 7 (b, inset).
- PND 3 (figure b) to 14: zymogen granules are rapidly depleted in response to suckling. Pancreas weight decreases nearly 50% in first 3 postnatal days. Note the decrease in the eosinophilic cytoplasm when the acinar cells (*) from PND 3 are compared to those of PND 0.
- After PND 14 (not shown), epithelial growth factor and insulin-like growth factor in maternal milk stimulate cellular expansion in the pancreas (as well as other gastrointestinal tissues and related glands).
- By PND 21 (not shown), the pancreas has a high mitotic rate, acinar cells are basophilic, and the eosinophilic zymogen granules are confined to the apex of acinar cells.

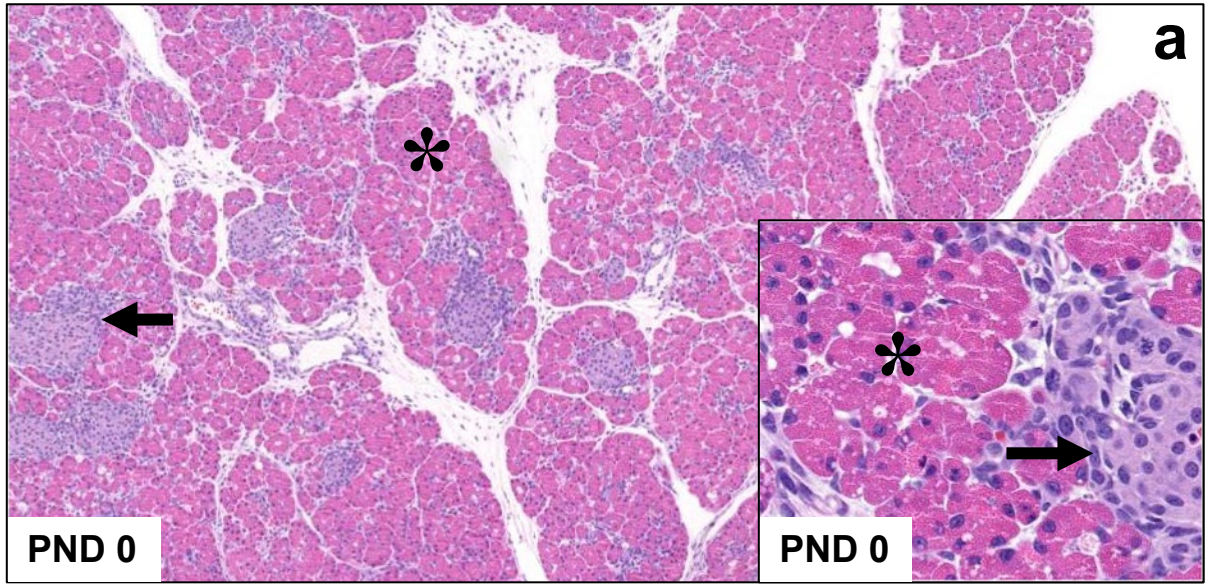

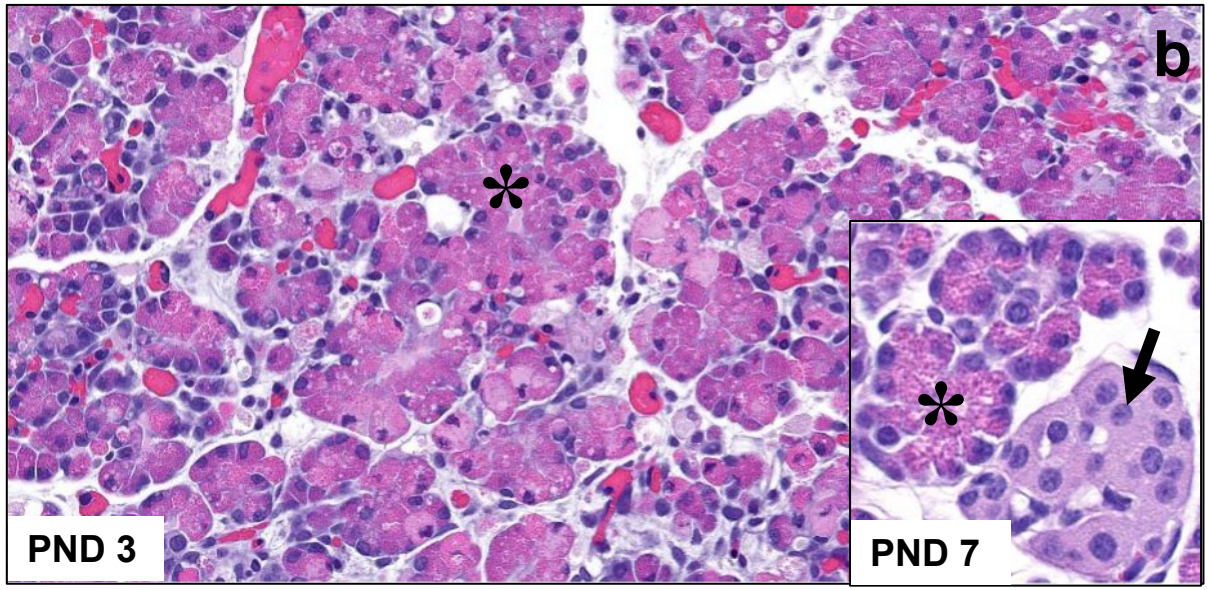

Liver, rat, PND 1

- At birth, hepatic cords are at least 3 cells thick, and the normal hepatic cords are difficult to detect. Glycogen is abundant in fetal liver but rapidly disappears after birth.
- Prominent extramedullary hematopoiesis (EMH – the production of blood cells outside of the bone marrow) is present in the liver at birth but is substantially diminished at PND 10. A small amount of EMH may be present up until 6-8 weeks of age.
- In this figure of the liver at PND 1, note the prominent EMH (dashed ovals), occasional megakaryocyte (arrow), and the abundant vacuolation (glycogen) of the individual hepatocytes. H&E stain.

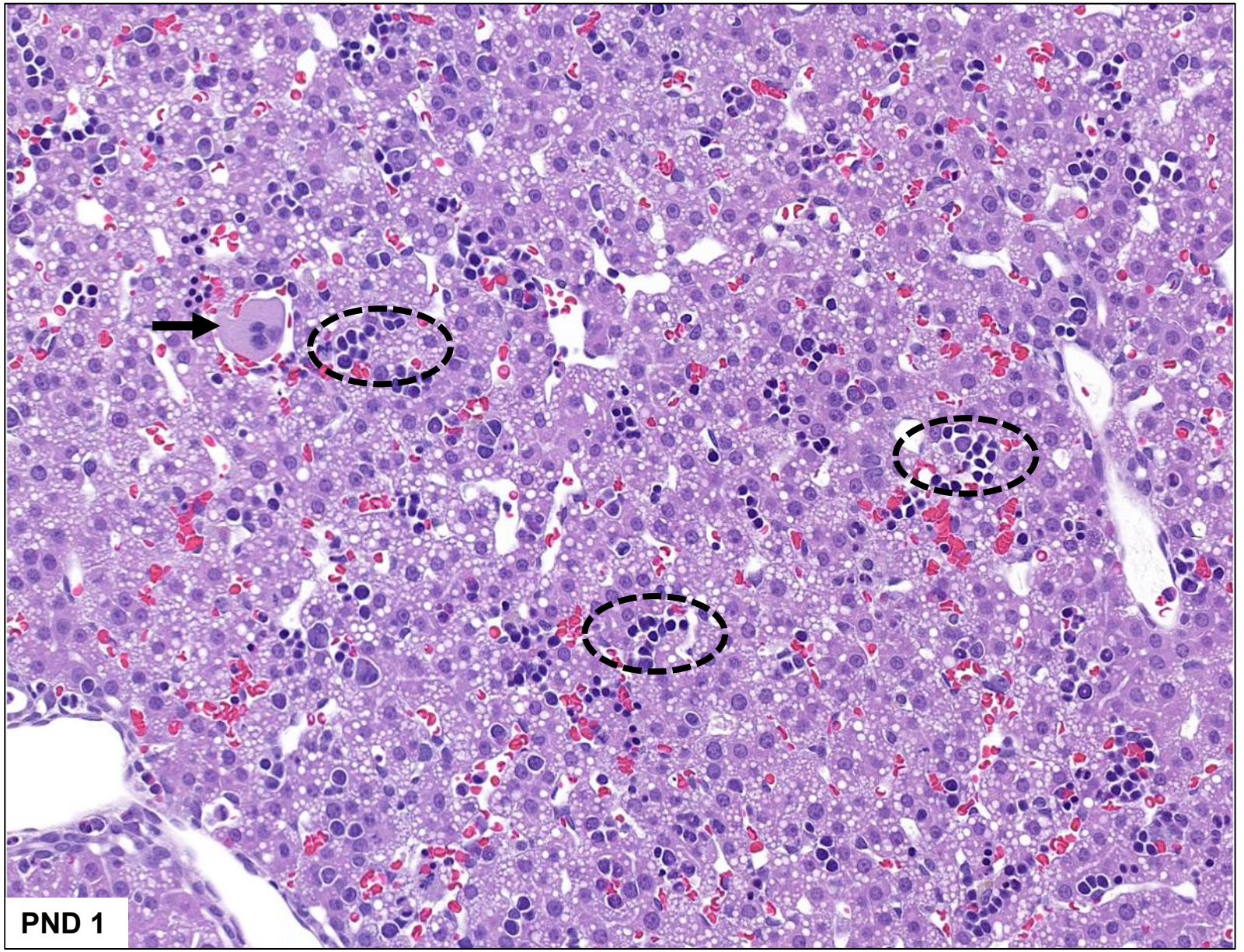

Liver, rat, PND 14

- At PND 14, there is a greatly reduced level of hepatic extramedullary hematopoiesis (EMH) (arrow), when compared to PND 1 on prior slide. H&E stain.
- A minor level of hepatic extramedullary hematopoiesis may persist in rats at 6 to 8 weeks of age, which is the typical age of rats at the onset of safety assessment toxicity studies.

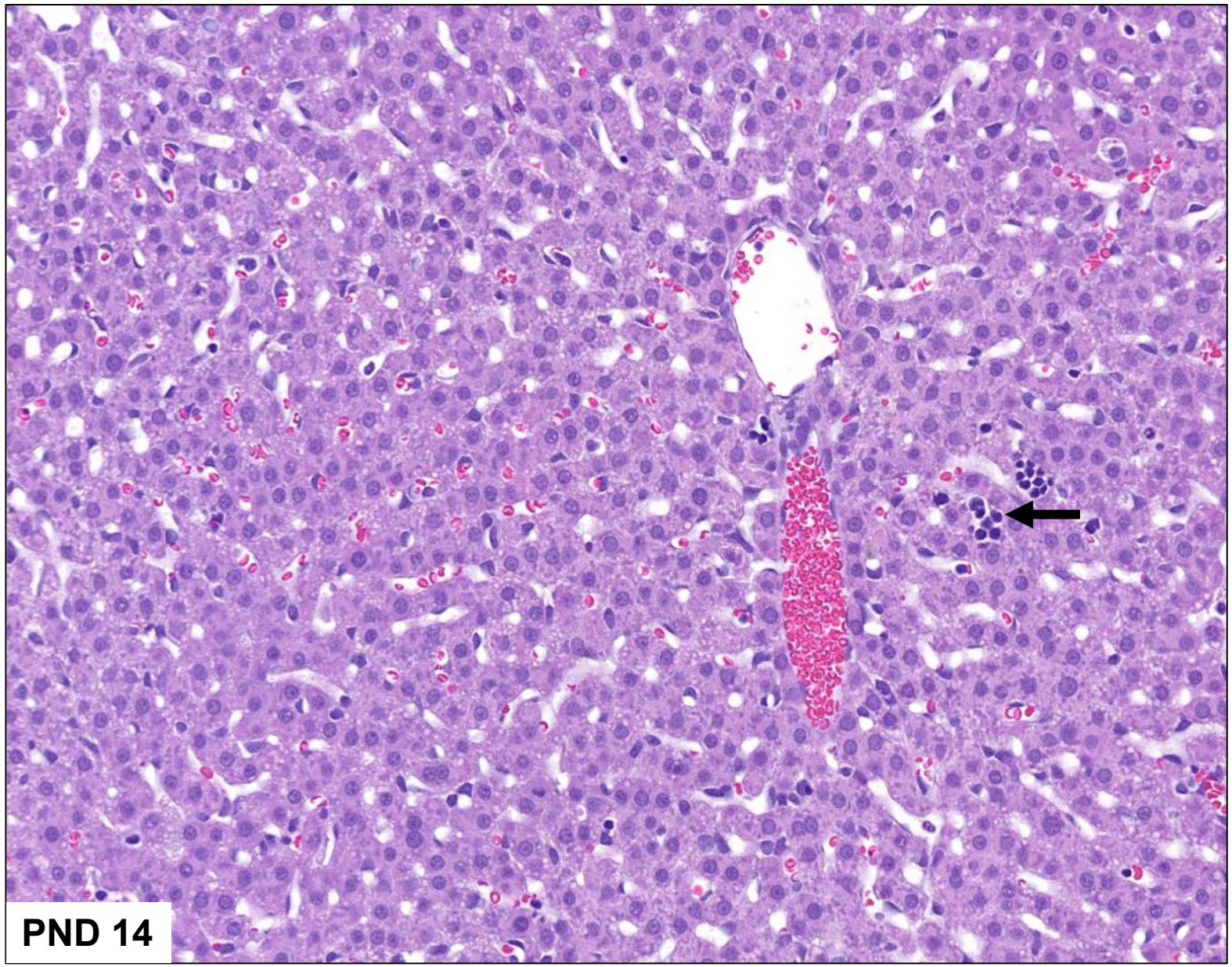

Liver, juvenile rats, PND 21 and 28

- a) The liver of a control group male rat at PND 21 has a moderate number of mitotic figures (arrows). At PND 21, the hepatic cords are one cell in thickness. H&E stain.

- b) The liver of a control group male rat at PND 28 has subcapsular necrosis (N) and inflammation (INF) of the liver. This finding may be secondary to handling of juvenile rats, which may result in physical injury to subcapsular hepatic tissue. H&E stain.

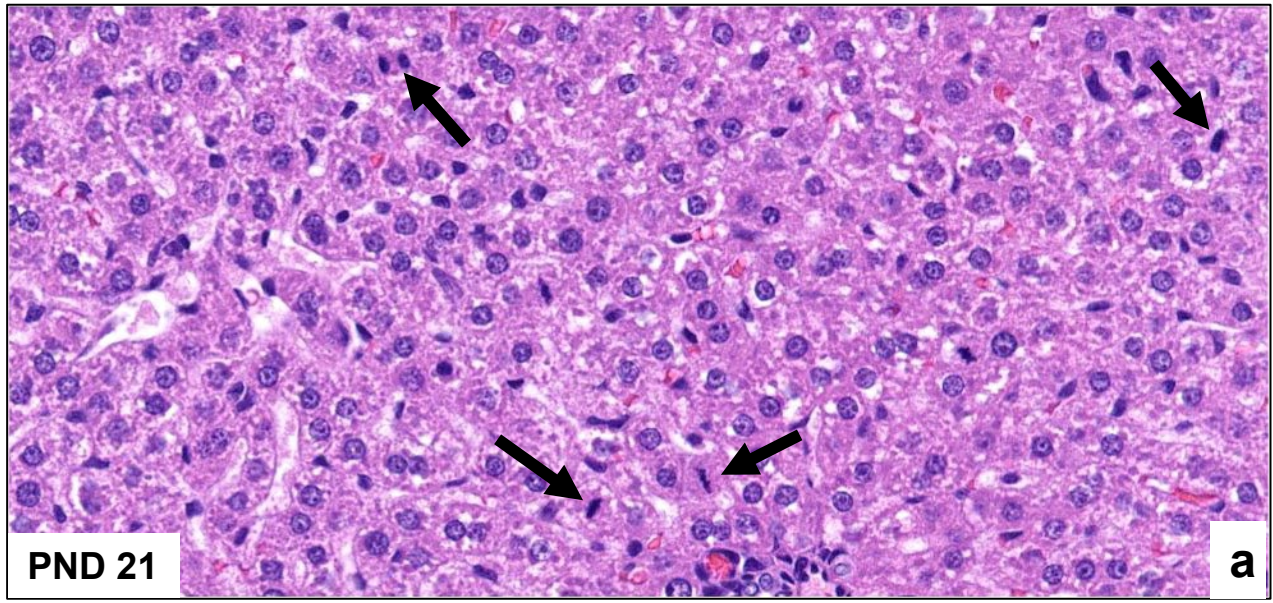

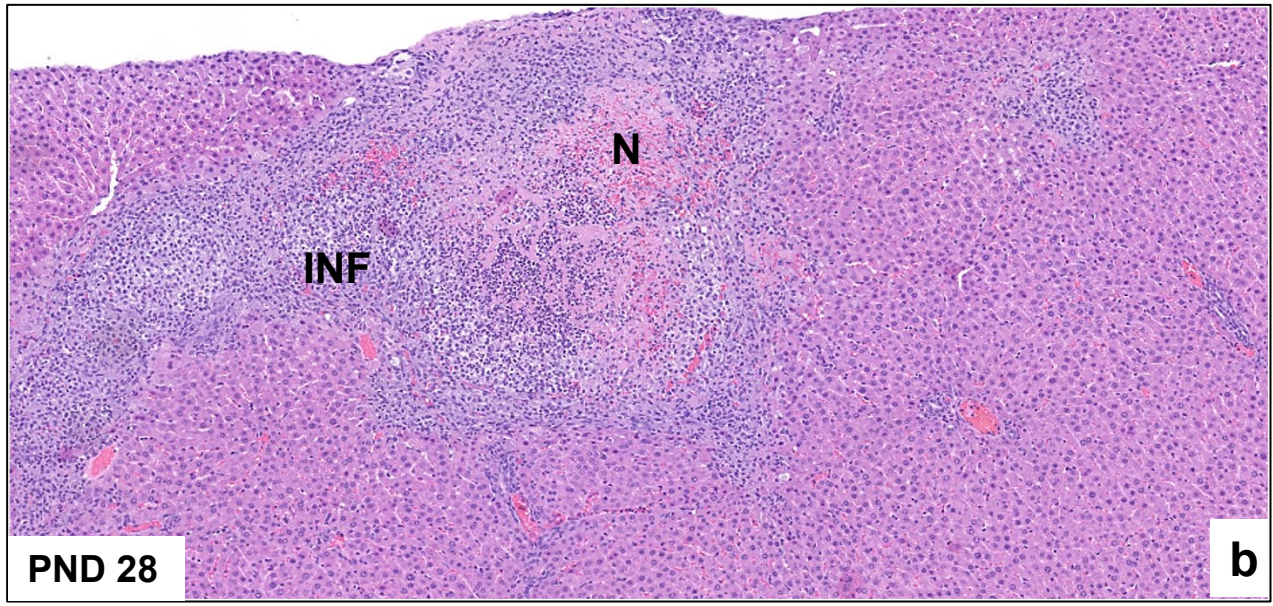

Salivary gland, rat, PND 0

- At birth, the rat has distinctive but under-developed submandibular (Sm), sublingual (Sl), and parotid (P) salivary glands. The mandibular lymph node (M) is clearly visible but poorly developed at this age. Note the dilated subcapsular lymphatic channels (arrow), indicating active fluid movement through the lymph node. H&E stain.
- The sublingual gland is the most developed gland at birth, and the parotid gland is the least developed gland at birth.

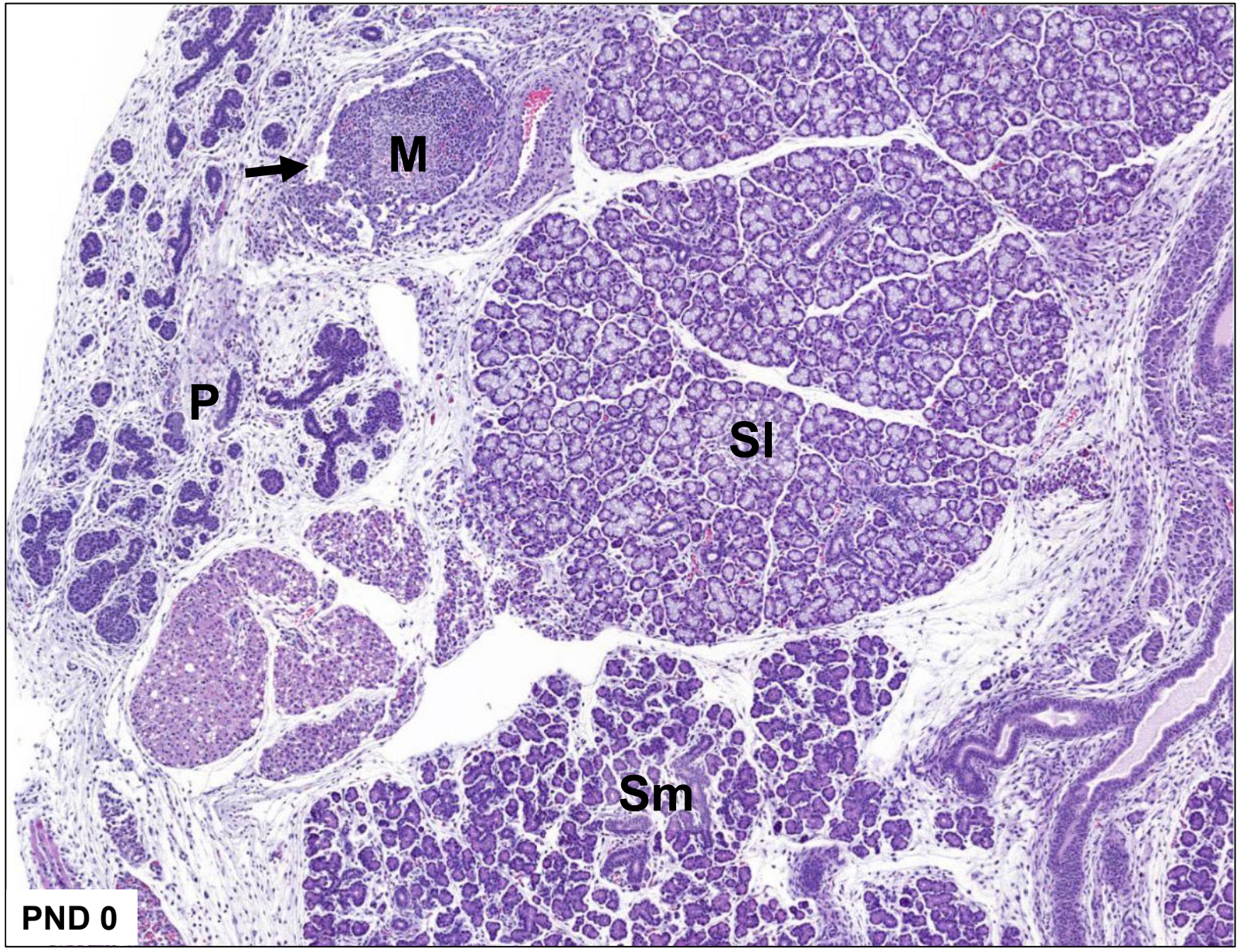

Female Reproductive Tract

Ovary:

- At birth, the ovary contains “fetal-appearing” tubular structures known as ovigerous nests, each containing an oogonia, which is the precursor of the oocyte, and lined by a single layer of undifferentiated granulosa cells.
- The ovigerous nests transform into primordial follicles, which are oocytes surrounded by a layer of flattened epithelial-like cells, during the first several postnatal days. Primordial follicles subsequently transform into primary follicles, which are surrounded by a single layer of cuboidal cells that represent undifferentiated granulosa cells.
- Follicle development is pituitary independent until PND 10. When the follicles start developing an antrum, they are controlled by pituitary gonadotropins.
- A wave of follicular atresia occurs at approximately PND 27.
- First ovulation in the rat occurs at approximately PND 36.

Vagina:

- Hormonal influence on the vagina (i.e., mucification) is visible as early as PND 25, before the first ovulation.

Ovary, rat, PND 1 and PND 6

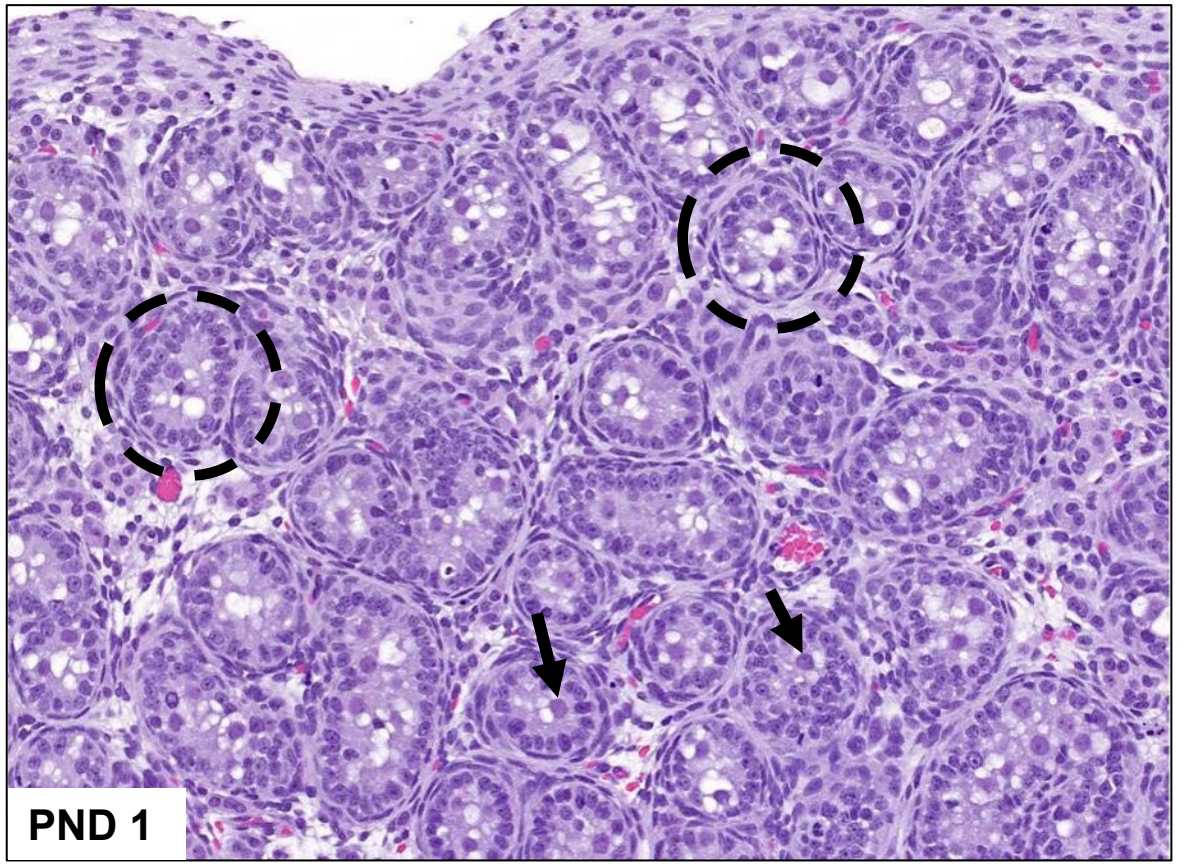

At PND 1, the ovary consists of ovigerous nests (dashed circles) containing oogonia (arrows), which are early diploid cells that have not undergone meiosis. These are bordered by a layer of undifferentiated cells that become nurturing granulosa cells. H&E stain.

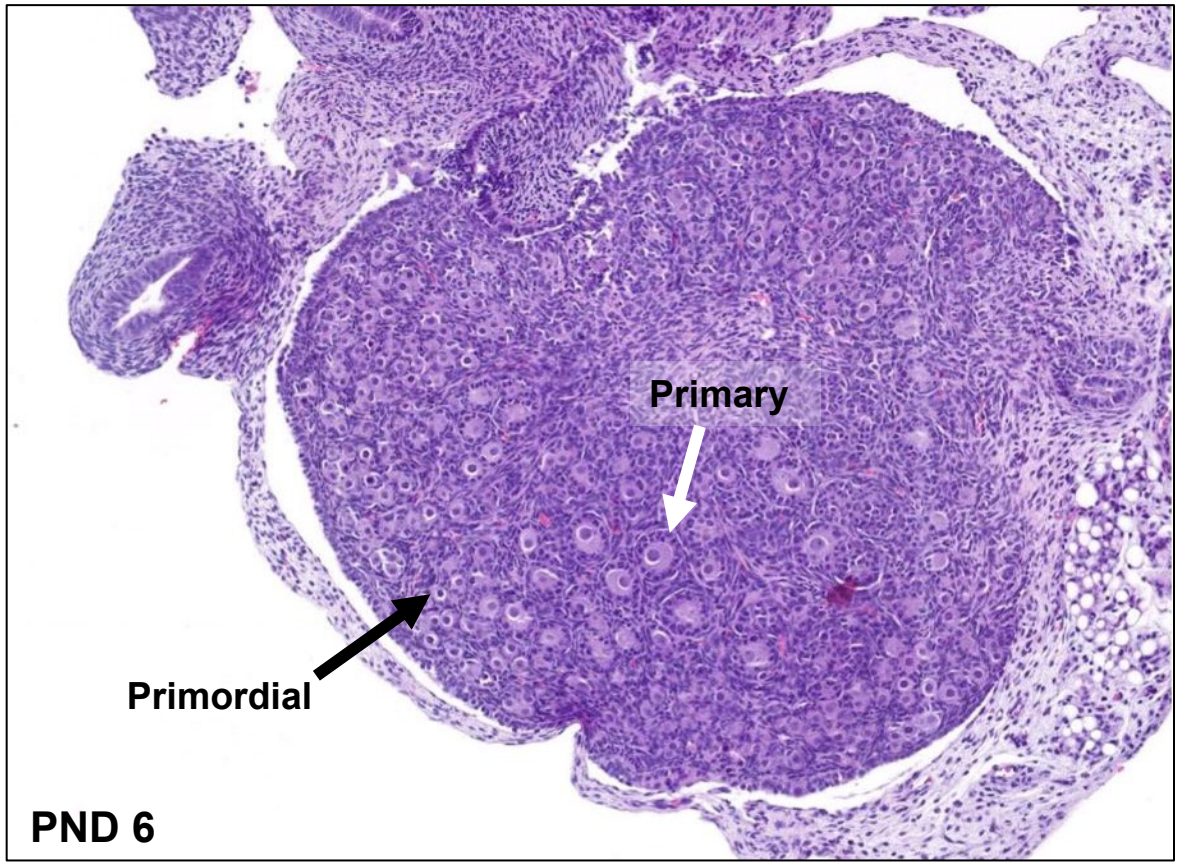

At PND 6, the nests have transformed into primordial (black arrow) and primary (white arrow) follicles, each containing one oocyte that has undergone the first meiotic division. Primary follicles are distinguished by a single layer of cuboidal to columnar cells surrounding the central oocyte, while primordial follicles have a single layer of flattened cells. H&E stain.

Ovary and vagina, rat, PND 28

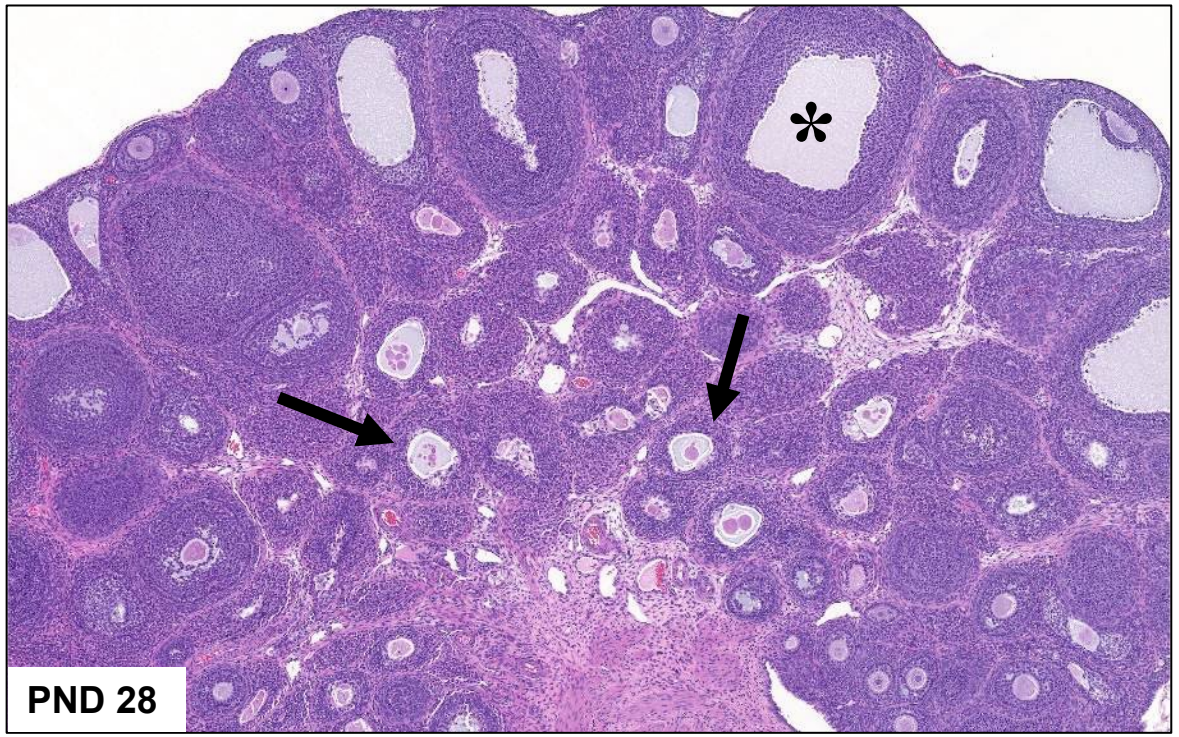

At PND 28, there are fluid-filled (antral) follicles (*) that are prepared to ovulate. Corpora lutea are not present, which indicates ovulation has not occurred. There are many atretic follicles (arrows), which are follicles that failed to develop to the antral stage and are involuting. H&E stain.

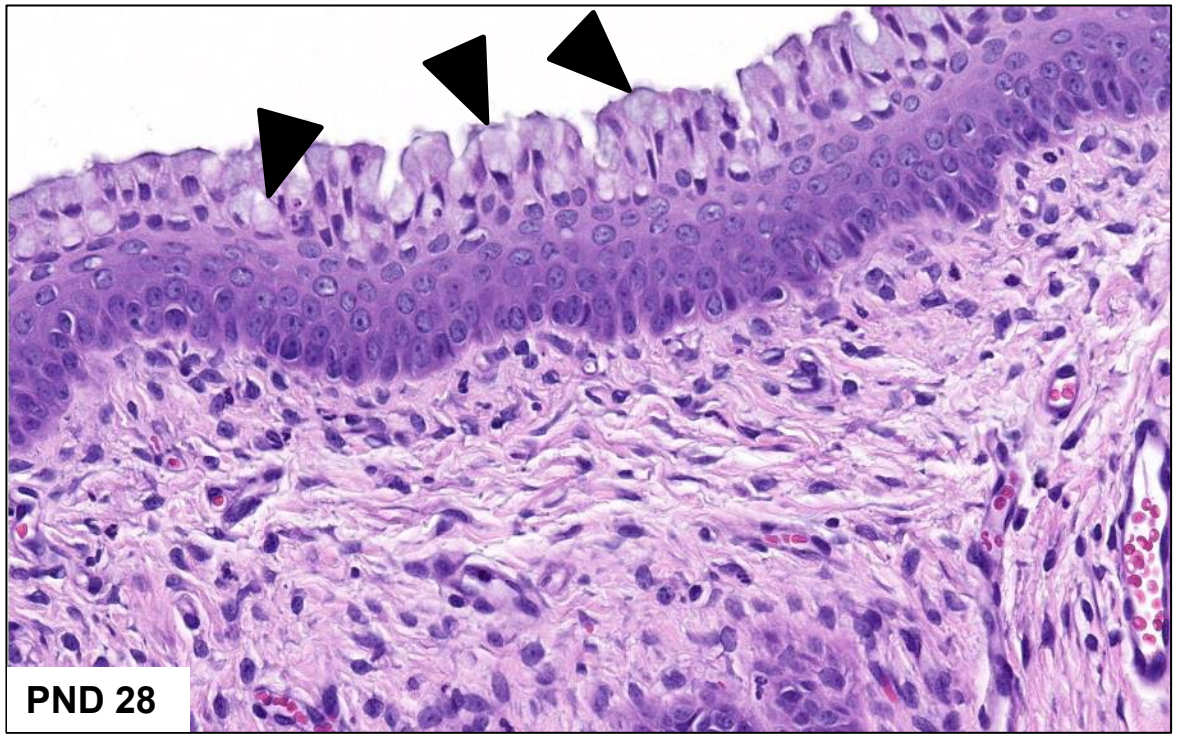

At PND 28, the vagina may have evidence of hormonal influence. Note the population of mucin-containing superficial epithelial cells (arrowheads). This manifestation of hormonal effects is known as “mucification”. H&E stain.

Male Reproductive Tract

Testis

- At birth, the rat testis consists of small tubules containing gonocytes, which are precursors to the spermatogonia, that are lined by immature Sertoli cells.
- From PND 1 to PND 15 (neonatal through early infantile stages), there is proliferation of spermatogonia and Sertoli cells.
- At PND 15 to 18 (late infantile stage), spermatocytes appear as the first wave of spermatogenesis starts. The tubules form a lumen, Sertoli cells mature and stop dividing, and a blood testis barrier becomes functional at this stage.
- Around PND 26 (juvenile stage), round spermatids develop.
- At PND 27 to 28 (juvenile stage), a prominent physiological apoptosis of pachytene spermatocytes occurs.

Epididymis

- From PND 27 until puberty, expect to see sloughed germ cells and/or cellular debris in the epididymal duct.
- At PND 35 (peri-pubertal stage), sperm appear in the epididymal duct.

Testis, rat, PND 1 and PND 3

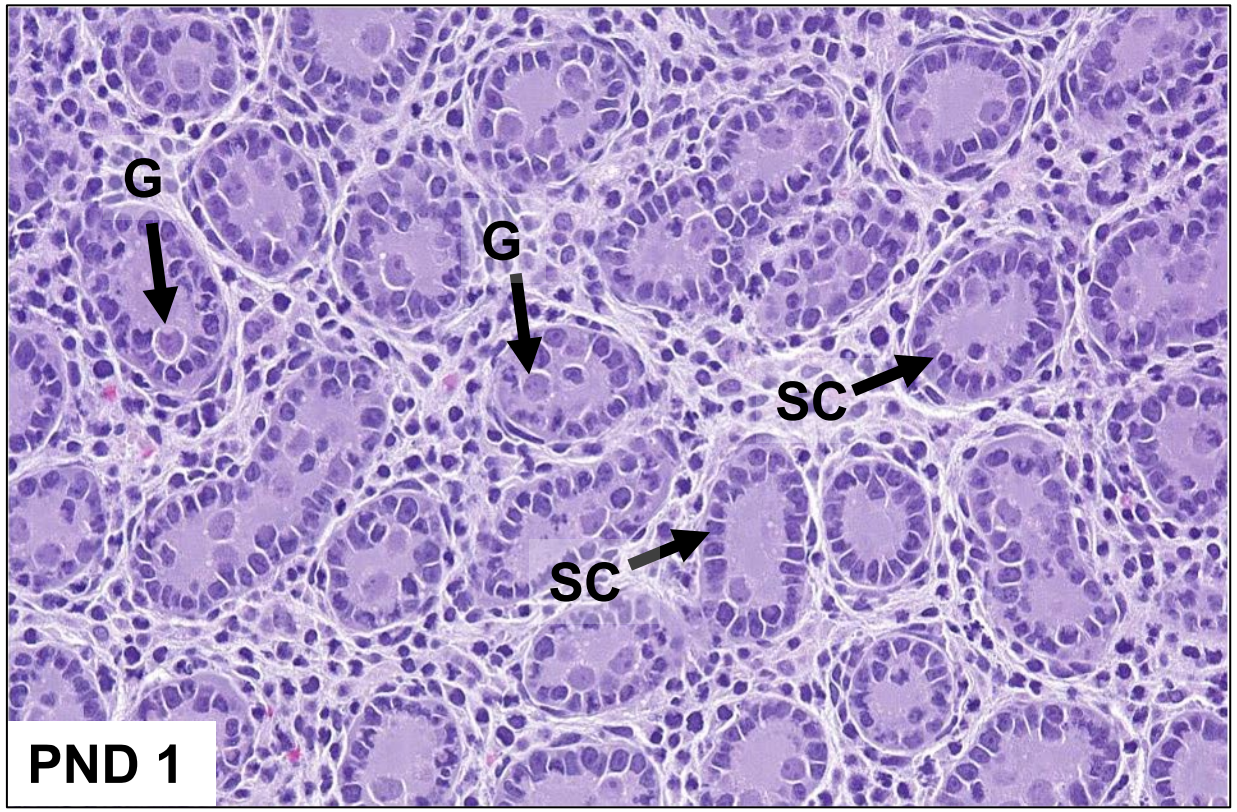

At PND 1, most cells lining the seminiferous tubules are Sertoli cells (SC), and the tubules contain gonocytes (G). There is no tubule lumen, and few to no spermatogonia are present. H&E stain.

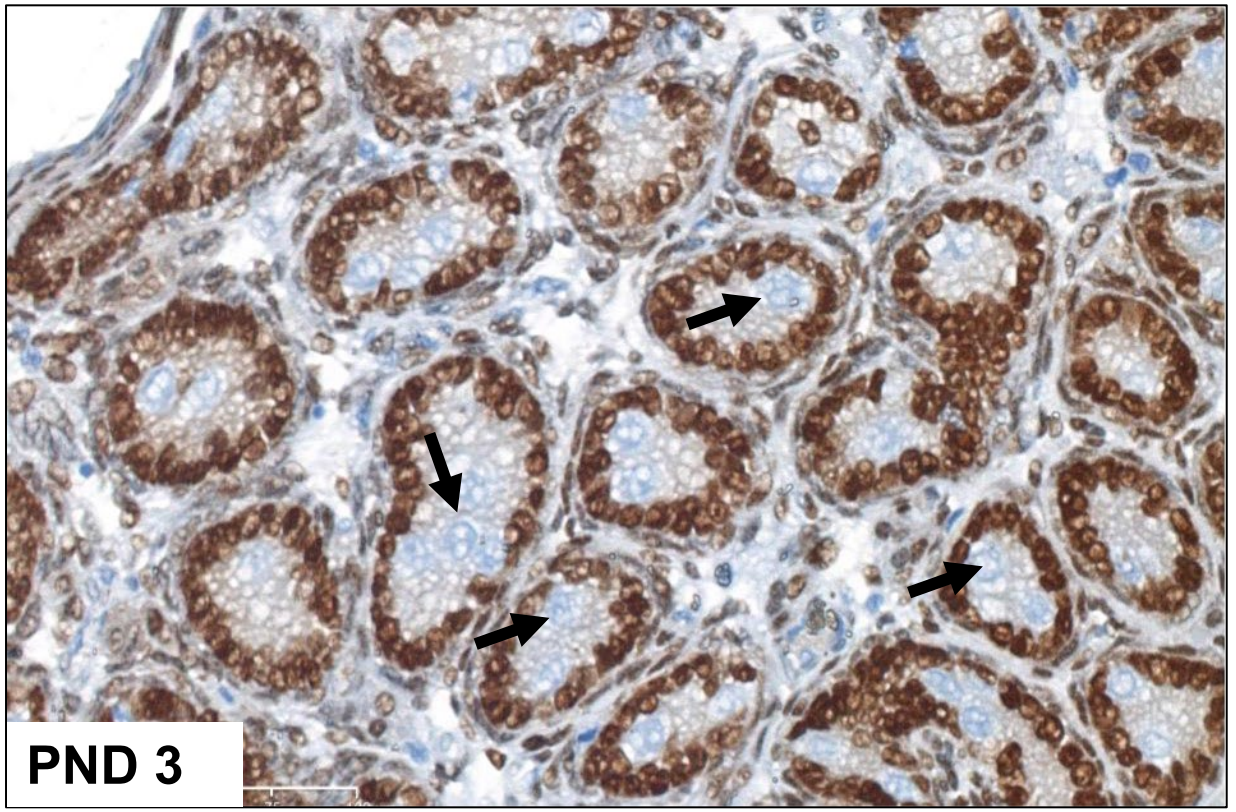

In this PND 3 testis, Sertoli cells are stained positively (brown) with the GATA-4 immunohistochemical (IHC) stain. These Sertoli cells are crowded on the basement membrane with a few pale blue profiles of gonocytes (arrows) barely visible within the tubule itself. GATA-4 stain.

Testis, rat, PND 18 and PND 27

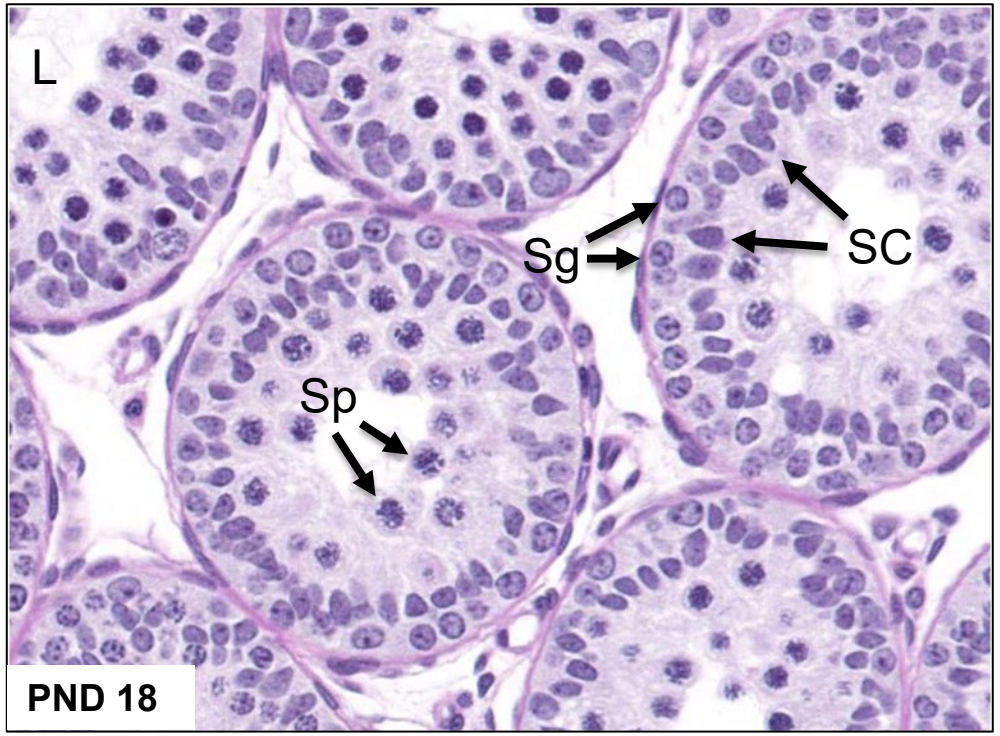

At PND 18 (late infantile stage), the crowded Sertoli cell (SC) nuclei are oval and pushed toward the lumen to line up internally to the spermatogonia (Sg). Spermatogonia have a round nucleus and rest on the basement membrane. The spermatogonia and Sertoli cells form a double layer. Spermatocytes (Sp) begin to develop during this first wave of spermatogenesis. A lumen (L) is now apparent. PAS/H stain.

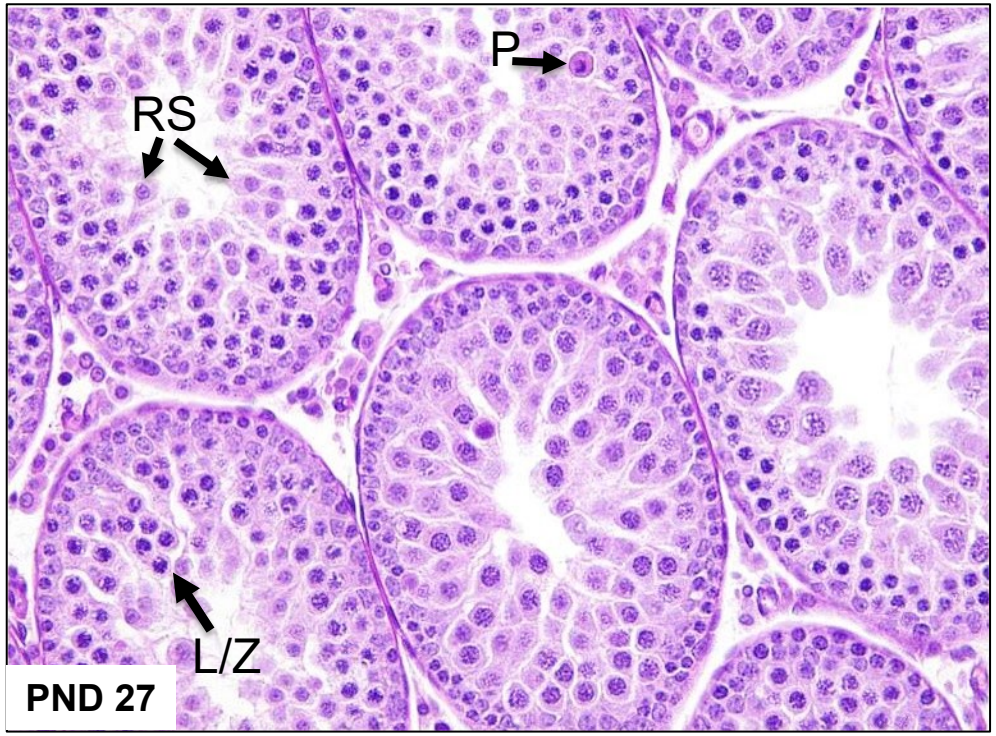

At PND 27 (juvenile stage), round spermatids (RS) form. There is physiologic apoptosis of pachytene spermatocytes (P) due to insufficient gonadotropin levels. Normal Leptotene/Zygotene spermatocytes (L/Z) (arrow) are plentiful, have highly condensed chromatin, and should not be misinterpreted as apoptotic or degenerative cells. PAS/H stain.

“Degenerative-like” changes in the normal juvenile testis

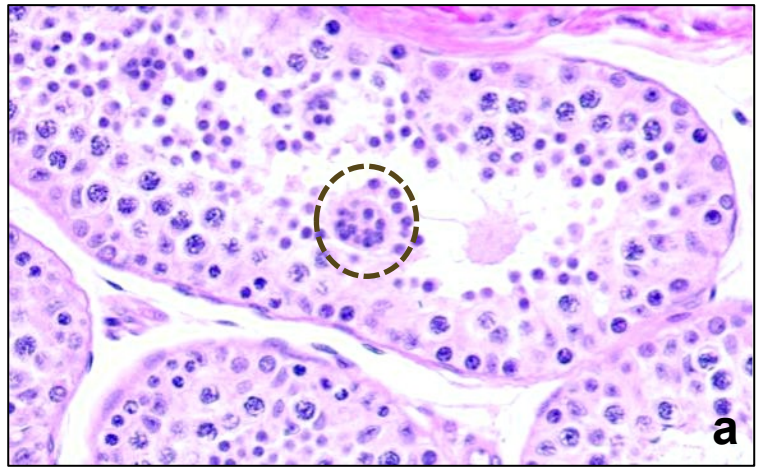

Multinucleated giant cells, nonhuman primate (cynomolgus macaque). H&E stain.

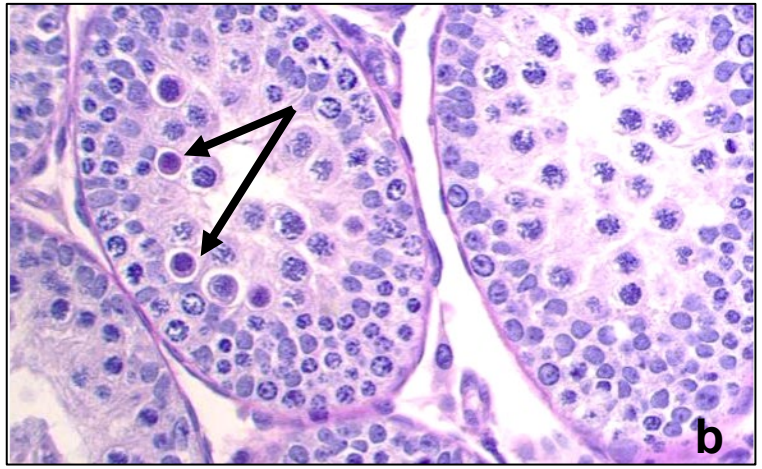

Physiologic apoptosis of pachytene spermatocytes, rat. PAS/H stain.

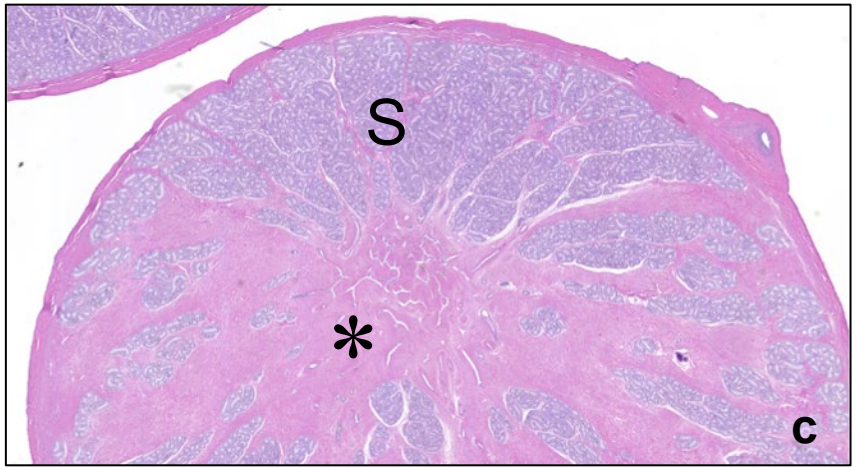

Increased stromal collagen, testis, nonhuman primate (cynomolgus macaque). H&E stain.

In pre- and peri-pubertal laboratory animals (nonhuman primates, rats, pigs, & mice), changes are present that would be considered degenerative in the adult animal. These include (a) multinucleated giant cells (dashed circle), (b) apoptosis of pachytene spermatocytes (arrows), and (c) increased stromal collagen (*). These findings should not be interpreted as a xenobiotic effect when dealing with the male reproductive tract of juvenile animals.

The specific change (*) in cynomolgus macaques (c) is called “increased stromal collagen”. Note the basophilic areas (S) which consist of normal seminiferous tubules.

“Degenerative-like” changes in the normal juvenile testis

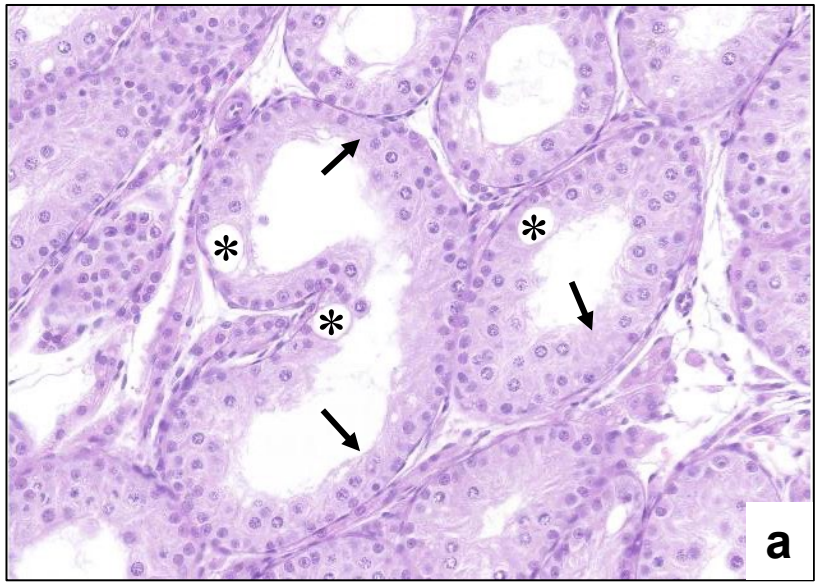

Paucity of germ cells and vacuolated Sertoli cells, peripubertal dog, H&E stain, 40x.

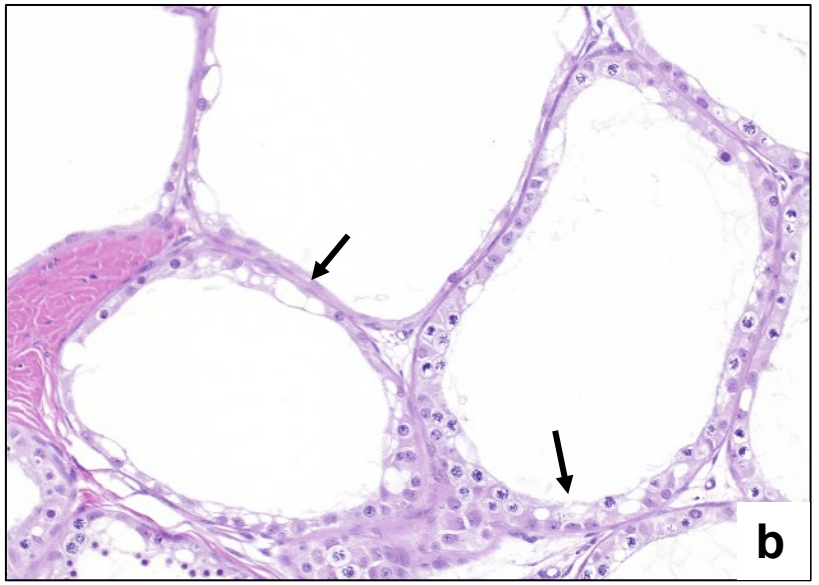

Tubule dilatation, prepubertal nonhuman primate, H&E stain, 20x.

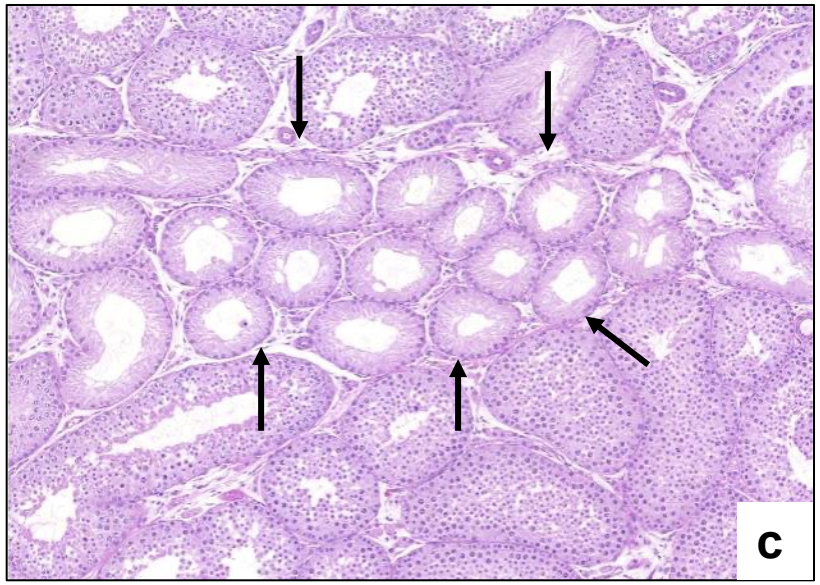

Tubule hypoplasia, peripubertal rat, H&E stain, 10x.

Additional “degenerative-like” findings that are considered background findings in pre- and peri-pubertal laboratory animals include:
(a) a paucity of germ cells with occasionally vacuolated Sertoli cells in dogs (10 months old). The tubules have an irregularly thin germ epithelium that could be described as “moth-eaten with fewer than expected germ cells” (arrows). Vacuolated cells (*) represent vacuolation of Sertoli cell cytoplasm. Normal tubules are not present in this image. (b) Dilatation of tubules in a peripubertal nonhuman primate is commonly multifocal. The dilated tubules are empty and lined by a thin, nearly imperceptible layer of germ cells (arrows). (c) Hypoplastic tubules in a peripubertal rat is a common incidental finding that may persist into adulthood. These hypoplastic tubules generally occur in clusters (outlined by arrows) and the tubules are lined only by Sertoli cells and have not been populated with germ cells.

Testis, rat, decreased tubule diameter due to thyrotoxicant

- Test articles may cause decreased tubule size (decreased tubule diameter). This finding is commonly associated with decreased numbers and delayed maturation of the germ cells.
- a) At PND 21, the tubules of a control rat are beginning to form a lumen (L) and have Sertoli cells lining up internal to the spermatogonia in a double layer (box). There are many spermatocytes (arrows) forming as well.
- b) When compared to an untreated control rat (a), the tubules in the thyrotoxicant (propylthiouracil, PTU) treated animals have decreased tubule size (b). These F1 animals are at age PND 21 and PTU was administered to their pregnant dams during gestation and lactation. The affected testis (b) has no lumen formation and rare spermatocytes (arrow). The seminiferous tubule contains a crowded pseudostratified layer of Sertoli cells and spermatogonia with no double layer formation. Sertoli cells tend to have oval nuclei while spermatogonia have round nuclei.

Untreated control testis, PAS/H stain, 20x.

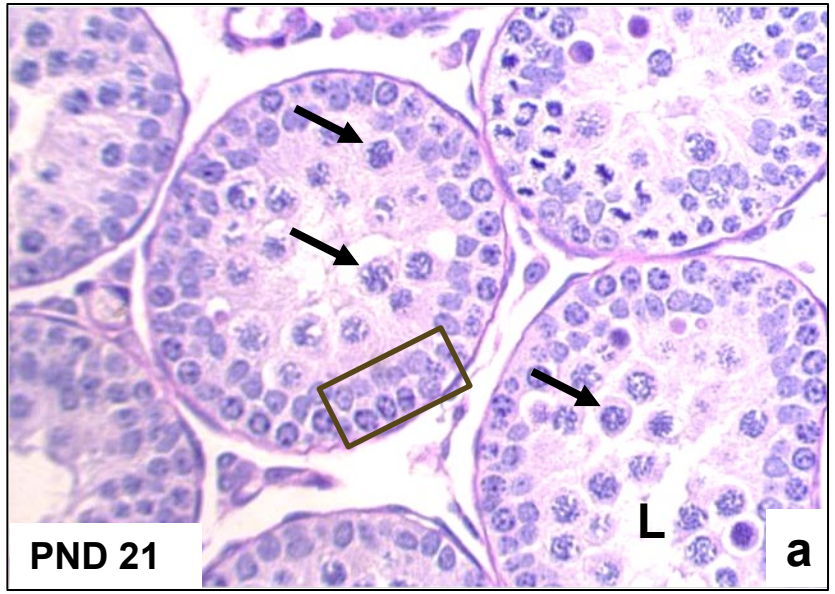

PTU-treated testis, PAS/H stain, 20x.

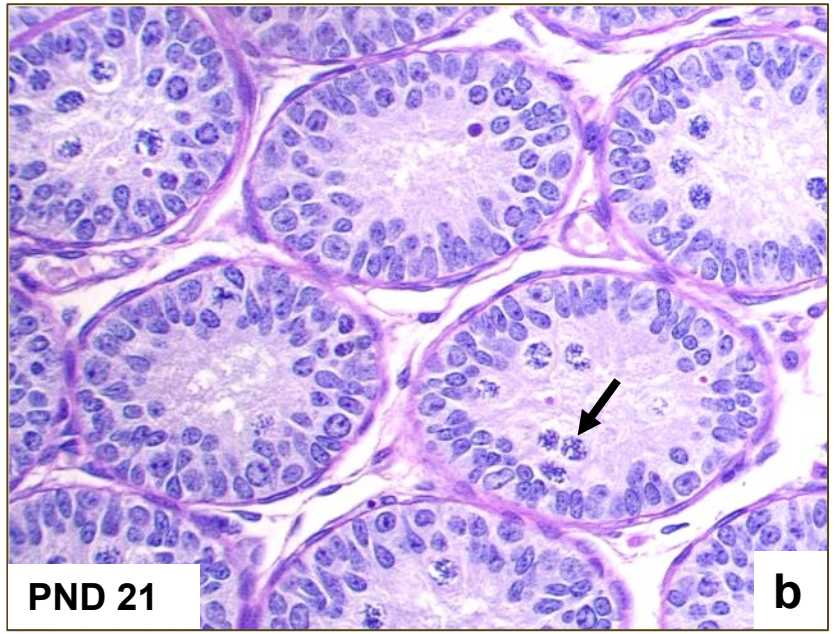

Testis, rat, PND 3, tubule dysgenesis associated with phthalate exposure

- Testes from prenatal exposure of pregnant dams to di(2-ethylhexyl) phthalate are present in these two images (a) and (b). The testes are from rats at PND 3. Exposure to phthalates resulted in tubule dysgenesis, Leydig cell aggregation, and multinucleated gonocytes (MG). PAS/H stain.
- Tubule dysgenesis is characterized by tubules lined by only Sertoli cells and forming abnormal convoluted profiles (arrowheads). Leydig cell aggregation (white asterisks) is characterized by abnormal clusters of Leydig cells, commonly adjacent to abnormal tubules. Multinucleated gonocytes (MG, arrows) is also an abnormal finding in some tubules. PAS/H stain.

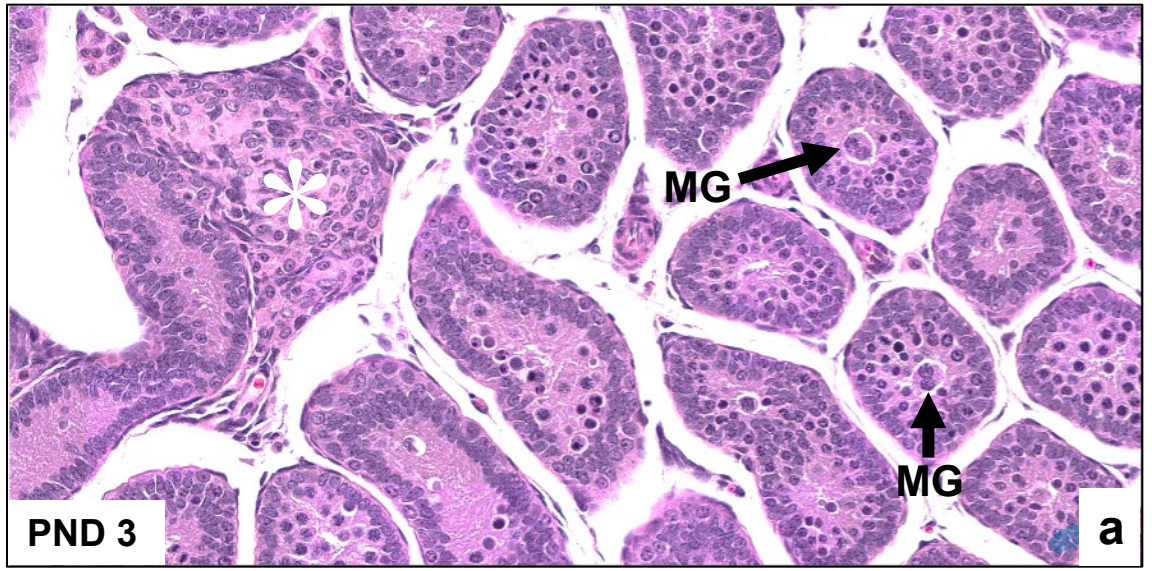

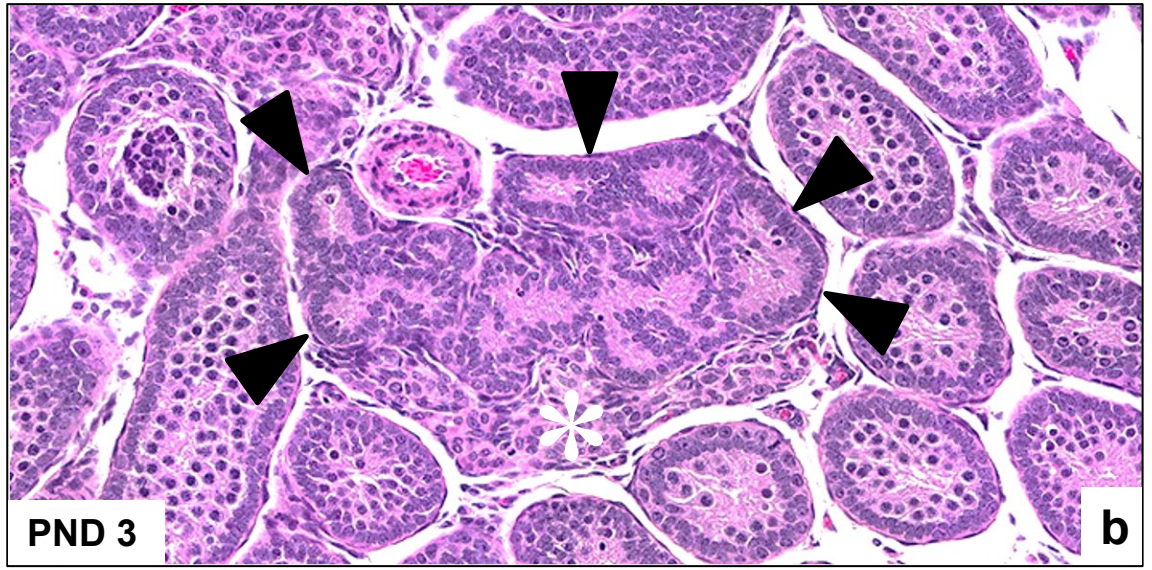

Epididymis, cauda region, rat, PND 20 and PND 28

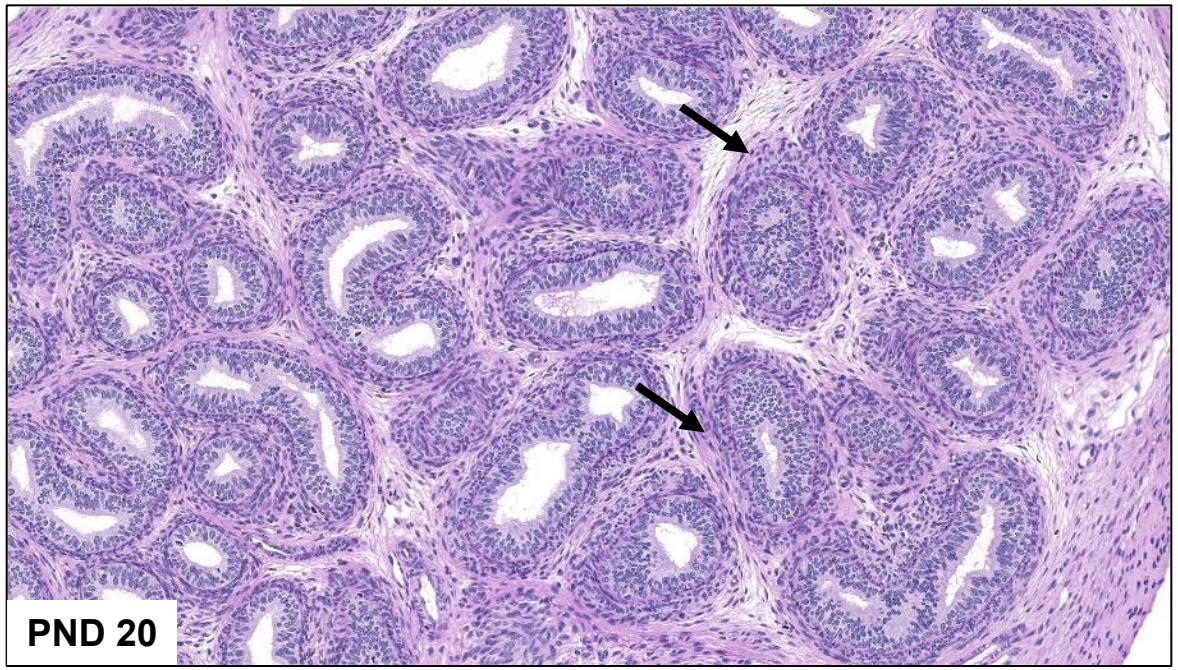

At PND 20, the cauda duct profiles are contracted and small, and the peritubular contractile smooth muscle (arrow) is developing. PAS/H stain, 15x.

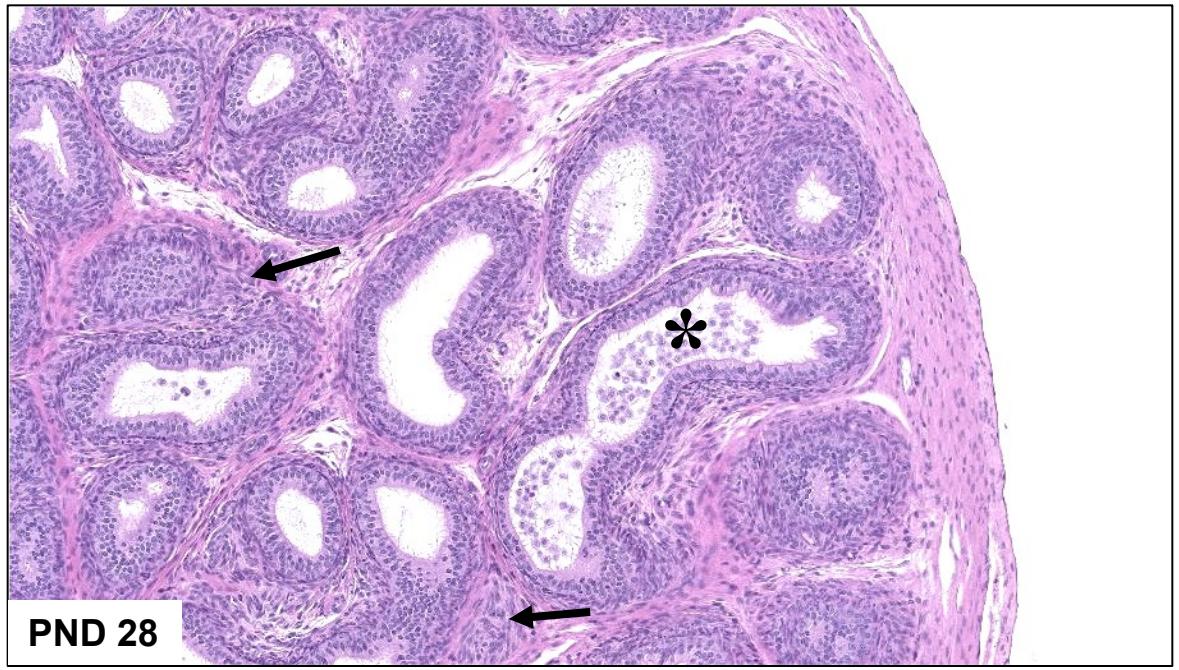

At PND 28, peritubular contractile smooth muscle (arrow) continues to develop. Sloughed germ cells may appear in the lumina of the duct profiles. This cellular debris (*) should be considered normal before sexual maturation is achieved. No spermatozoa are present at this age. Note the increased diameter of duct profiles as compared to PND 20. PAS/H stain, 15x.

Summary of immune system maturation in rats

N = not present
I = immature
A = adult
PND = postnatal day
BALT = bronchus-associated lymphoid tissue
GALT = gut-associated lymphoid tissue
NALT = nasopharynx-associated lymphoid tissue
PALS = periarteriolar lymphoid sheath

	PND0		PND7		PND14		PND21		PND28		PND35		PND42	
Organ/structure	M	F	M	F	M	F	M	F	M	F	M	F	M	F
Bone marrow, sternum	I	I	I	I	A	A	A	A	A	A	A	A	A	A
Bone marrow, femur	I	I	A	A	A	A	A	A	A	A	A	A	A	A
GALT														
Peyer's patches	I	I	I	I	I	I	I	I	A	A	A	A	A	A
Diffuse lymphocytic population	N	N	N	N	N	I	I	I	I	I	A	A	A	A
Lung (BALT)	N	N	I	I	I	I	I	I	A	A	A	A	A	A
Lymph node, axillary	I	I	I	I	I	I	I	I	A	A	A	A	A	A
Lymph node, mandibular	I	I	I	I	I	I	I	I	A	A	A	A	A	A
Lymph node, mesenteric	I	I	I	I	I	I	A	A	A	A	A	A	A	A
NALT	N	N	N	N	N	I	I	I	I	N	A	A	A	A
Spleen														
PALS (T cell)	N	N	I	I	I	I	I	I	A	A	A	A	A	A
Follicles (B cell)	N	N	N	N	N	N	N	N	N	N	I	I	A	A
Thymus	I	I	I	I	A	A	A	A	A	A	A	A	A	A

- The primary immune system organs (thymus and bone marrow) mature first.
- Secondary lymphoid organs associated with the GI tract mature somewhat later.
- Non-enteric secondary lymphoid organs mature last.

Thymus, rat, PND 0

- The thymus is a primary immune system organ. As such, thymus development is a genetically determined process with no external environmental influence.
  - The thymus originates from the third and fourth branchial arches. Two distinct lobes of the primitive thymus migrate down to the anterior aspect of the thoracic cavity by the time of birth
  - PND 0 – thymus is moderately developed with cortex (C), medulla (M), and distinct corticomedullary boundary (arrows). H&E stain
  - PND 7 – cortex cellularity approaches adult level
  - PND 14 – thymus development complete
  - Any additional increase in size is parallel to increased size of rat

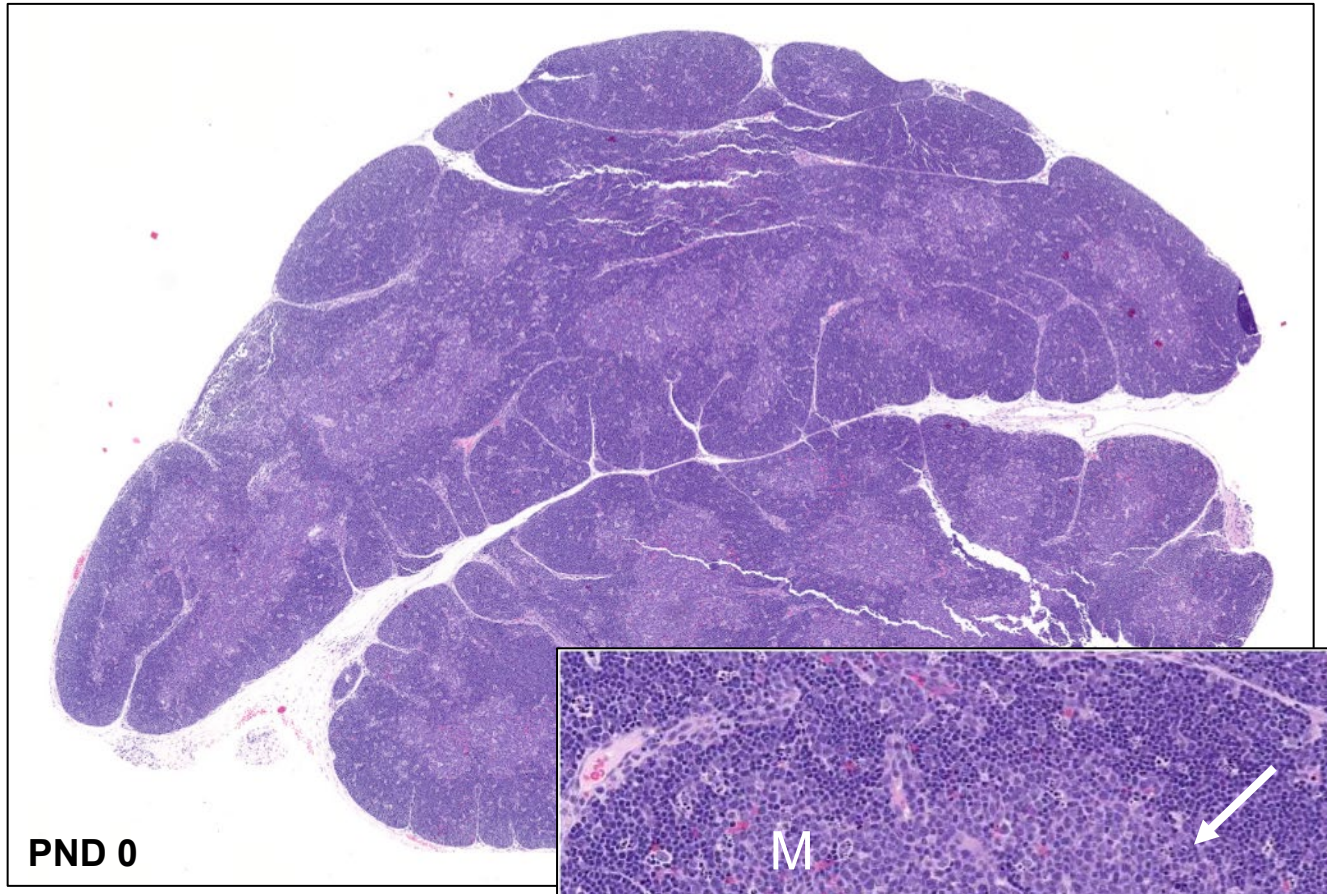

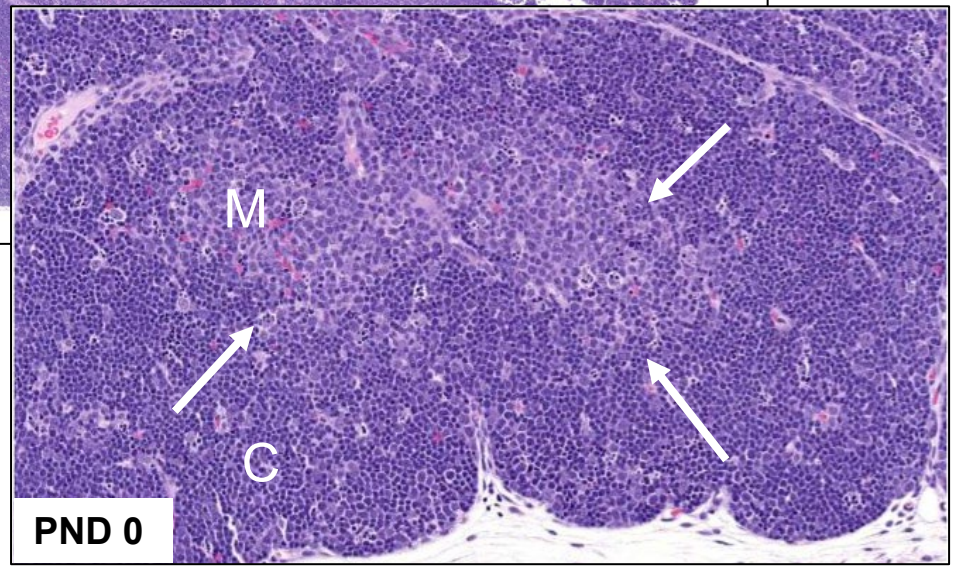

Bone marrow, rat, GD 15, PND 0 and PND 4

- Bone marrow is a primary immune system organ. Development is a genetically determined process, with no environmental influence. Fetal hematopoiesis commences with blood spots on the yolk sac of the embryo. Hematopoiesis subsequently migrates from yolk sac → adrenal gonadal metanephros → liver → bone marrow.
- Bone marrow developmental sequence:
- PND 0 – myeloid and erythroid precursors present. M:E ratio high (approx. 3.0)
- PND 7 – megakaryocytes present. Lymphocyte population approx. 20%
- PND 14 to 42 – Lymphocytes population increases to approx. 45%

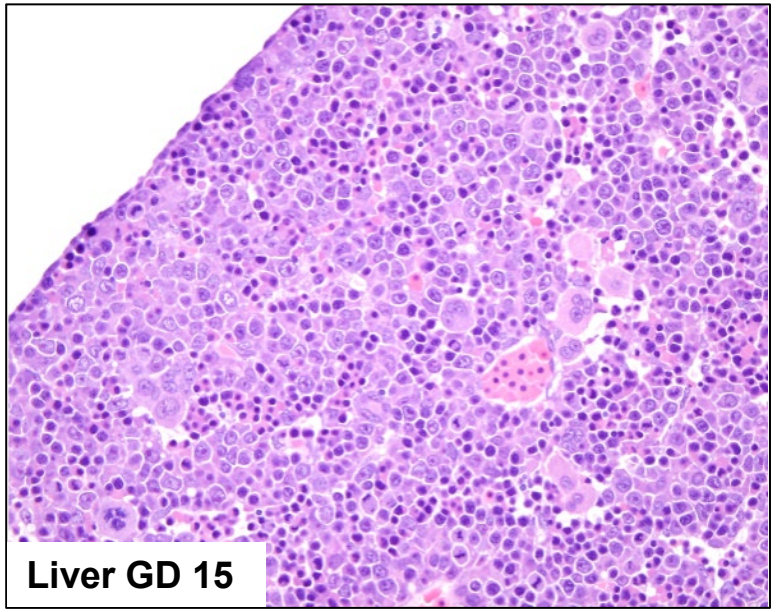
Liver GD 15

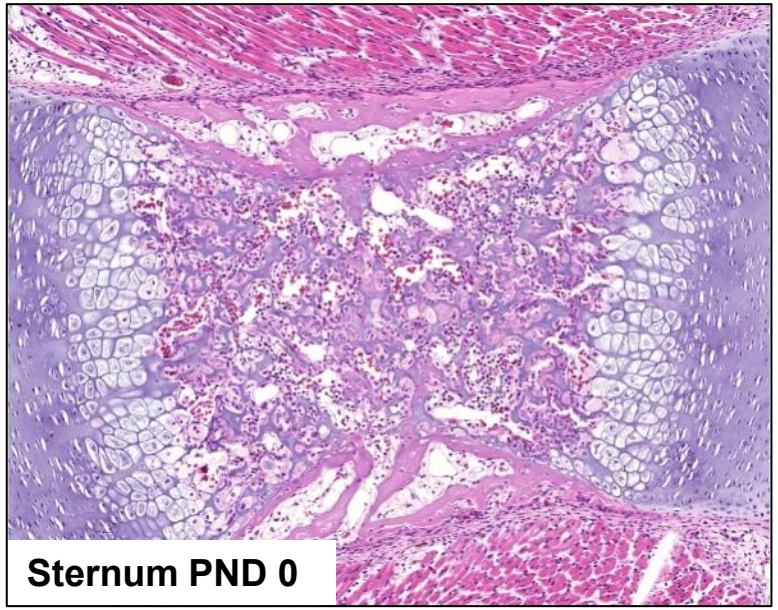
Sternum PND 0

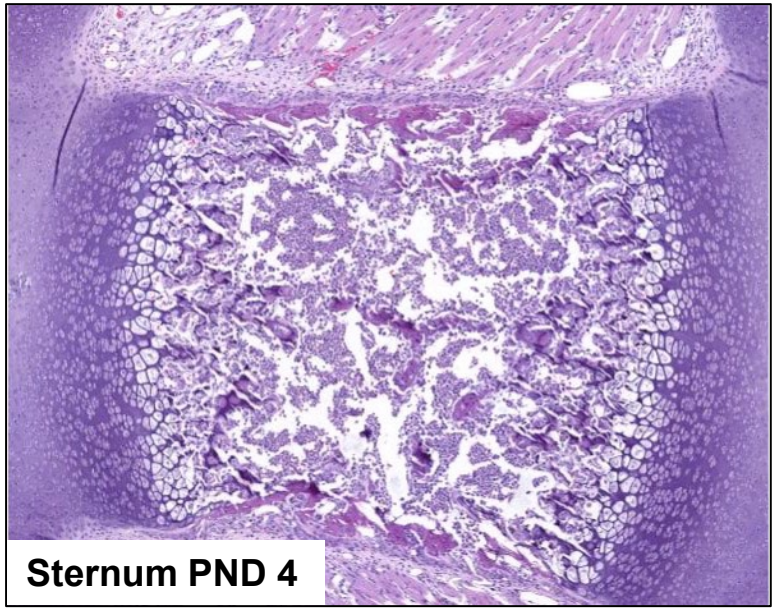
Sternum PND 4

Figure legend:

Liver, gestation day (GD) 15 – liver is the primary hematopoietic organ. H&E stain.

Sternum, PND 0 – sparse marrow cell population. H&E stain.

Sternum, PND 4 – increased marrow cell population. H&E stain.

Spleen, rat, PND 0

- The spleen is a secondary immune system organ
- Developmental sequence:
  - PND 0 – spleen parenchyma is a uniform population of cells except for slight collection of periarteriolar cells in region of future periarteriolar lymphoid sheath (PALS)
  - PND 7 – PALS are distinct
  - PND 14 to 21 – increase in overall size of spleen
  - PND 28 – incipient lymphoid follicles appear
  - PND 35 – approximately 50% of rats have well-developed splenic lymphoid follicles
  - PND 42 – splenic development complete, with follicles, germinal centers, PALS, and marginal zones
- Image legend: arteriole (A), periarteriolar lymphoid sheath (PALS), marginal sinus (MS) interfollicular (red) pulp (RP). H&E stain.

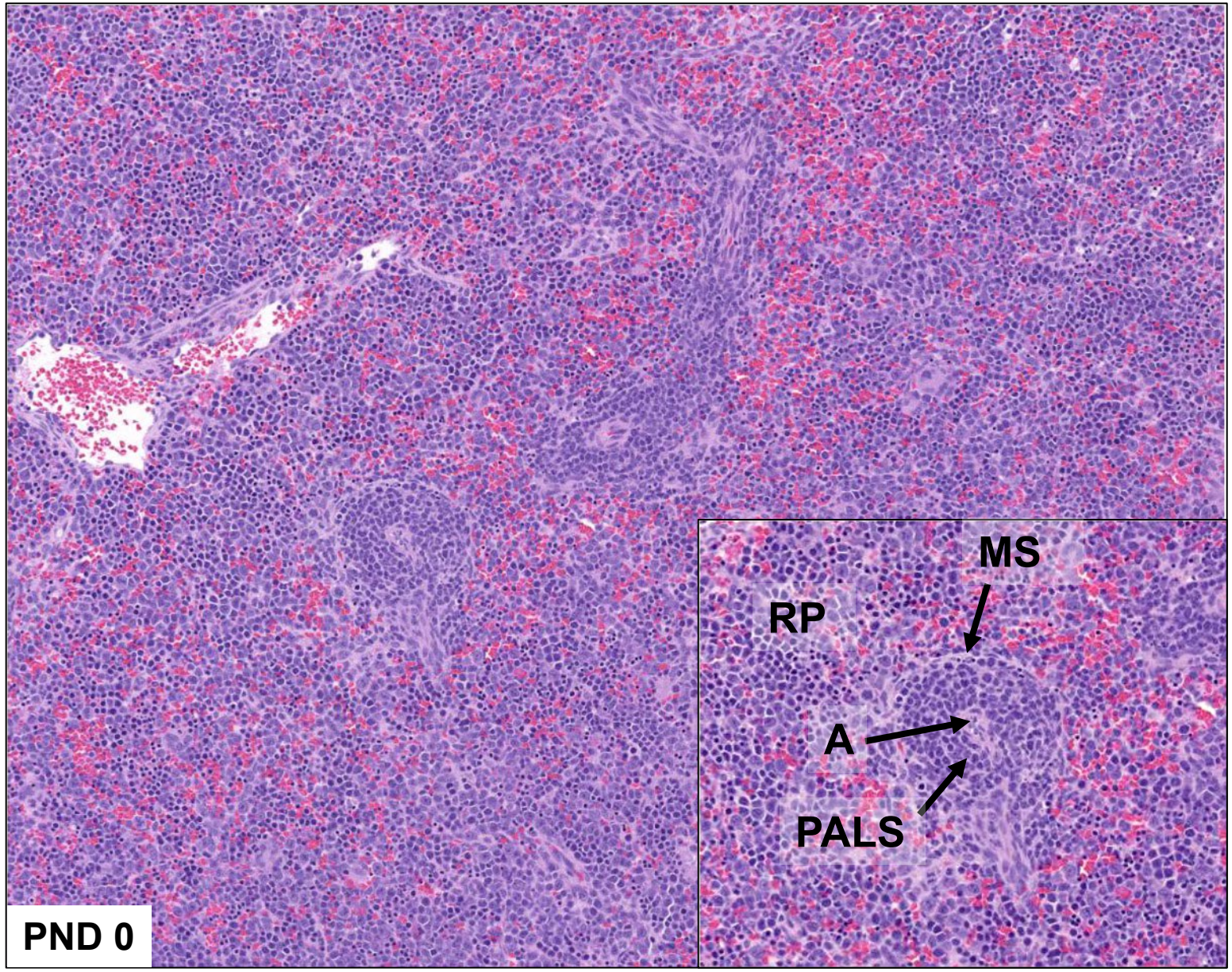

Mandibular lymph node, rat, PND 1

- PND 0 – lymph nodes poorly developed. Mesenteric lymph nodes are slightly more developed than mandibular or axillary lymph nodes.
- PND 7 – mesenteric lymph nodes have follicles and paracortex with high-endothelial venules
- PND 14 – germinal centers present in mesenteric lymph node follicles of 40% of rats
- PND 28 – Mesenteric lymph nodes fully developed. Follicles and germinal centers are commonly present in mandibular lymph nodes.
- PND 35 – Mandibular lymph nodes fully developed
- PND 42 – Axillary lymph nodes fully developed but rare germinal centers in follicles

- Lymph node figure legend: H = hilus with blood vessels and lymphatics; C = immature cortex; arrows = dilated lymphatic sinuses. H&E stain.

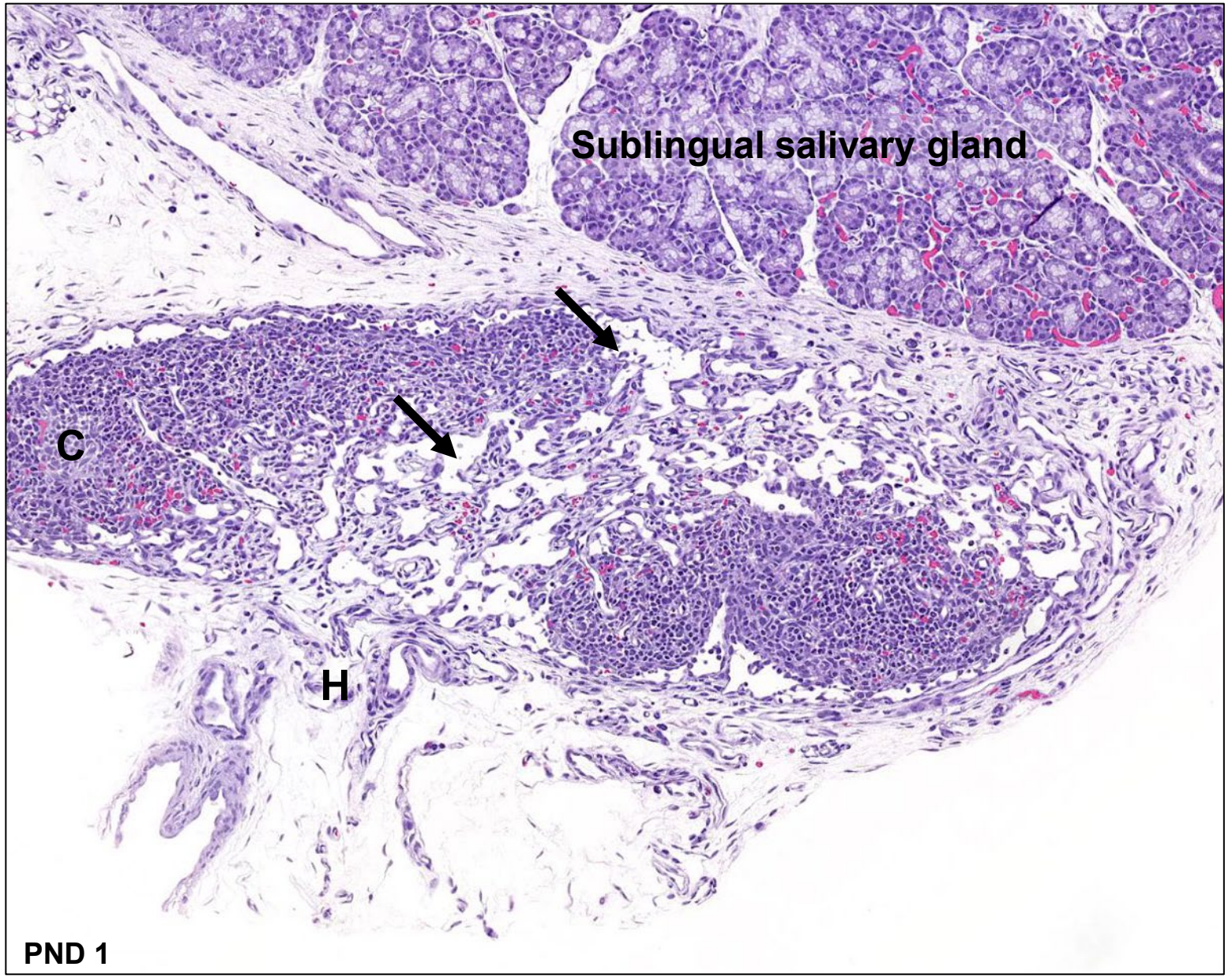

Small intestine, rat, PND 7

- PND 0 – small intestine has small cellular aggregates consistent with incipient Peyer's patches
- PND 7 to 21 – Peyer's patches become more prominent (arrowheads), with variable germinal centers
- PND 28 – Peyer's patches are fully developed
- Development of diffuse intestinal lymphocytic population lags behind Peyer's patch development and is not at adult level until PND 35

Figure legend:

Arrowheads = immature Peyer's patch (PP) in small intestine. D = dome associated with a PP lymphoid follicle. FAE = follicle-associated epithelium. Note protein/lipid vacuoles in epithelial cells. H&E stain.

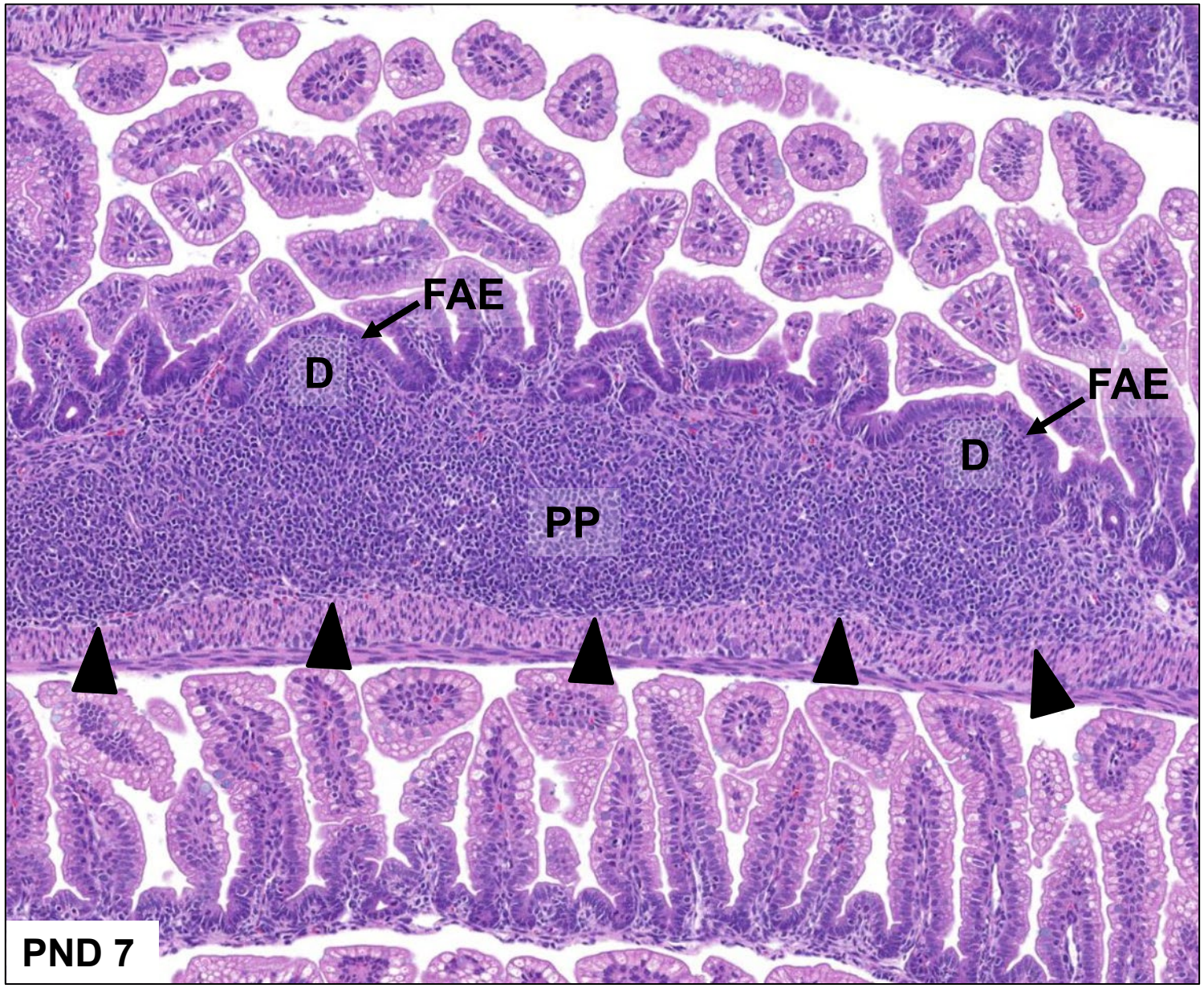

Small intestine, rat, PND 1 and PND 21

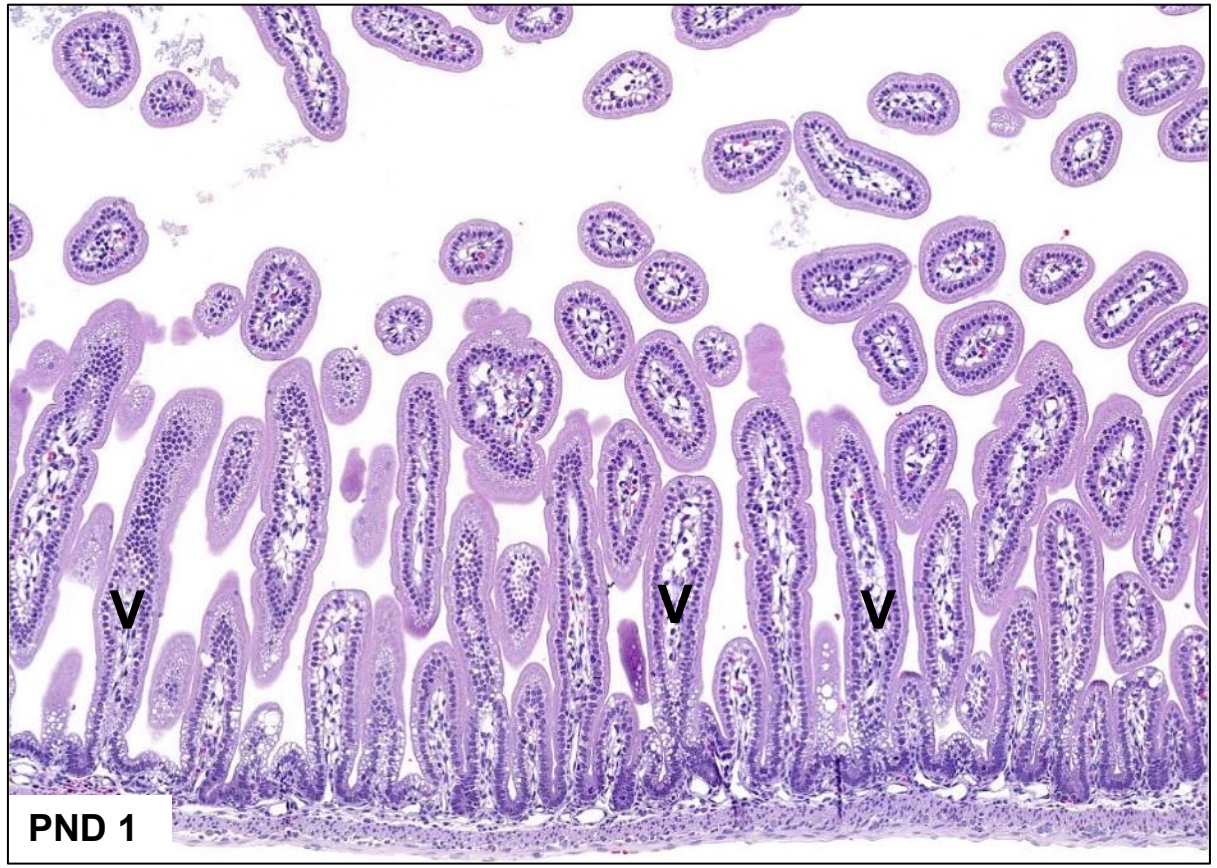

PND 1 – Note sparse diffuse lymphocyte population in lamina propria of villi (V). H&E stain.

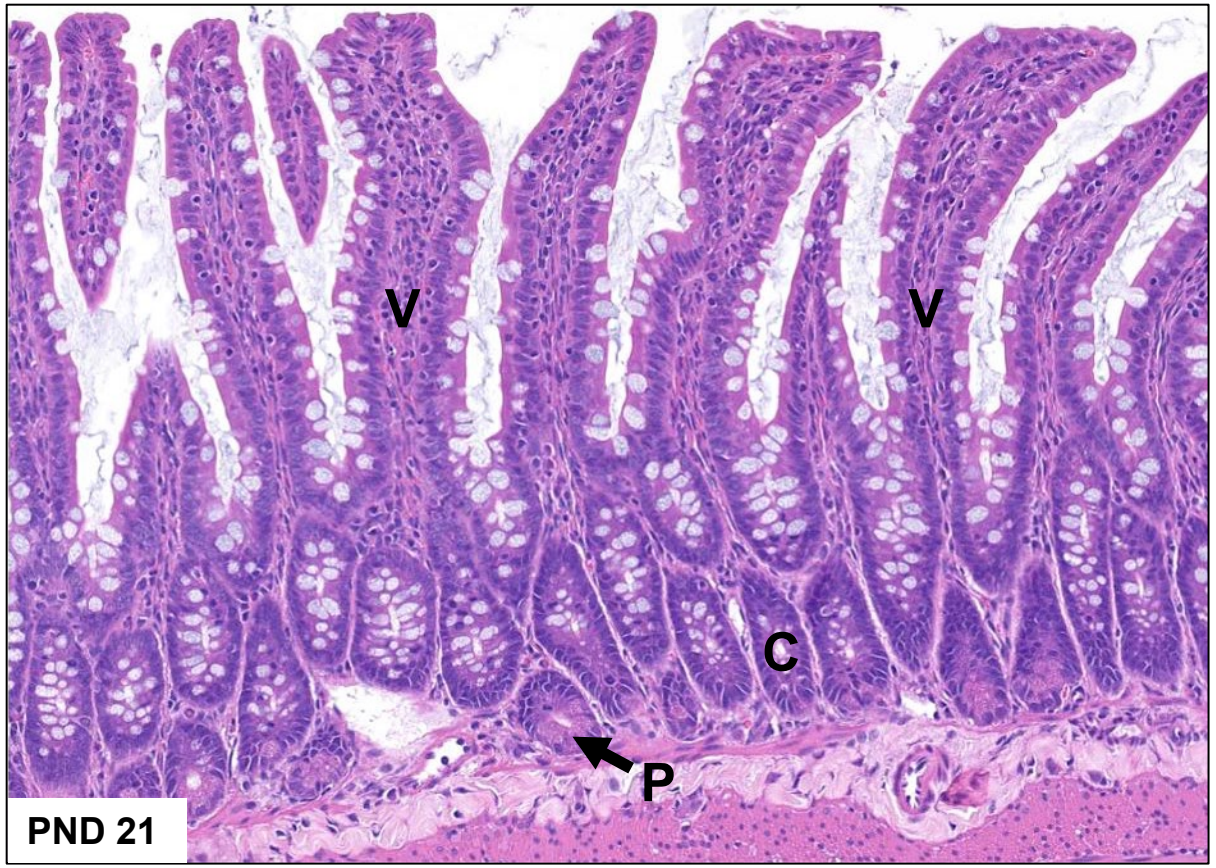

PND 21 – Note more extensive diffuse lymphocyte population in lamina propria of villi (V). Also note the active-appearing crypt epithelium (C) and eosinophilic Paneth cells (P) in depth of crypts. H&E stain.

Bronchus-associated lymphoid tissue (BALT), rat, PND 14

Developmental sequence:

- PND 7 – Incipient bronchus-associated lymphoid tissue (BALT) is present
- PND 28 – BALT is present in 90% of rats
- PND 42 – BALT uniformly present in rats
- BALT is constitutively expressed in rats but is induced in mice. Should be called iBALT in mice.

Figure legend:

A = arteriole; B = bronchiole; V = venule; * = BALT

Note the proximity of BALT to bronchiolar epithelium, which facilitates presentation of airborne antigens to the immune system. H&E stain.

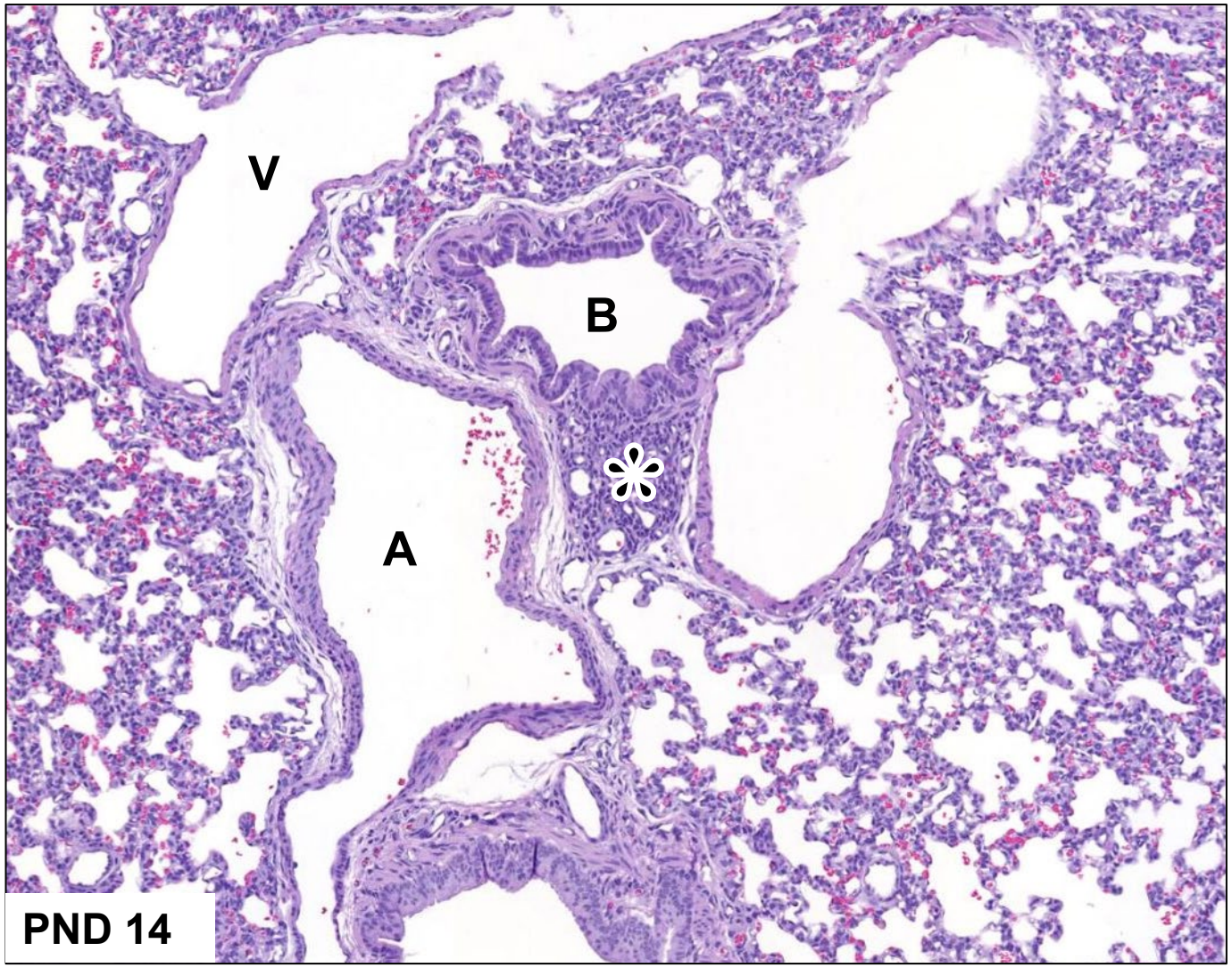

Thigh muscle, rat, PND 1 and PND 21

Developmental sequence:

- Skeletal muscle undergoes maturation during first three (3) postnatal weeks.
- Skeletal muscle is generally considered to be nonregenerative but, in the rat, myofiber replication is part of the maturation process. Occasional mitotic figures are noted.
- PND 1 (top image): The thigh muscle has high nuclear density with sparse sarcoplasm and abundant interstitial spaces. Occasional nuclei are present within the sarcoplasm, as opposed to the peripheral location of nuclei in mature skeletal muscle. H&E stain.
- PND 7 to 14 (not pictured): slight increase in sarcoplasm, with cross-striations evident.
- PND 21 (bottom image): marked increase in sarcoplasm to essentially mature status. H&E stain.
- Subsequent change is limited to minor increases in sarcoplasm.

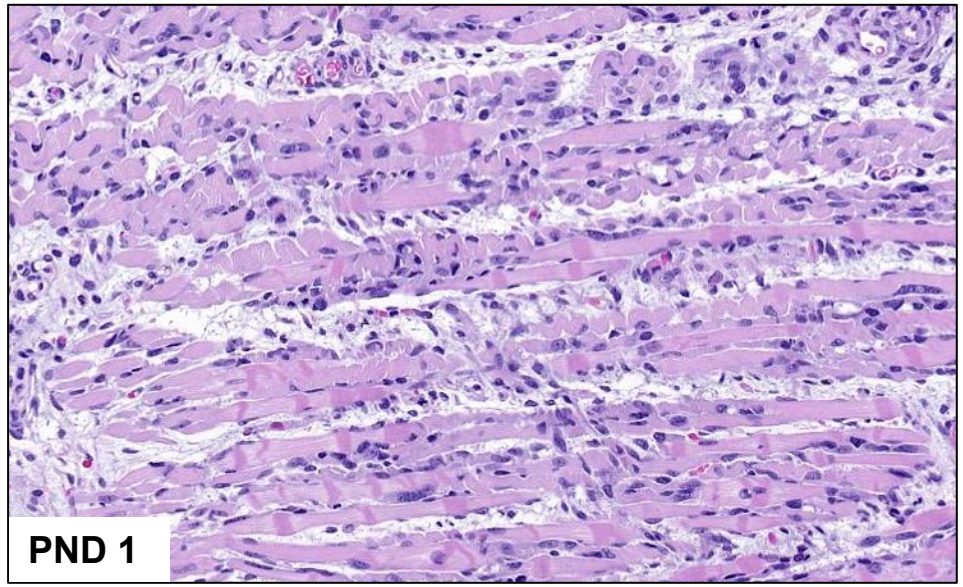

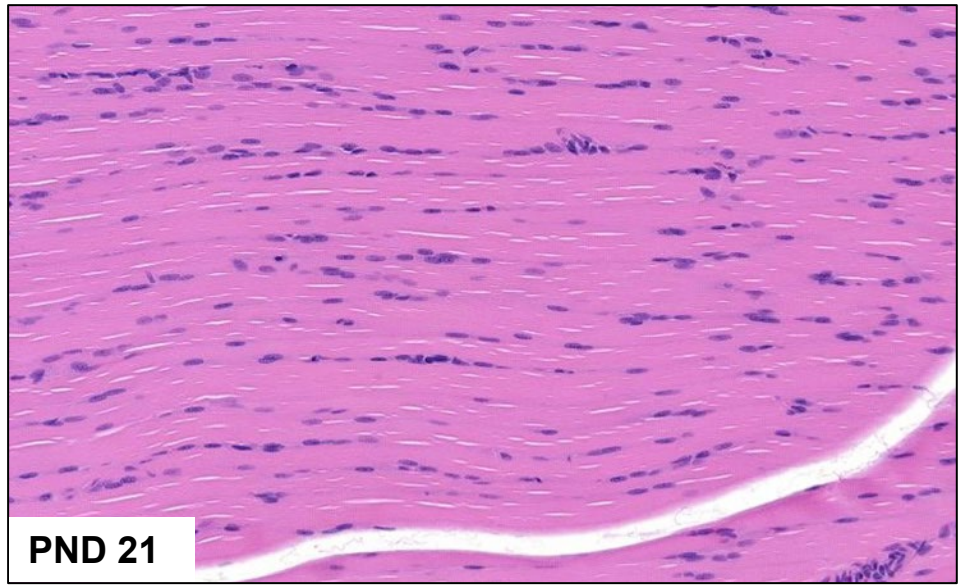

Femur, rat, PND 0

Developmental schedule:

- PND 0 – primary ossification center is well developed
- PND 7 – growth plate has matured
- PND 21 – secondary growth plate forms beneath distal articular surface of femur.
- PND 21 to 42 – constant growth from epiphyseal growth plate
- PND 42 – cortical bone is morphologically mature

Figure legend for PND 0 : C = hyaline cartilage; H = zone of cartilage hypertrophy; O = primary ossification center; B = endochrondral bone formation results in increased length of long bones; CB = immature cortical bone undergoes intramembranous ossification to form mature cortical shaft; T = tip of ossification center at opposite end of femur. H&E stain.

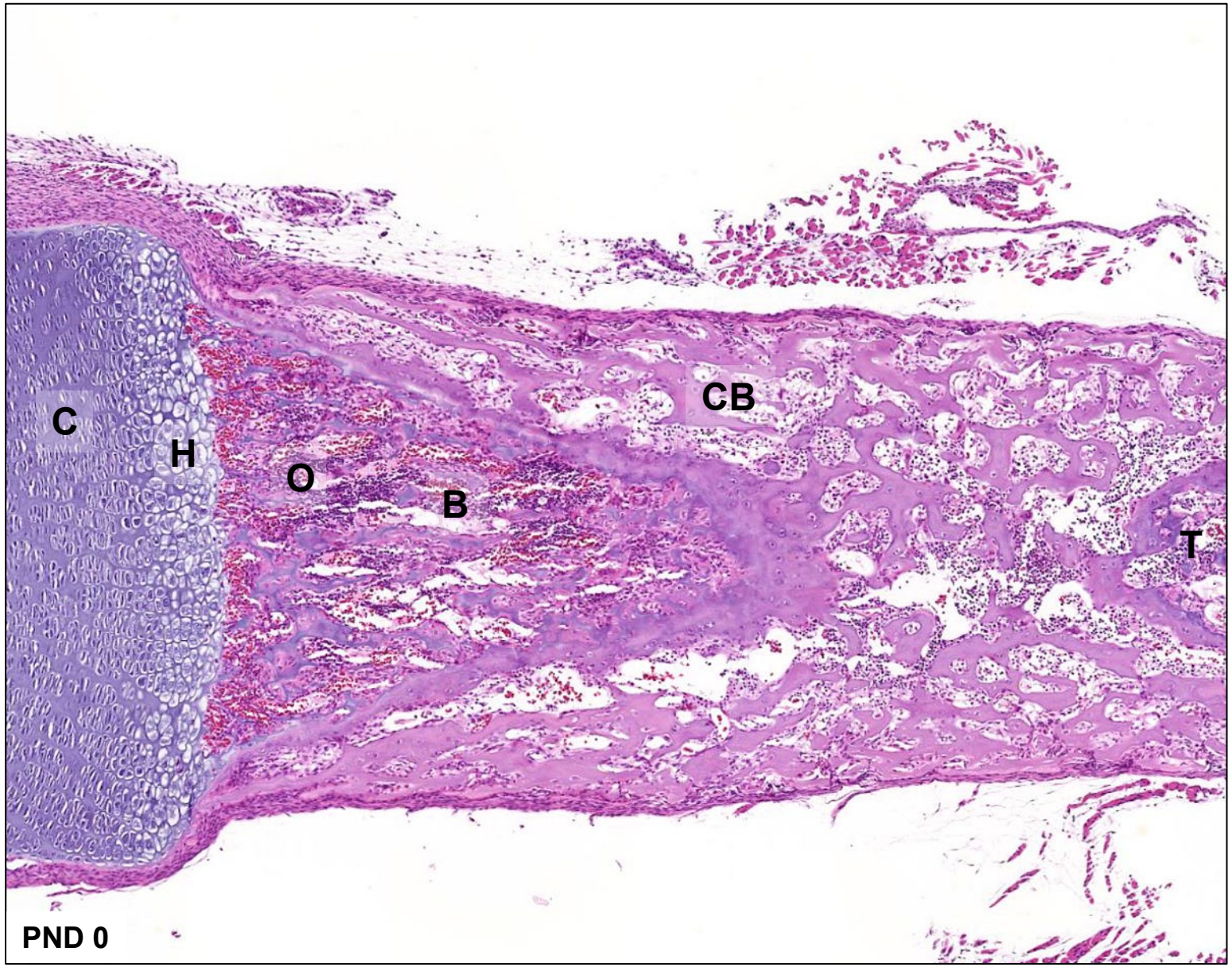

Thyroid gland, rat, PND 4, 7 and 21

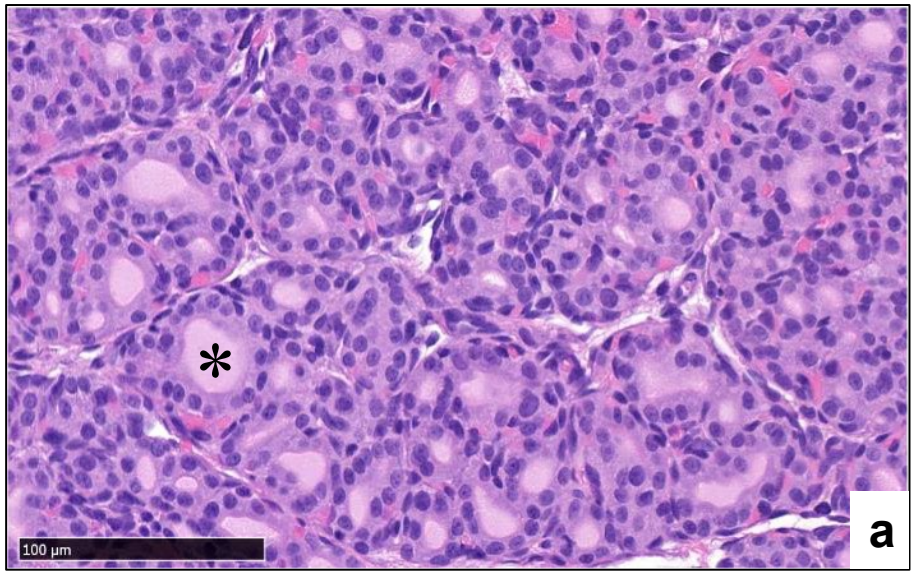

PND 4, H&E stain, 30x.

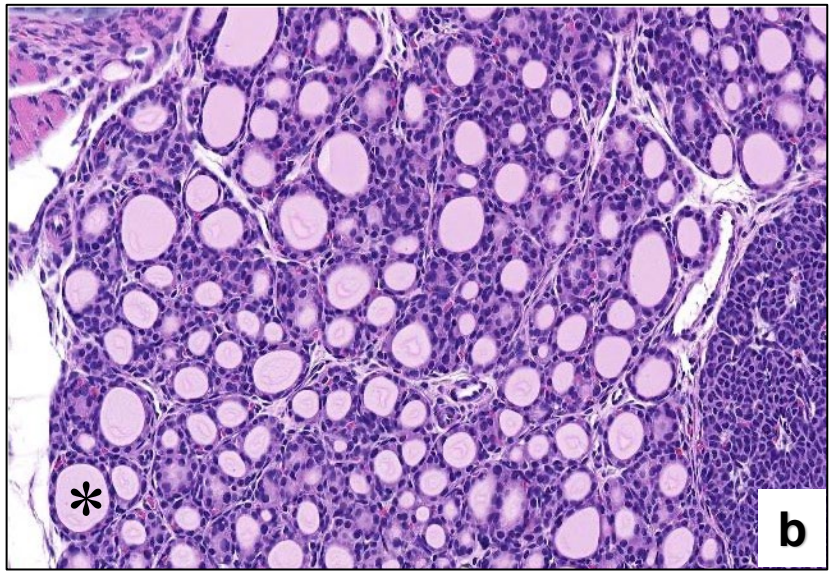

PND 7, H&E stain, 25x.

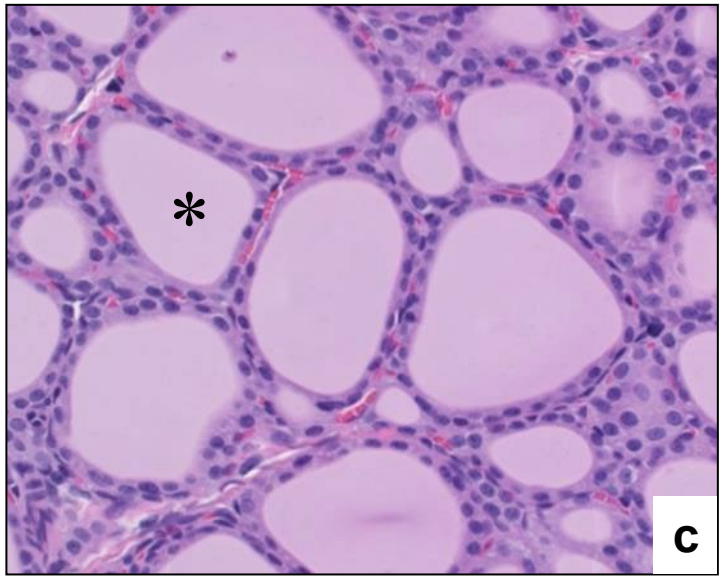

PND 21, H&E stain, 35x.

- These images show the normal postnatal development of the thyroid gland. The thyroid gland begins to develop follicles and colloid 1-2 days prior to birth. From PND 1 to 21, there is progressive accumulation of colloid (*) and a corresponding flattening of the follicular epithelial cells.
  - a) PND 4 – the thyroid gland has few follicles with some colloid (*). Epithelial cells are plump cuboidal.
  - b) PND 7 – the colloid containing follicles (*) are more abundant.
  - c) PND 21 – the thyroid gland is histologically mature. Follicles are distended with colloid (*) and follicular epithelial cells are flattened.
- PND 40 to 42 (not shown) – sexual dimorphism of thyroid follicular cells becomes apparent. The follicular cells of males are plumper with more vacuolation than in females. The testosterone produced by the post-natal Leydig cells render the thyroid epithelial cells more sensitive to thyroid stimulating hormone.

Thyroid gland, rat, PND 21, hypertrophy/hyperplasia of follicular epithelium

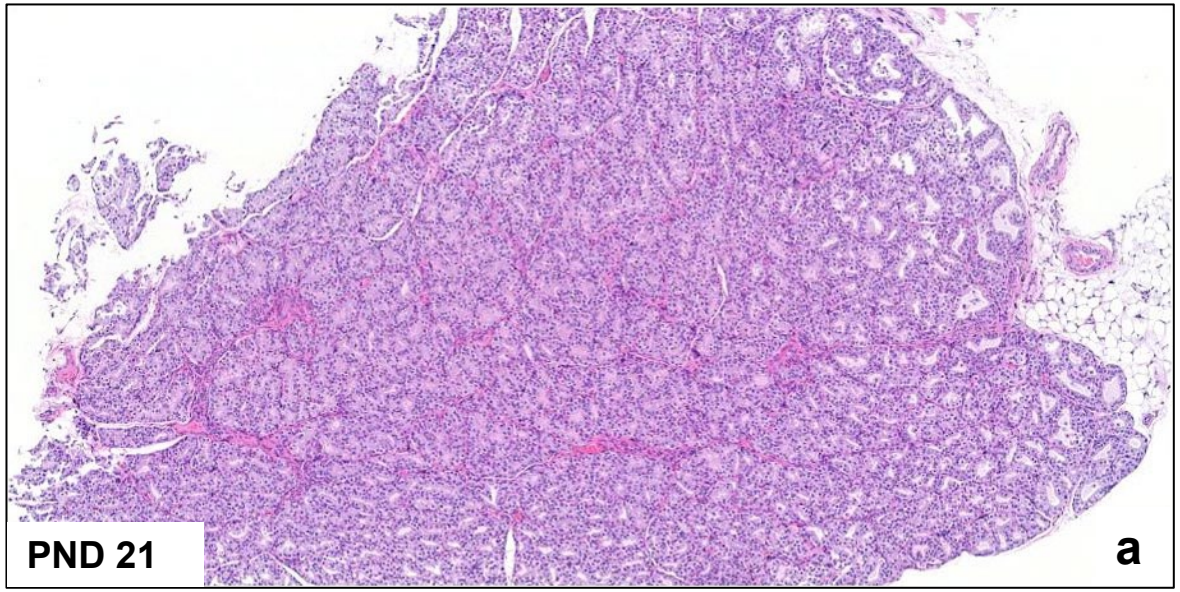

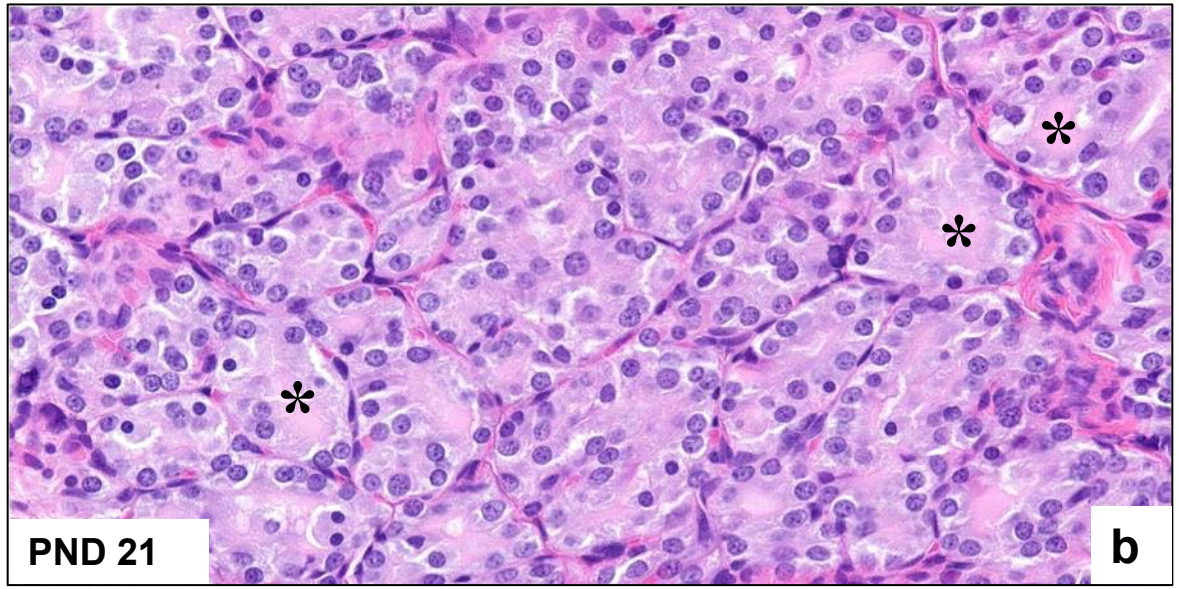

- When rats are exposed to a thyrotoxicant indirectly throughout gestation and lactation (by exposure of the dam), the typical tissue change is hypertrophy/hyperplasia of the thyroid follicular cell with decreased colloid. This change can be seen in first generation (F1) rats at PND 21. a) Following exposure of the dam to propylthiouracil (PTU), the thyroid gland of the PND 21 pups has hypertrophy/hyperplasia and appears as a solid tissue with only a few small follicle contours at the periphery. H&E stain, 5x. b) The follicles have little colloid (*), and the follicular epithelial cells are plump and crowded. H&E stain, 33x.

- Thyrotoxicants generally cause lower circulating thyroid hormone with release of any available colloid from the gland. The lower circulating thyroid hormone levels cause increased production and release of thyroid stimulating hormone (TSH) from the pituitary gland. TSH has a trophic effect on the thyroid follicular epithelial cells, leading to hypertrophy/hyperplasia.

Endocrine: pituitary, pancreatic islets, parathyroid, and adrenal gland

- **Pituitary gland** of the rat is functional at PND 0 but acidophils and basophils are not distinguishable until PND 7.
  - PND 7 to 14 – basophils more numerous; PND 21: equal proportions of basophils and acidophils; PND 28: acidophils more numerous; PND 35 – no predominant cell type, chromophobes recognizable.
- **Pancreatic islets** are present at birth: A cells (glucagon), B cells (insulin), D cells (somatostatin), PP cells (pancreatic polypeptide).
  - PND 0 to 4 – proliferation of all 4 cell types; PND 5 to 10: accelerated growth of A and B cells; after PND 10: slow but constant growth of all 4 cell types.
- **Parathyroid gland** has two cell types: dark cells actively secrete PTH, light cells are resting status
  - Sexual dimorphism in parathyroid gland: PND 28 – parathyroid glands of females are 44% larger than males; PND 90 – parathyroid glands of females are 66% larger than males.
- **Adrenal gland** is endocrinologically active at birth:
  - PND 0 – Zona reticularis (ZR) is not discernible. PND 10 to 14 – ZR becomes discernible
  - Corticosterone production starts as early as GD 18.
  - Corticosterone production increases until PND 40 in males and PND 60 in females.
  - Aldosterone production is minimal prenatally, increases from PND 1 to 20, then declines and stabilizes.
  - Sexual dimorphism in adrenal gland:
    - PND 49 – adrenal cortex and medulla are larger in female rats compared to males.
    - Larger size in females possibly associated with higher levels of corticosterone in females.

Skin, rat, PND 1 and PND 21

Developmental schedule:

- PND 0 – epidermis (E) is thicker than adult rat (5-6 cells thick) with thick keratin layer (K). Hair follicles bud downward from the epidermis to form hair pegs (P).
- PND 7 – epidermis remains thick, more adipocytes in deep dermis (D)/panniculus adiposus. High density of hair follicles (F). No additional budding of pegs from epidermis. The absolute number of hair follicles remains fixed from this point onward.
- PND 14 – epidermis becomes thinner. Arrector pili muscles and adnexal glands (A) are prominent.
- PND 28 – skin is histologically mature.

Figures legend: E = epidermis; K = superficial keratin layer; P = hair peg; D = dermis; F = follicles; A = adnexal gland. H&E stain.

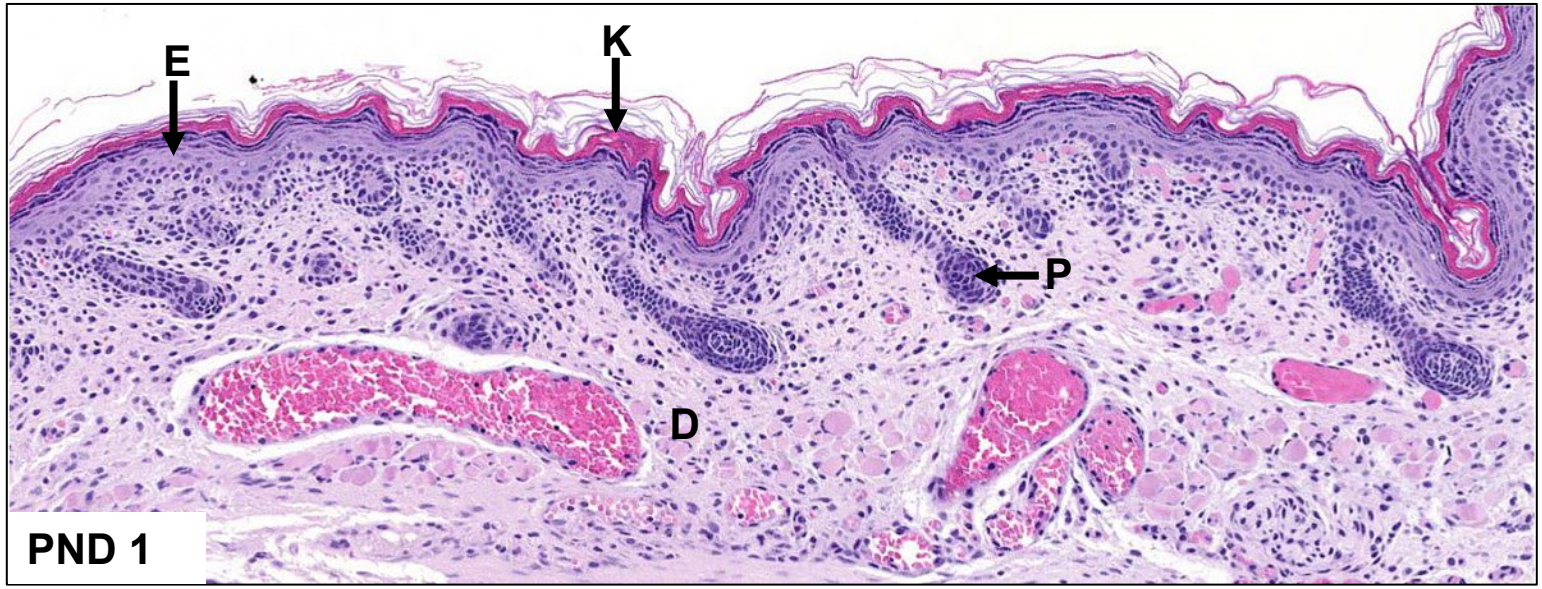

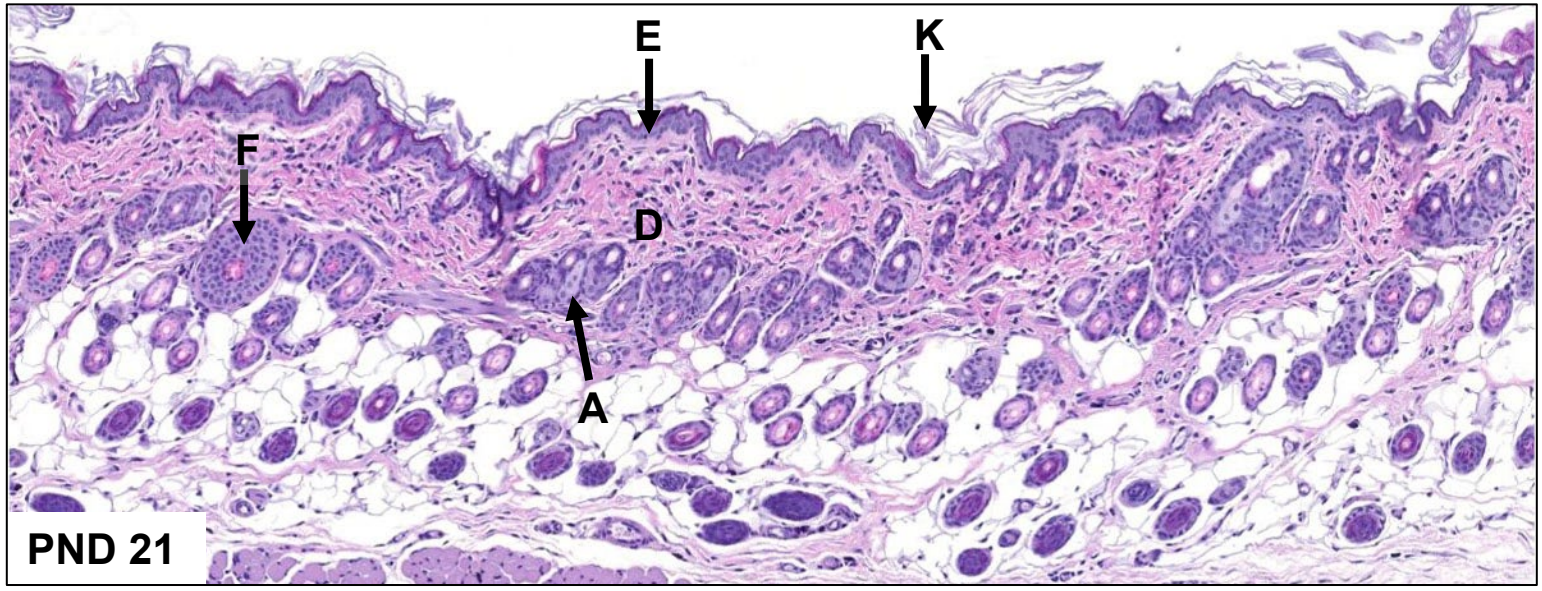

Mammary gland, rat, PND 1

- Developmental sequence
  - Mammary gland tissue is present at birth, consisting of simple tubular glands (arrowheads). The mammary glands become more complex during following weeks. H&E stain.
  - In rats, terminal end buds (TEBs) (arrow, inset) are apparent by PND 14. H&E stain.
  - PND 21 to 84 – TEBs divide with each successive estrous cycle to form additional alveolar buds and alveolar lobules. TEBs are not commonly visible in typical 5 micrometer (µm) histologic sections but are abundantly visible in mammary gland whole mounts.
- Sexual dimorphism of rat mammary gland commences at time of puberty. The mammary gland is tubuloalveolar in females and lobuloalveolar in males.
- There are species-specific differences in response to hormonal influences on the mammary gland.
- Chemically-mediated hormonal influences may alter any step in mammary gland development.
- Note immature inguinal lymph node (*) in the PND 1 image.

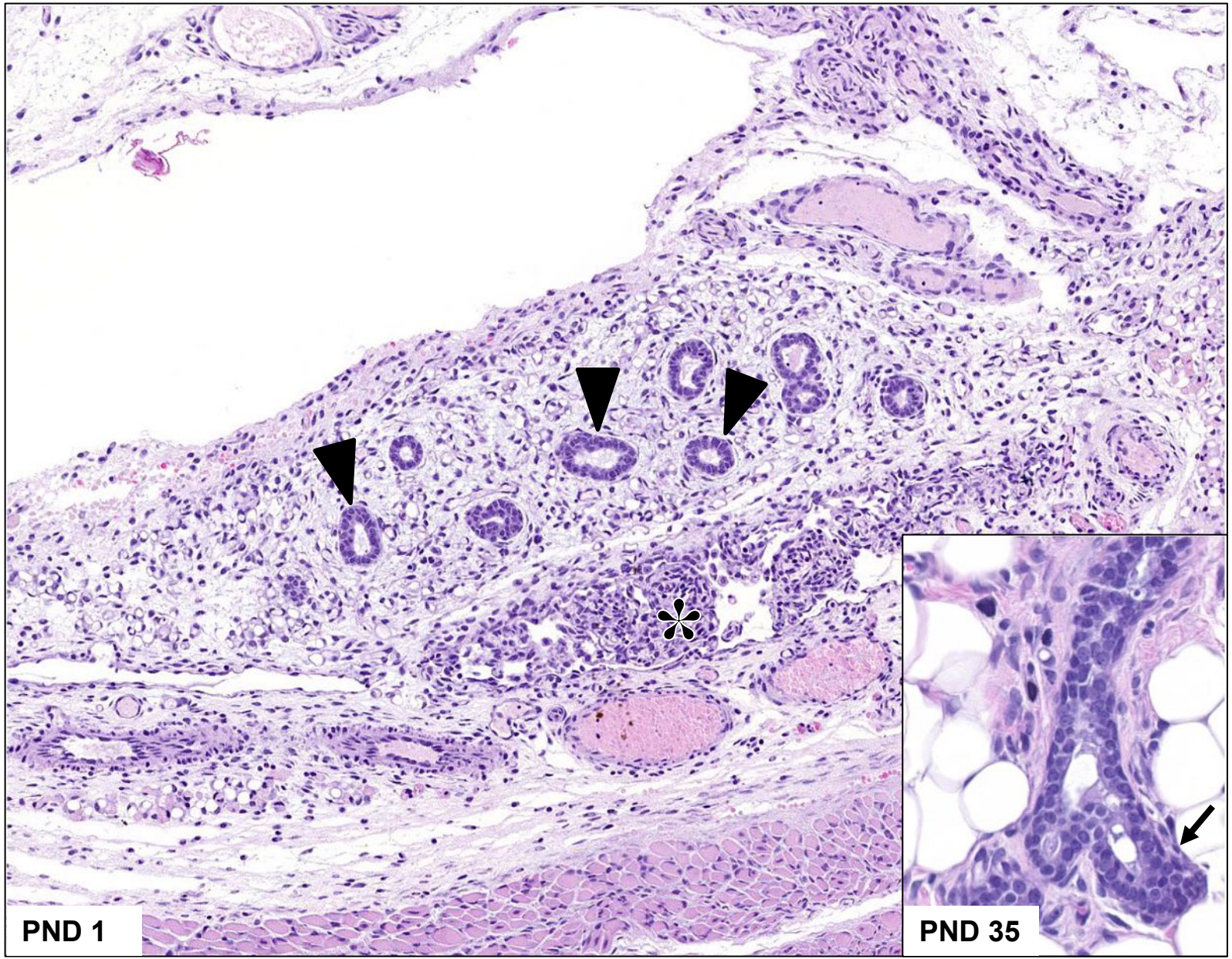

Specific factors to consider in studies involving juvenile animals

Organ weight interpretation in juvenile animals

- Certain organ weights, e.g., testis and brain weights, are spared in the adult animal when the animal experiences loss of body weight due to nutrition or toxicity. This organ weight sparing is not absolute in the juvenile animal during organ system development. With test article-related body weight loss during postnatal life in the pup, there also may be lower absolute brain and testes weights.
- Body weight loss in suckling pups may not necessarily be the result of direct test article-related toxicity. If maternal toxicity prevents the dam from nurturing the pups properly, this lack of nurturing may result in lower pup body weight gain and, accordingly, lower brain and testis weights.

Complications with dose adjustment in feeding studies

- When conducting feeding studies involving juvenile rats, food consumption (by the dams during gestation and lactation or F1 rats during the first week following weaning) can drastically change due to changing nutritional demands. Nutritional demand in the dams increases during gestation and especially during lactation. Thus, the xenobiotic level in the diet must be adjusted downward to maintain a target xenobiotic dose.
- Feed adjustment is most critical during gestation, lactation, and for pups during the first week following weaning. Food consumption by dams during gestation increases up to 8%, and, during lactation, food consumption by dams can increase 95-100%. For pups during the first week after weaning (PND 21 to 28), food consumption suddenly begins and can result in 130% increase in the xenobiotic target dose.

Example of brain lesions associated with failure to adjust for feed consumption in rat pups

In a study of benzoic acid administered to rats in an EOGRT, dosages in feed were not adjusted for body weight. Pups at PND 21 to 28 were exposed to 130% target dose due to higher food consumption relative to body weight during this first post weaning week. This higher-than-expected food consumption (and dose) resulted in massive acute neuronal necrosis and mineralization of multiple sites in the brain.

- This panel of images from brain of PND 90 rats exposed to benzoic acid at 130% of the target dose during the first week following weaning, resulting in a) dystrophic mineralization of the hippocampus, b) globular mineralized deposits in the habenular commissure; and c) neuronal depletion of the dentate gyrus (DG). Panel (d) is a control rat with normal neuronal density in the DG. H&E stain.

- This example underscores the importance of dosed feed adjustments in juvenile animals.

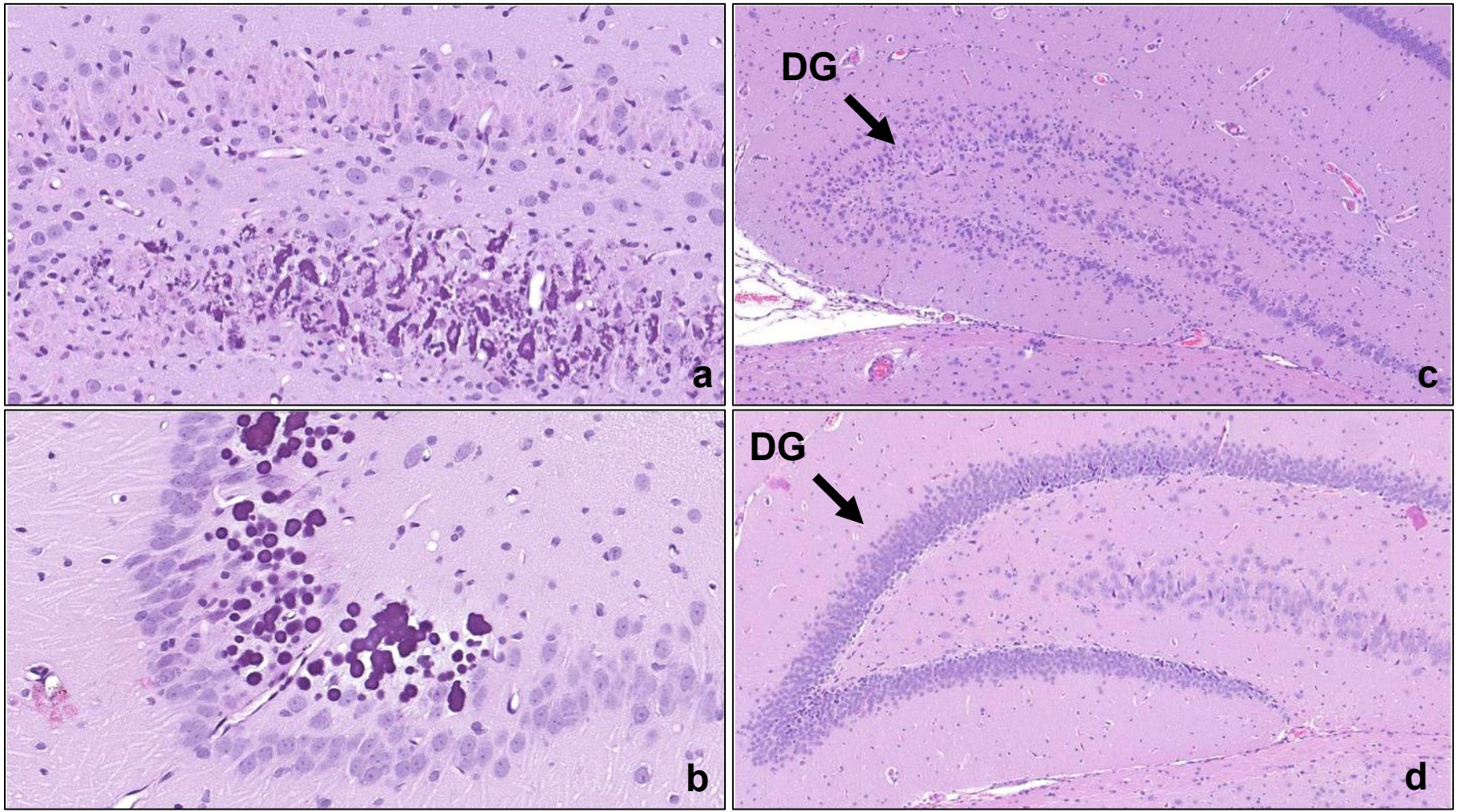

Specific factors to consider in studies involving juvenile animals, cont.

Effects of inflammation in dams

- Maternal inflammation and stress are particularly important in developmental and reproductive (DART) studies.
- Inflammation-associated activation of the maternal immune system has been linked to various developmental disorders.
  - In-utero inflammation in murine dams is associated with expansion of lymphoid-biased progenitor cells that persist postnatally, resulting in increased lymphoid responsiveness in offspring.
  - When rhesus macaque dams were injected with a viral mimic during pregnancy, offspring had volume reductions in cerebral cortex and frontal cortex white matter.

Maternal failure to nurture pups

- Maternal failure to properly nurture pups can affect development of multiple organ systems in the pups. When pups are orphaned or there is a failure of maternal nurturing, effects on the GI tract, immune system and brain may occur.
  - The stress associated with lack of nurturing may result in increased glucocorticoid surge due to stress. Glucocorticoids are known to result in precocious gastrointestinal development.
  - Under normal circumstances, vertical transmission of maternal microbiota (exposure to feces of the dam) during the early postnatal period promotes immune system development and provides substrates for brain development. With altered maternal nurturing, altered interactions between the intestinal microbiome and the immune system may have an impact on maturation and function of the central nervous system.

References

- Bandeira, F., Lent, R., & Herculano-Houzer, S. (2009). Changing numbers of neuronal and non-neuronal cells underlie postnatal growth in the rat. *Proceedings of the National Academy of Sciences, 106*(33), 14108–14113. https://doi.org/10.1073/pnas.0804650106
- Barnes, D. and Altman, J. (1973). Effects of different schedules of early undernutrition on the preweaning growth of the rat cerebellum. *Experimental Neurology, 38*(3), 406–419. https://doi.org/10.1016/0014-4886(73)90163-5
- Bolon, B., Dostal, L. A., & Garman, R.H. (2021). Neuropathology evaluation in juvenile toxicity studies in rodents: comparison of developmental neurotoxicity studies for chemicals with juvenile animal studies for pediatric pharmaceutical. *Toxicologic Pathology, 49*(8), 1405–1415. https://doi.org/10.1177/01926233211045321
- Coder, P., Picut, C., Walling, B., & Parker, R. (2019). Critical windows for feed adjustment in developmental and reproductive toxicology (DART) studies: A case study. Poster presentation, Society of Toxicologic Pathology annual meeting, Raleigh, NC.
- Downs, N. and Mullins P. (2014). The development of myelin in the brain of the juvenile rat. *Toxicologic Pathology, 42*(5), 913–922. https://doi.org/10.1177/0192623313503518
- Frazier, K.S. (2017). Species differences in renal development and associated developmental nephrotoxicity. *Birth Defects Research, 109*(6), 1243–1256. https://doi.org/10.1002/bdr2.1088
- Groseclose, M.R., Laffan, S.B., & Frazier, K.S. (2015). Imaging MS in toxicology: An Investigation of Juvenile Rat Nephrotoxicity Associated with Dabrafenib Administration. *Journal of American Society for Mass Spectrometry, 26*(6),887–898. https://doi.org/10.1007/s13361-015-1103-4
- Keane, K. A., Parker, G. A., Regan, K. S., Picut, C., Dixon, D., Creasy, D., Giri, D., & Hukkanen, R. R. (2015). Scientific and Regulatory Policy Committee (SRPC) points to consider. Toxicologic Pathology, 43(8), 1047–1063. https://doi.org/10.1177/0192623315579943

References

- Parker, E., McElroy, P., Picut, C., Szabo, K., & White-Hunt, S. (2018). Soy-deficient diet induces renal lesions in juvenile rats. *Food and Chemical Toxicology*, *121*, 467–471. https://doi.org/10.1016/j.fct.2018.09.044
- Parker, G. A., Picut, C. A., Swanson, C., Toot , & J. D. (2015). Histologic features of postnatal development of immune system organs in the Sprague-Dawley rat. *Toxicologic Pathology, 43*(6), 794-815. https://doi.org/10.1177/019262331557872
- Parker, G. and Picut, C. A. (2016). *Atlas of histology of the juvenile rat.* San Diego, CA, Elsevier/Academic Press.
- Parker, G, and Picut, C.A. (2024). Development of immune system organs. In C. McQueen (Ed.), *Comprehensive Toxicology*, 4th ed. Elsevier.
- Petrere, J. (1994). Developmental toxicity studies in mice, rats, and rabbits with the anticonvulsant gabapentin. *Fundamental and Applied Toxicology, 23*(4), 585–589. https://doi.org/10.1006/faat.1994.1144
- Picut, C. A., Remick, A. K., Asakawa, M. G., Simons, M. L., & Parker, G. A. (2014). Histologic features of prepubertal and pubertal reproductive development in female Sprague-Dawley rats. *Toxicologic Pathology, 42*(2), 403–413. https://doi.org/10.1177/0192623313484832
- Picut, C. A., Remick, A. K., de Rijk, E. P., Simons, M. L., Stump, D. G., & Parker, G. A. (2015). Postnatal development of the testis in the rat: Morphologic study and correlation of morphology to neuroendocrine parameters. *Toxicologic Pathology, 43*(3), 326–342. https://doi.org/10.1177/0192623314547279
- Picut, C. A., Ziejewski, M. K., & Stanislaus, D. (2018). Comparative aspects of pre- and postnatal development of the male reproductive system. *Birth Defects Research, 110*(3): 190–227. https://doi.org/10.1002/bdr2.1133

National Institute of Environmental Health Sciences
Division of Translational Toxicology

Authors

- George A. Parker, DVM, PhD, DACVP, DABT, FIATP – Charles River Laboratories
- Catherine A. Picut, VMD, JD, DACVP, DABT, FIATP – Charles River Laboratories

Reviewers

- Cynthia Willson, MS, PhD, DVM, DACVP, DABT – Inotiv-RTP
- Beth Lubeck, PhD, MBA – Division of Translational Toxicology, NIEHS
- Vanessa Vrolyk, DVM, MSc, PhD, DACVP – Charles River Laboratories

Acknowledgments

- All images presented are from the personal collections of the authors.

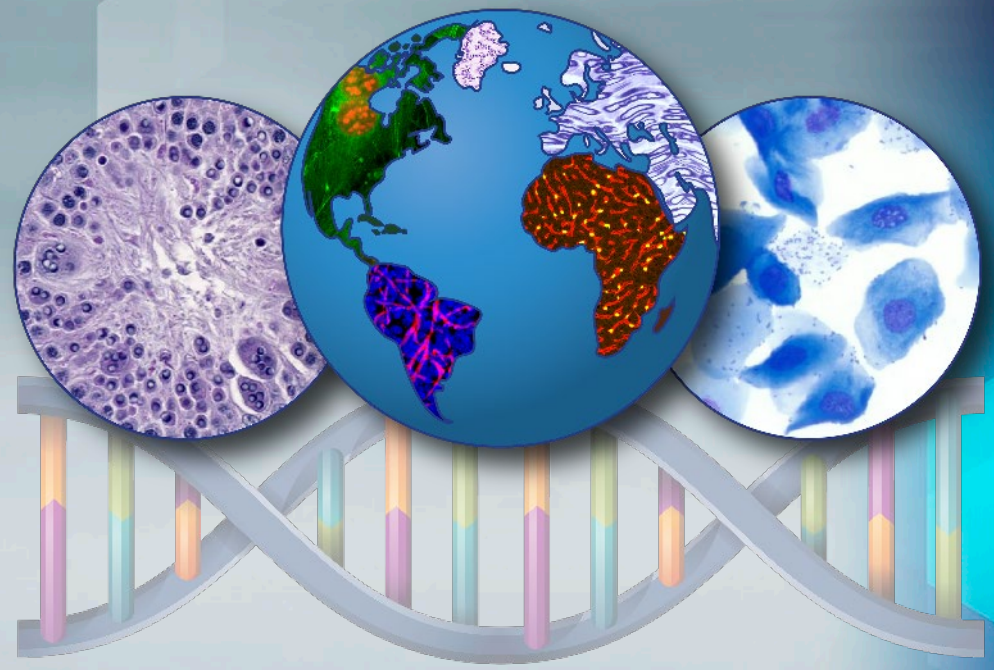

Division of Translational Toxicology
Global Toxicologic Pathology Training Program